Chair of Pico and Nano Satellites, and Satellite Constellations
TUM School of Engineering and Design
Technical University of Munich

Effect of Ground Stations in Satellite Networks for Task Distribution in Centralized and Decentralized Approaches

Sarvesh Jagadish [03764730]

Semester Thesis Report

Master of Science (M.Sc.) in Aerospace Engineering

at the TUM School of Engineering and Design of the Technical University of Munich.

Examiner:

Prof. Dr. Alessandro Golkar

Supervisor:

M.Sc. Vincenzo Messina

Submitted:

Munich, 02.06.2024

I hereby declare that this thesis is entirely the result of my own work except where otherwise indicated. I have only used the resources given in the list of references.

Munich, 02.06.2024 Sarvesh Jagadish [03764730]

Abstract

This thesis explores the optimization of satellite constellations to enhance ground station coverage and task distribution efficiency. By comparing centralized, decentralized, and partially centralized network configurations, the research aims to determine the optimal setup for minimizing total time delay and improving performance metrics. This study investigates how ground stations influence task distribution and evaluates the benefits of adding one or more ground stations to enhance network performance. By evaluating 44 optimization algorithms across two satellite configurations, the study identifies the top algorithms for maximizing coverage at the lowest altitude.

The results demonstrate that an optimized satellite configuration significantly enhances coverage and reduces latency. Increasing ground station density markedly improves performance in centralized and partially centralized networks, though less so in decentralized configurations. The inclusion of multiple ground stations shows significant improvements in network efficiency, highlighting the benefits of both centralized and decentralized approaches. Additional central nodes show nuanced impacts on time delay and post-capture time, indicating areas for further refinement. The link budget analysis confirms that effective communication can be maintained in optimized configurations, with potential improvements through enhanced error correction methods.

This study provides valuable insights into optimizing satellite network design, contributing to more efficient and reliable space communication systems.

Contents

List of Figures

List of Tables

Glossary

EIRP Equivalent isotropic radiated power. 101

EO Earth Observation. 5, 65

ISL Inter-Satellite Link. iv, 4, 6

LEO Low Earth Orbit. v, 1, 4, 6, 22–24

NLOPT Non Linear Optimizer. ix, 14, 30, 36, 72

PNT Position, Navigation, and Timing. 4

SAT Satellite. 23

SIN Space Information Networks. 7

1 Introduction

Satellite networks have witnessed unprecedented growth in recent years, with a surge in deployments driven by both private ventures and national projects. Currently, over 9,000 spacecraft orbit the Earth, predominantly in the Low Earth Orbit (LEO) region, within approximately 2,000 kilometers from the Earth's surface [1]. This dense satellite population serves diverse purposes, including communication, Earth observation, scientific research, and technological advancements. The projected deployment of up to 57,000 new satellites by the end of the decade underscores the accelerating pace of expansion in the satellite industry [2].

Among the entities driving this expansion is SpaceX, whose ambitious Starlink satellite program aims to deploy over a thousand new satellites annually. With communication satellites comprising a significant portion of the operational satellites, surpassing half of the total, initiatives like Starlink are poised to further increase satellite numbers, particularly in LEO [2]. This proliferation of satellites necessitates efficient management and optimization strategies to ensure seamless operation and resource utilization within satellite networks.

Ground stations play a pivotal role in satellite operations, serving as the vital link between satellites and terrestrial infrastructure. These stations facilitate communication, data transmission, and command execution, thereby enabling the efficient functioning of satellite-based services. As satellite networks continue to expand, understanding the impact of ground stations on task distribution becomes increasingly crucial [3].

The motivation behind this research is to comprehensively investigate the effect of ground stations on task distribution within satellite networks, particularly in centralized and decentralized approaches. Ground stations are intermediaries for communication, data reception, and command execution between satellites and terrestrial infrastructure. Understanding their role and influence is essential for optimizing satellite deployment, enhancing communication networks, and ensuring efficient service delivery.

Centralized and decentralized approaches represent distinct paradigms for managing satellite networks. Centralized control involves a single authority making decisions for the entire network, while decentralized approaches distribute decision-making across multiple nodes within the network [4]. The choice between centralized and decentralized approaches impacts task distribution efficiency, latency, and overall network performance [5].

1.1 Research Statement

This research addresses several critical questions related to the impact of ground stations on task distribution in satellite networks. Specifically, it seeks to elucidate how ground stations influence task

distribution under different control paradigms, identify critical parameters affecting task distribution decisions, and assess the benefits of integrating ground stations into satellite networks.

By examining the interplay between ground stations and satellite networks, this study aims to provide valuable insights into designing and optimizing satellite networks for efficient task distribution, reduced latency, and enhanced network performance.

1.2 Problem Description

As satellite networks become increasingly integral to various applications such as communication, Earth observation, and scientific research, optimizing task distribution within these networks emerges as a critical challenge. Ground stations serve as essential intermediaries between satellites and terrestrial infrastructure, facilitating communication, data transmission, and command execution. However, the influence of ground stations on task distribution efficiency in satellite networks remains poorly understood.

The effectiveness of task distribution mechanisms in satellite networks is directly impacted by the presence and deployment of ground stations. Factors such as communication latency, bandwidth limitations, and ground station coverage areas significantly influence the speed and reliability of data transmission between satellites and terrestrial infrastructure. Moreover, the trade-offs between centralized and decentralized approaches to task distribution further complicate the optimization of ground station deployment strategies.

Understanding the impact of ground stations on task distribution efficiency is essential for optimizing satellite network performance and resource utilization. Centralized control mechanisms offer a centralized decision-making authority, potentially streamlining task distribution processes but also introducing challenges related to scalability and fault tolerance. On the other hand, decentralized approaches distribute decision-making among individual satellites or clusters, offering greater flexibility and resilience but requiring efficient coordination and communication mechanisms [6].

Furthermore, the comparison between centralized and decentralized approaches necessitates a thorough analysis of their respective advantages and limitations in the context of ground station influence. Identifying the optimal balance between centralized control and decentralized decision-making, considering the specific requirements and constraints of satellite networks, is crucial for maximizing task distribution efficiency and network performance [7].

To tackle these challenges, it is necessary to create innovative models that combine the features of ground stations and strategies for distributing tasks. Additionally, the research seeks to conduct a comprehensive comparison of satellite network architectures, including decentralized, centralized, and partially centralized models, to determine their respective advantages and suitability under different operational scenarios.

1.3 Research Questions

1. What are the key parameters and variables affecting task distribution decisions in satellite networks, considering the presence of ground stations?

2. How do ground stations impact task distribution in satellite networks under centralized and decentralized approaches?
3. What benefits can be derived from the addition of one or more ground stations to satellite networks in terms of task distribution efficiency and network performance enhancement?

1.4 Outline

The remainder of this Thesis is structured as follows:

1. **Chapter 1: Introduction**
   This chapter serves as an introduction to the thesis, presenting the research statement that defines the scope and purpose of the study. It describes the problem that the thesis aims to address, providing context for the research questions posed. Additionally, this chapter outlines the structure of the thesis, providing readers with a roadmap of what to expect in the subsequent chapters.
2. **Chapter 2: Literature Review**
   Examines existing methodologies and technologies in Constellations, Decentralized and Centralized approaches, identifying gaps and innovation opportunities. This review lays the foundation for the development of our novel framework.
3. **Chapter 3: Methodology**
   In this chapter, the methodology employed in the research is detailed. It begins by discussing the choice between Kepler and J2 Brouwer-Lyddane elements and proceeds to outline the various design parameters considered. Assumptions made during the research are also explicitly stated. The chapter then introduces the layout and optimization objectives, followed by a discussion on setting up the optimizer. Simulation setups for disaster monitoring are explained, including objectives and specific configurations. The chapter concludes with an analysis of propagation delays and link budgets.
4. **Chapter 4: Results**
   This chapter presents the results obtained from the research. It starts by discussing initial contact with ground stations and the optimization of contact time. Various optimization methods are compared, and the outcomes of different algorithms are analyzed in detail. Results related to total time delay, impact of additional nodes, task distribution, and link budget are presented and discussed comprehensively. The chapter also includes a discussion on the implications of the results and their significance in addressing the research questions.
5. **Chapter 5: Future work and Conclusion**
   This final chapter outlines potential future directions for research based on the findings of the study. It discusses areas that could benefit from further exploration or refinement and proposes potential avenues for extending the current work. Additionally, the chapter provides a concise summary of the key findings and conclusions drawn from the research. It reflects on how the research has contributed to the existing body of knowledge and offers insights into the broader implications of the findings. Finally, the chapter concludes with a closing statement that encapsulates the overall significance of the research and its potential impact on the field.

2 Literature Review

Chapter 2 provides a overview of Low Earth Orbit (LEO) satellite constellations, emphasizing their role in global communications and navigation. It discusses the challenges and opportunities presented by the rapid expansion of LEO constellations, alongside exploring the principles and advantages of the Walker Constellation in optimizing task distribution. Additionally, the chapter examines the significance of Inter-Satellite Links (ISLs) in enhancing ground station communication efficiency and task distribution within LEO mega-constellations. Furthermore, it delves into the dynamics of centralized and decentralized routing solutions, highlighting their importance in optimizing network performance and resource utilization within space information networks. Understanding these concepts is crucial for devising efficient task distribution strategies and enhancing the resilience of satellite networks.

2.1 State of Low Earth Orbit (LEO) Satellite Constellations

Low Earth Orbit (LEO) satellite constellations are becoming increasingly important, in the field of communications and navigation. The rise of Earth orbit (LEO) satellite networks like Starlink, Kuiper and OneWeb are rapidly expanding due to their capacity to provide internet access and enhanced Position, Navigation and Timing (PNT) services. These LEO satellites travel around the Earth at heights ranging from 500 km, to 2000 km resulting in reduced latency compared to satellites thus aiding in data transmission. These constellations have effectively bridged the digital divide, offering connectivity in remote and underserved regions where traditional terrestrial infrastructure is lacking [8].

However, the rapid expansion of LEO satellite constellations also presents significant challenges. Key issues include space traffic management, collision avoidance, and spectrum allocation. As highlighted by Prol et al. (2022), the dense deployment of LEO satellites necessitates advanced coordination mechanisms to prevent collisions and mitigate space debris risks [8]. Additionally, the competition for radio frequency spectrum intensifies as more satellites are launched, potentially leading to interference issues [9]. Despite these challenges, the opportunities presented by LEO constellations are immense, particularly in enhancing global connectivity and providing robust PNT services.

The continuous innovation in satellite technology and the development of comprehensive regulatory frameworks will be crucial in addressing these challenges and realizing the full potential of LEO satellite networks [10].

2.2 Walker Constellation

The Walker Constellation, also known as the Walker Delta Pattern, is a class of circular orbit geometries commonly used in satellite network design. Named after John Walker [11], who proposed a notation to describe this pattern, the Walker Constellation aims to optimize the spatial distribution and operational efficiency of satellite networks. This section delves into the principles, advantages, and application of the Walker Constellation in satellite networks, particularly in relation to the research topic of ground station effects on task distribution in centralized and decentralized approaches.

Principles of Walker Constellation
The Walker Constellation is designed to maintain a systematic and balanced arrangement of satellites in orbit. The fundamental notation for describing a Walker Constellation is given as:

$$i : t/p/f \tag{2.1}$$

$Where,$

- *i is the inclination of the orbit,*
- *t is the total number of Satellites*
- *p is the number of equally spaced orbital planes*
- *f is the relative spacing betweeen satellites in adjacent planes. The change in true anomaly (in degrees) for equivalent satellites in neighbouring planes is equal to* $(f * 360/t)$.

2.2.1 Benefits of the Walker Constellation

- Consistent Coverage; One key advantage of the Walker Constellation is its capability to offer coverage across the Earths surface. By spacing out satellites, in orbits the constellation ensures that every point on Earth remains within view of at least one satellite at all times [12]. This feature is vital for applications that rely on dependable coverage, such as communication and Earth Observation (EO).
- Orbit Maintenance; Satellites within a Walker Constellation share orbits, eccentricity and inclination. This uniformity means that external influences like forces from the Earth and the Moon impact all satellites, in a way. As a result maintaining the constellations geometry requires station keeping maneuvers leading to reduced fuel usage and prolonged operational life span of the satellites. [12].
- Satellites are strategically positioned in orbits to prevent collisions, at intersections ensuring the safety and reliability of the satellite network as more satellites populate Low Earth Orbit (LEO) [13]. The Walker Constellations circular orbits maintain an altitude simplifying communication by keeping signal strength consistent. This stability benefits data transmission quality. Streamlines ground station operations [14].

2.2.2 Application in Task Distribution

In the context of task distribution within satellite networks, the Walker Constellation offers several benefits:

- Distribution for Decentralized Systems; In scenarios where individual satellites independently make decisions on task allocation the uniform coverage offered by the Walker Constellation ensures a distribution of satellites. This enables sharing of tasks based on proximity and availability.
- Reduced Delay in Centralized Systems; In systems for task allocation, the consistent and reliable coverage of the Walker Constellation can help reduce delays in sending commands and collecting data. Ground stations strategically positioned to leverage the constellations coverage can effectively communicate with satellites thereby boosting network responsiveness.
- Improved Disaster Surveillance; In tasks like disaster surveillance the Walker Constellations capability to swiftly and dependably transmit data is highly valuable. The predictable pattern of Walker Delta simplifies forecasting satellite passes, over affected regions enhancing monitoring efforts responsiveness and dependability [15]. The constellation's design supports low-latency communication and quick data relay to ground stations, which is essential for timely decision-making in emergency situations. The regularity of the Walker Delta pattern simplifies the prediction of satellite passes over affected areas, enhancing the responsiveness and reliability of monitoring efforts.

2.3 Inter-Satellite Link (ISL)

In the context of Low Earth Orbit (LEO) mega-constellations, inter-satellite links (ISL) significantly enhance the efficiency of ground station communication and task distribution. By enabling direct satellite-to-satellite communication, ISLs reduce the need for frequent data downlinks to ground stations, alleviating bottlenecks common in centralized network configurations. This improvement is especially beneficial in decentralized networks [16][17], where distributing data evenly across the constellation is crucial. ISLs extend the effective range of ground stations by allowing data to be relayed through multiple satellites, thereby reducing latency and increasing transmission efficiency, which ensures faster and more reliable ground station connectivity.

Moreover, ISLs facilitate dynamic task distribution by providing multiple data pathways and optimizing overall network performance. In decentralized configurations, tasks can be assigned based on satellite positions and ISL status, leading to efficient task execution. Minimizing hop-count in ISL routing is essential for reducing delays and enhancing task distribution, particularly for time-sensitive operations. While centralized configurations may suffer from congestion at the central node, decentralized networks leverage ISLs for more flexible and resilient data routing, thereby reducing delays and improving network robustness. The findings from Chen et al. (2021) [18] underscore the critical role of ISLs in maximizing the operational efficiency of LEO mega-constellations.

2.4 Centralized and Decentralized Networks

Routing solutions, whether centralized or decentralized, play a crucial role in shaping the present and future landscape of space information networks (SINs). Fraire and Gasparini (2021) explores the intricate dynamics of these solutions, highlighting their importance in optimizing network performance and resource utilization within SINs SINs [19]. As elucidated by Russell Carpenter (2002), centralized approaches entail a hierarchical structure where a central controller orchestrates task distribution and routing decisions across the satellite network. On the other hand, decentralized control mechanisms explored by Belanger et al. (2006), distributes decision making authority among individual satellites, enabling autonomous operation and resilience against communication failures [20][21]. Understanding the nuances of centralized and decentralized routing solutions is paramount for devising efficient task distribution strategies and enhancing the resilience of satellite networks in the face of dynamic operational challenges.

3 Methodology

Chapter 3 is sectioned as follows: First, we define the selection of Brouwer-Lyddane J2 elements by comparing it against Keplerian elements. Then we talk about the Design parameters addressing the satellite layouts, objectives of optimization, setting up the simulation and followed by Link budget analysis. All simulations of the optimizer and disaster monitoring were conducted using Freeflyer, a software used for satellite mission analysis, design, and operations [22]. For the link budget and data visualization and plotting, MATLAB was utilized.

3.1 Kepler vs J2 Brouwer-Lyddane Elements

In this study, Brouwer-Lyddane J2 (BLJ2) [22] elements were utilized instead of the classical Keplerian elements [23] to model the satellite's orbits. This was because BLJ2 elements provide better accuracy in dealing with the Earth's oblateness, which is one of the most important perturbations for Low Earth Orbit (LEO) constellations; due to this, comparing the relative distances between the neighbouring spacecraft over time is essential.

To illustrate the effectiveness of Keplerian versus Brouwer-Lyddane J2 (BLJ2) elements in maintaining satellite formation stability, the relative distance between neighbouring spacecraft over time was plotted. The x-axis represents elapsed time in days, while the y-axis shows along-track drift in kilometers.

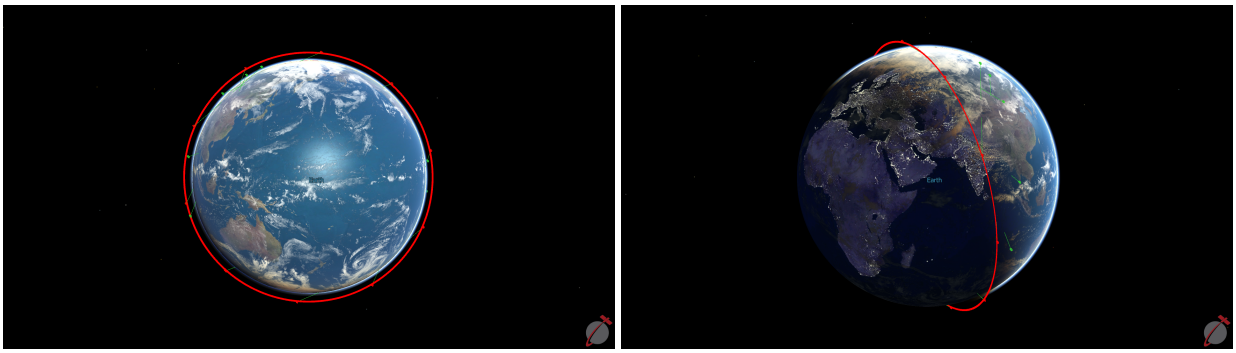

(a) Keplerian Orbital Elements **(b)** Deviation of Satellites

Figure 3.1 Constellation Initialized using Keplerian Elements

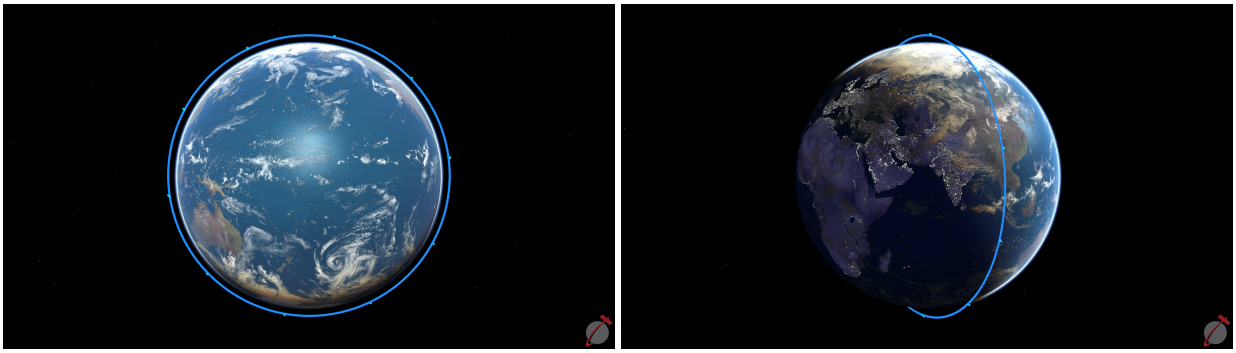

(a) Brouwer Lyddane J2 Orbital Elements **(b)** Deviation of Satellites

Figure 3.2 Constellation Initialized using Brouwer Lyddane J2 Elements

When the satellites were initialized using the Keplerian elements as seen in Fig.3.1a, there was a significant drift of Satellites ranging from -11000 km to 2500 km due to not accounting for the perturbations as shown in Fig.3.3. Whereas when the satellite formation was re-initialized using BLJ2 elements as seen in Fig.3.2a and the results show that the drift was considerably low around -17 km to +15 km, as shown in Fig.3.4 highlighting the improved stability. By incorporating J2 perturbations, which account for the Earth's oblateness, BLJ2 elements provided a more precise and stable satellite formation.

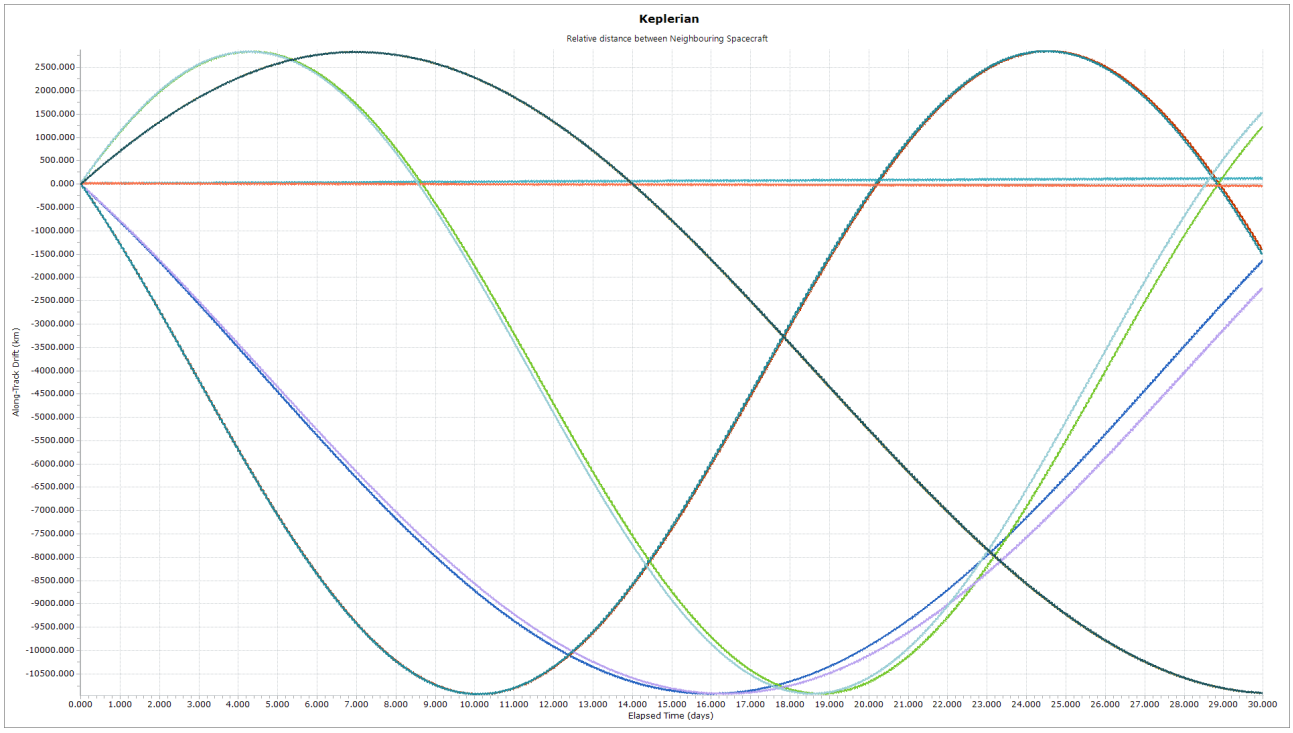

Figure 3.3 Keplerian Formation Relative distance between neighbouring satellites

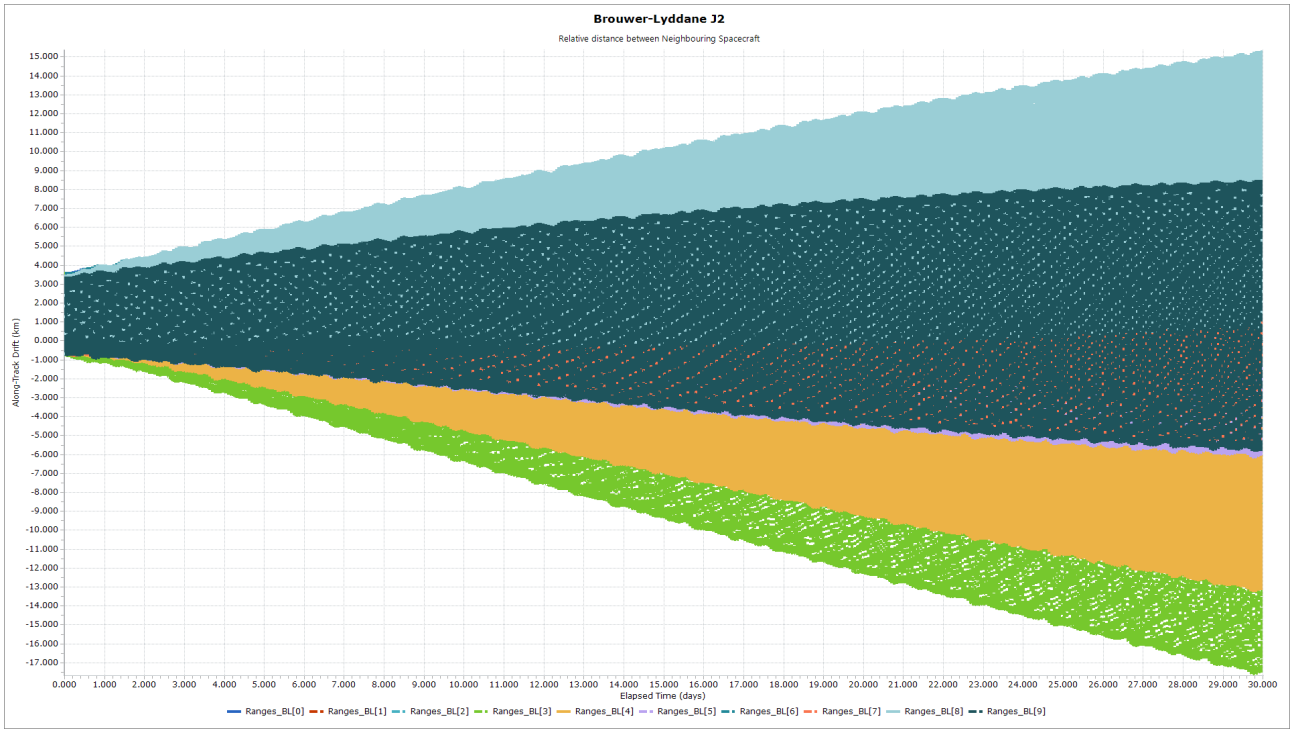

Figure 3.4 BLJ2 Formation Relative distance between neighbouring satellites

Additionally, Fig.3.1b illustrates how much the satellite has drifted from its initial position when using Keplerian elements. The initial position is indicated in red, and the final position, marked in green, shows the significant displacement experienced due to the lack of perturbation considerations in Keplerian elements.

All simulations in this study were conducted using BLJ2 elements to ensure consistent and accurate results.

3.2 Design Parameters

This section outlines the key design parameters and variables used in the analysis of task distribution within the satellite network. The parameters encompass orbital characteristics, satellite sensor capabilities, constellation configuration, ground station specifications, and communication details. These variables are crucial in defining the performance and efficiency of the satellite network, particularly in terms of coverage and task distribution. Table 3.1 summarizes these parameters.

Here, T_g is Ground-station Transmitter,
R_g is Ground-station Receiver,
T_s is Satellite Transmitter,
R_s is Satellite Recevier.
These parameters form the basis for simulating and analyzing the satellite network's performance in task distribution, particularly focusing on maximizing coverage and ensuring reliable communication links under different network configurations.

Table 3.1 Parameters

Orbital Parameters	Semi Major Axis (Km)	6878 to 10000
	Inclination (deg)	10 to 108
	RAAN	360 * (i / Planes)
	Eccentricity	0,0000005
Sensor	Fov	2 deg
	Number of sensors on body (Communications)	4 per satellite
	Number of sensors in Zaxis	1 Per satellite
Constellation	Number of satellites	1,5,10,20,30,40,50,100,200,300,400,500,600,700,800,900,1000
	Number of satellites per plane	1 to 1000
	Number of planes	1 to 1000
Groundstation	Number of Groundstations	1, 2, 5
Target	Number of Target location	1
	Region (Km^2)	20446,22
Nodes	Centralized nodes	1, 2, 3, 4, 5, 10
Communication	L1	Uplink
	L2	Downlink
	L3	Crosslink
	Groundstation Antenna Diameter (m)	7,3
	Tg Feeder Loss (dB)	2
	Tg HPA Power (dBW)	14
	Tg Antenna Gain (dBi)	30
	Rg G/T (dB/K)	17
	Rg Feeder Loss (dB)	1
	Frequency (GHz)	2.02-2.40
	Required Eb/No (dB)	10
	Satellite Antenna Diameter (m)	0.1
	Half Beamwidth (deg)	72
	Data Bit Rate (Mbps)	0.125
	Ts Feeder Loss (dB)	1
	Ts HPA Power (dBW)	3
	Ts Antenna Gain (dBi)	6,8
	Rs G/T (dB/K)	2,5
	Rs Feeder Loss (dB)	1
	Polarization Mismatch Loss (deg)	45
	Antenna Mispointing loss (dB)	1

3.2.1 Assumptions

For this study, several assumptions are made: The satellite can transmit and receive data if another satellite is in line of sight. We do not consider any data packet size. Each Satellite is equipped with 4 antennas, broadcasting and receiving signals uniformly in all directions. Additionally, we assume the Satellite has no restrictions in data storage capacity and it has enough power to transmit data at all times. The nadir sensor half angle used is 20 degrees. However, for the simulation of disaster monitoring commercially available sensors optics [24] and S band transceiver [25] were utilized

3.3 Satellites Layout Introduction

First, the centralized layout as shown in Fig.3.5, where a single satellite is capable of communicating with all the satellites in the constellation. In this mode all the other satellites are capable of crosslinking information only to the single satellite (highlighted in yellow) and this satellite is only one capable of downlinking to ground station. However, all the satellites can receive commands (uplink).

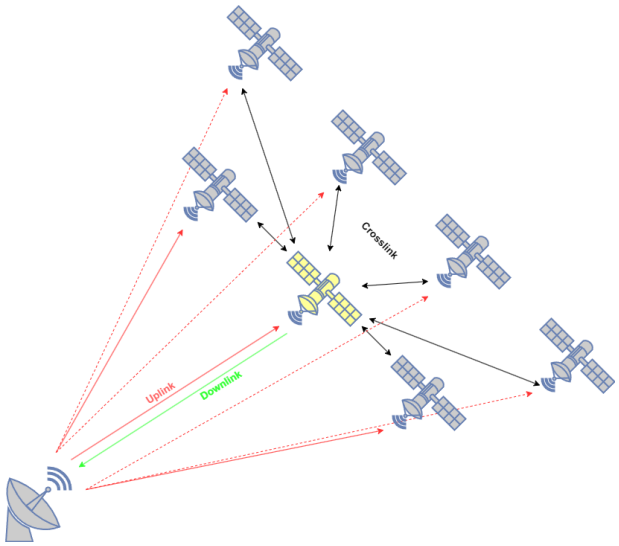

Figure 3.5 Centralized

The decentralized layout as shown in Fig.3.6, where all the satellites can communicate with each other. On top of that they can also downlink data back to ground station. Here all the satellites have same degree of authority.

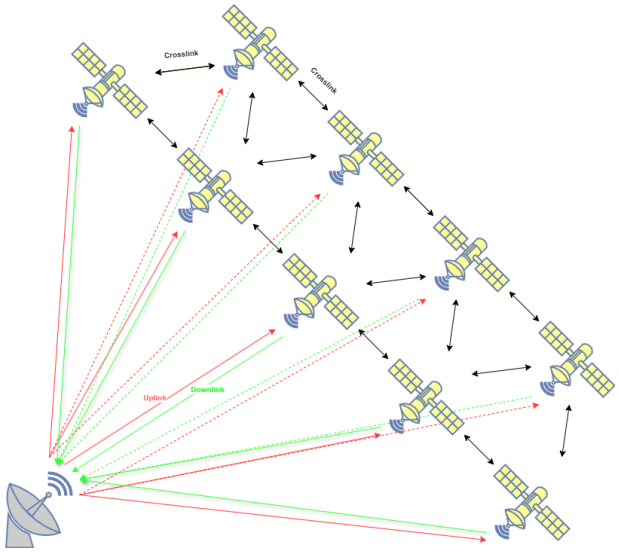

Figure 3.6 Decentralized

The partially centralized layout as shown in Fig.3.7, which is a combination of centralized and decentralized layouts. The only difference here is that all the satellites can communicate with each other. However, only one satellite can downlink to ground station.

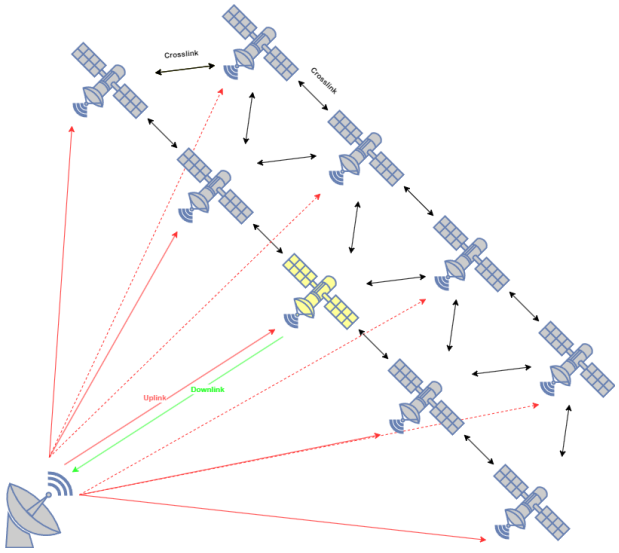

Figure 3.7 Partially Centralized

The Red arrow indicates the uplink from ground stations to satellites, while the Green lines indicate the downlink to ground stations. The Black arrow signifies the crosslink of data between satellites.

3.4 Optimization Objective

The objective of this optimization process is to configure a walker constellation comprising a specified number of spacecraft to achieve optimal coverage of a designated region over the course of a day. The constellation design involves dividing the spacecraft into multiple combinations, each characterized by a certain number of planes and spacecraft per plane. The optimization algorithm adjusts parameters such

as the inclination of the planes and the semi-major axis of the spacecraft [26]. A cost function, based on the semi-major axis, is established to guide the optimization process towards minimizing altitude while maximizing coverage. The optimization algorithm conducts 1000 iterations for each configuration to identify the configuration that achieves the best coverage at the lowest altitude. [26]

In the optimization study, Non Linear Optimizer (NLOPT) will be utilized to perform the optimization tasks.

3.5 Optimizer Set Up

The Fig.3.8 shows the optimization work flow. First, we need to load a region into Freeflyer. Once the region is loaded, we create it and populate points around it. Then, we initialize the constellation by selecting the number of planes and satellites per plane. After that, we choose the optimizer algorithm and run the simulation. The output includes coverage, cost and objective function.

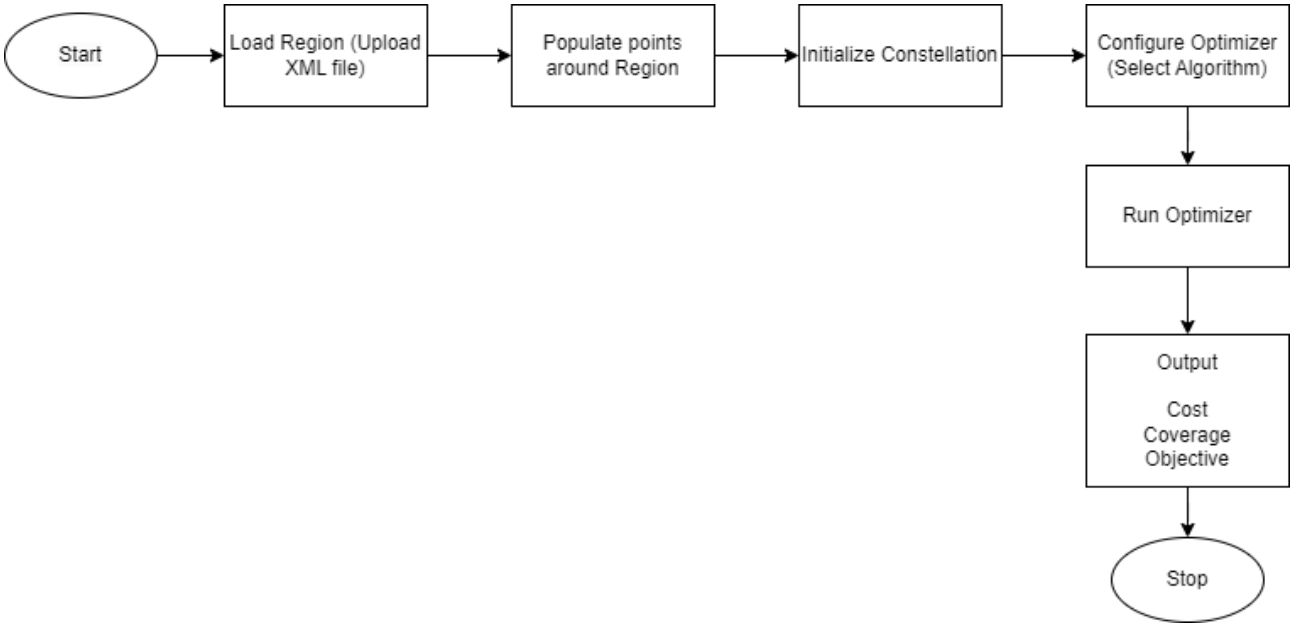

Figure 3.8 Optimization Work Flow

3.5.0.1 Coverage Function

The coverage function measures the proportion of the region covered by the spacecraft. It is defined as:

$$coverage = \frac{n}{N} \tag{3.1}$$

where,

- n is the number of points covered by the spacecraft during the coverage analysis.
- N is the total number of points defined by the point group representing the region.

The coverage value is 1 when the entire region is covered.

3.5.0.2 Cost Function

The cost function is designed to minimize the semi-major axis, thereby ensuring the lowest possible altitude for the spacecraft. The cost function is defined as follows:[26]

$$cost = \frac{(const[0].A - LowerBound)}{(UpperBound - LowerBound) * 2} \tag{3.2}$$

where,

- const[0].A is the Semi major axis of the first satellite in the constellation
- Lowerbound is the lowest value of semi major axis i.e, 6878 km
- Upperbound is the highest value of semi major axis i.e, 10000 km

This function normalizes the semi-major axis value within the defined bounds, ensuring that the cost increases as the semi-major axis increases.

3.5.0.3 Objective Function

The objective function aims to maximize the coverage while minimizing the semi-major axis (altitude). It is defined as:

$$Objective = coverage - cost \tag{3.3}$$

This function seeks to maximize coverage (ideally 1, when the entire region is covered) while minimizing the cost (ideally 0, when the spacecraft are at the lowest possible altitude).

3.5.0.4 Design Variables

The definition of the design variables is essential for adjusting design specifications and evaluating the factors that most significantly affect performance. The most relevant design variables are listed in Table 3.2.

Table 3.2 Design Variables

Design Variable	Description	Range	Unit
$nsats$	Number of Satellites	5 - 1000	-
A	Semi Major Axis	6878 - 10000	km
I	Inclination	10 - 108	degrees

The primary design variable is the number of satellites in the constellation. This variable influences the overall architecture and has a strong impact on the time required to disseminate information among the satellites. Additionally, the semi-major axis and inclination are crucial for optimizing the coverage of the ground station. By carefully adjusting these design variables, the performance and efficiency of the satellite network can be significantly enhanced.

3.5.1 Selection of Region for Optimizer

To effectively analyze the optimizer region for satellite coverage, the focus was on the area around Germany, where the first ground station is located. The objective was to maximize the coverage for this region using different satellite constellations, which is crucial for timely and effective disaster monitoring.

Next the optimizer was run for 5 Satellites which had a total of two combinations which can be seen in the Table. A.1.

Figure 3.9 Optimizer Coverage Region

3.5.2 Optimizer Region analysis

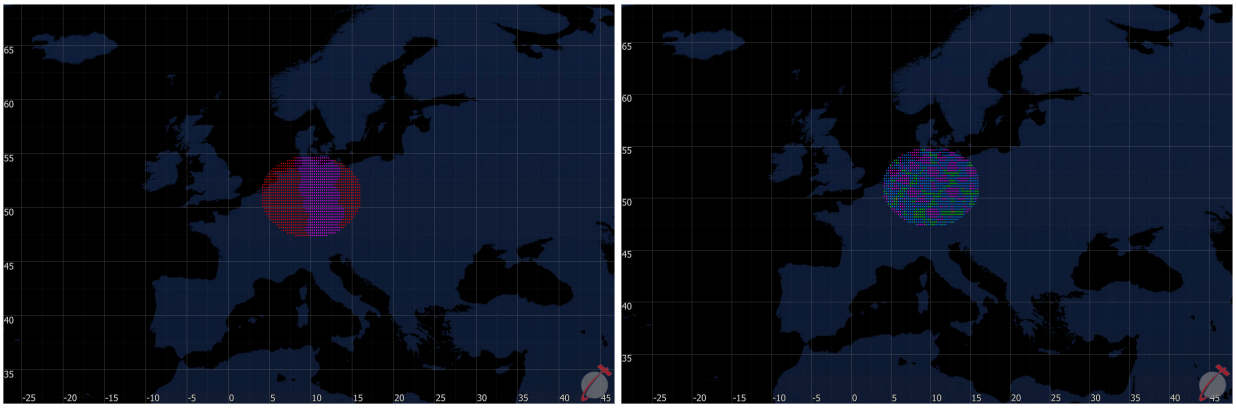

(a) Coverage 5 Satellites **(b)** Coverage 20 Satellites

Figure 3.10 Optimizer Coverage

The coverage analysis is visualized using a color-coded map, as shown in Fig.3.10:

- Red indicates areas where no satellites provided coverage.
- Purple indicates areas that were covered once by the satellites.
- Green indicates areas that were covered twice.
- Blue indicates areas that were covered more than three times
- **Coverage by 5 Satellites**:
  With only 5 satellites, the coverage was limited, with significant areas marked in red, indicating no coverage.
- **Coverage by 20 Satellites**:
  Increasing the number of satellites to 20 significantly improved the coverage. The red areas were drastically reduced, and there were substantial regions in purple, indicating robust and overlapping coverage. This demonstrates the effectiveness of a higher satellite count in ensuring comprehensive coverage.

3.6 Simulation Setup for Disaster Monitoring

The simulation setup for the bushfire monitoring in Australia involved steps to assess the effectiveness of satellite constellations with different configuration, shown in Appendix Table.A.1 are used in providing timely and comprehensive imagery of bushfire-prone regions. With the aim of optimizing disaster response and management efforts, the simulation focused on leveraging satellite technology to enhance situational awareness and facilitate timely decision-making in combating bushfires.

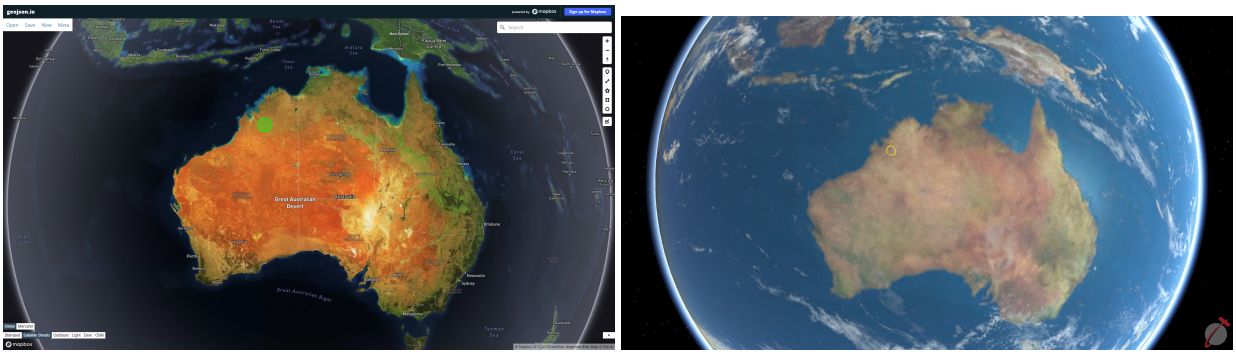

(a) Region with highest bushfires [27] **(b)** Region depicted in Freeflyer

Figure 3.11 Region of Interest

3.6.1 Objective

The primary objective of the simulation was to evaluate different satellite constellation configurations and optimization strategies to minimize the time required for image reception from satellites monitoring bushfire-affected areas in Australia. By optimizing the constellation design and ground station placement, the goal was to expedite the transmission of critical imagery for real-time assessment and response coordination.

3.7 Simulation Set up

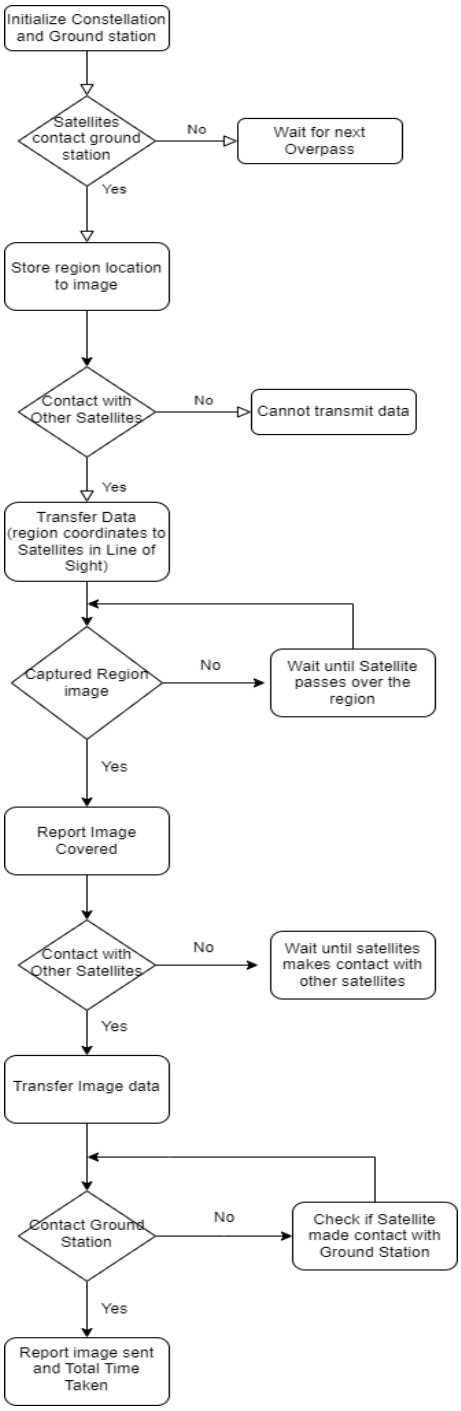

Figure 3.12 Simulation Flowchart

For the disaster monitoring simulation, the steps in the flowchart are as follows: First, I initialise the constellation and ground station. When any satellite makes contact with the ground station, it receives the command to capture the region of interest, specifically the northwestern part of Australia, and stores this data. Satellites not contacting the ground station must wait for the next overpass to receive commands. Satellites that have received commands can crosslink information to others that have not, provided they are in the line of sight. If they are not in the line of sight, the satellites with data cannot transmit information. Once a commanded satellite passes over the region, it captures images. If it is not over the region, it

cannot capture images. However, if it is in line of sight with other satellites that have captured images, other satellites can crosslink the image data. Satellites that receive or capture image data record the time when this occurs. If a satellite contacts the ground station after capturing the image, it downlinks the data; otherwise, it cannot downlink. Finally, once the image is downlinked to the ground station, the total time delay from when the first Satellite received the command is reported.

3.7.1 Region Selection

The simulation was centered around a strategically chosen region in Australia known for its susceptibility to bushfires [28]. This selection was based on historical data and assessments to ensure the relevance and representativeness of the simulation scenario.

3.7.2 Constellation Configuration

A satellite constellation tailored for bushfire monitoring was configured using parameters such as orbital altitude, inclination, and coverage area. These parameters were carefully selected to optimize the constellation's ability to capture high-resolution imagery of bushfire-affected regions with minimal latency.

3.7.3 Ground Station Placement

In this simulation, three distinct ground station configurations were employed to assess their impact on image reception efficiency:

1. **Case 1: One ground station in Neustrelitz [29]**

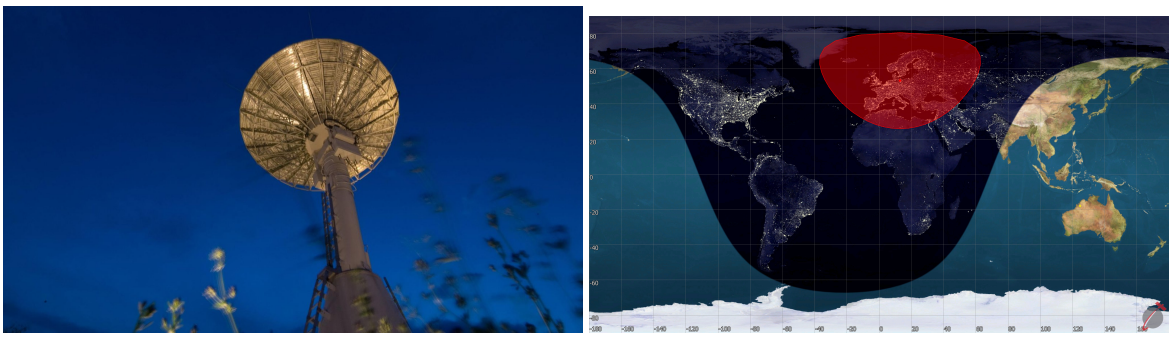

(a) 7.3-metre L- / S- / X-band recieving antenna
Credit: DLR (CC BY-NC-ND 3.0) [30]

(b) Neustrelitz groundstation coverage in Freeflyer

Figure 3.13 Ground station DLR Neustrelitz

- The DLR ground station located in Neustrelitz, Germany, was chosen as the primary ground station for the simulation case.
- Neustrelitz, Germany, situated at 53° 19.779' N, 13° 4.247' E, provides optimal coverage over Europe, making it an ideal choice for mission support.
- The simulation utilized the GSC-X2 (7.3 m) antenna, specifically designed for S-band uplink and downlink operations, ensuring efficient communication with the satellites.

2. **Case 2: Two Ground stations**
    - The simulation scenario involved the utilization of two ground stations: the DLR ground station in Neustrelitz, Germany, and the South African National Space Agency (SANSA) owned HBK-5 ground station located in Hartebeesthoek, South Africa.
    - SANSA HBK-5 positioned at 25°53’13.9"S 27°42’02.5"E, the ground station features a 10-meter S-band and X-band antenna offers a wide frequency range for both receiving and transmitting signals. [31]
3. **Case 3: Five Ground stations across continents**
    - In addition to DLR Neustrelitz, Germany, and SANSA HBK-5, Hartebeesthoek, South Africa, the simulation incorporates three other ground stations strategically positioned across the globe, one in each continent except Australia.
    - Bangalore, India: Operating at a latitude of 13.03° and a longitude of 77.51°, the ground station in Bangalore is equipped with an antenna capable of S-band uplink (2 kW) and both X-band and S-band downlink, enhancing mission support capabilities. [32]
    - Kourou, French Guiana: Located at a latitude of 5.23° and a longitude of 307.2243°, the Kourou S- and X-band station, also known as ’Kourou 93’, boasts a 15-meter dish antenna designed for transmitting and receiving signals in S- and X-band wavelengths, along with comprehensive facilities for tracking, telemetry, telecommand, and radiometric measurements.[33]
    - Vandenberg AFB, California: Positioned at 34º 49’ 21” N and 120º 30’ 07” W, Vandenberg Air Force Base in California operates in the 2025-2110 MHz Band, providing essential support for satellite missions with its strategic location and advanced infrastructure. [34]

3.8 Combination of all Satellites

The complete combination of the Satellites is presented in Appendix Table.A.1 and these satellite combinations were used to run the optimizer simulations.

3.9 Link Budget

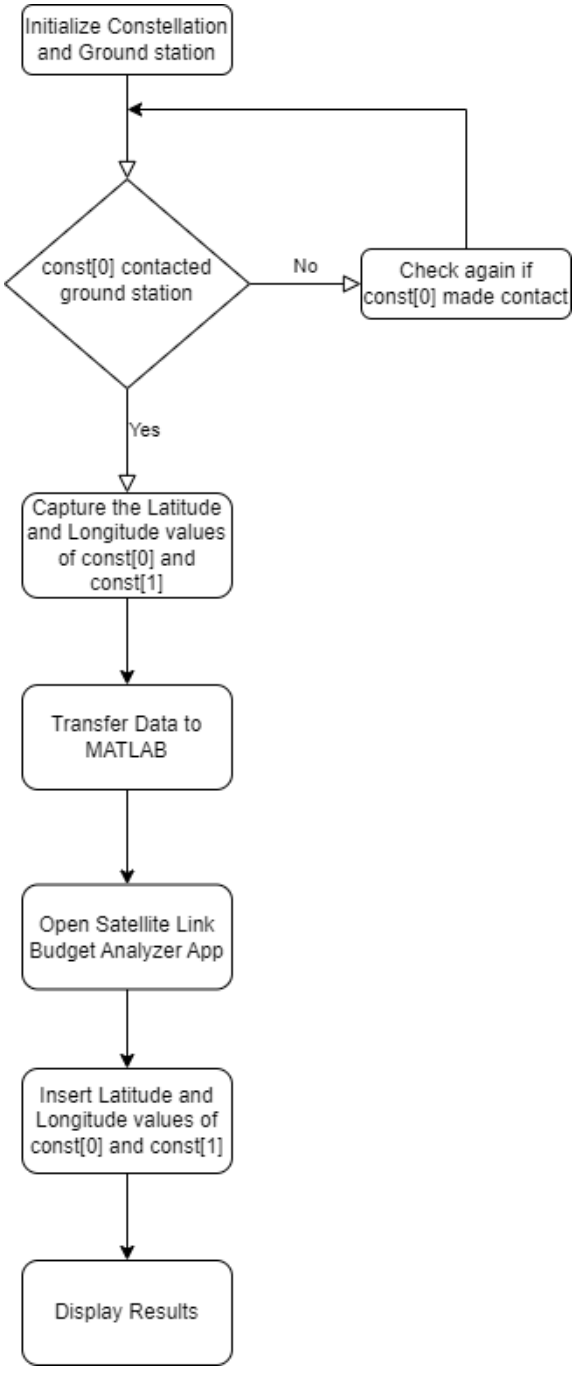

Figure 3.14 Link Budget Analysis

To effectively analyze the communication capabilities of the satellite network, a detailed link budget process is essential. The following flowchart outlines the systematic procedure used to evaluate the link budget. This process begins with the initialization of the satellite constellation and the selection of ground stations. A decision block then checks if the first satellite in the constellation (const[0]) contacts the ground station. If contact is not established, the system continuously checks until a connection is made. Once contact is confirmed, the latitude and longitude of both the first (const[0]) and second (const[1]) satellites are captured. The coordinates are transferred to MATLAB and inputted into the Satellite Link Budget Analyzer

app. The app processes the data and displays the results, such as the available margin (dB) and free space path loss (dB), thereby comprehensively analyzing the link budget.

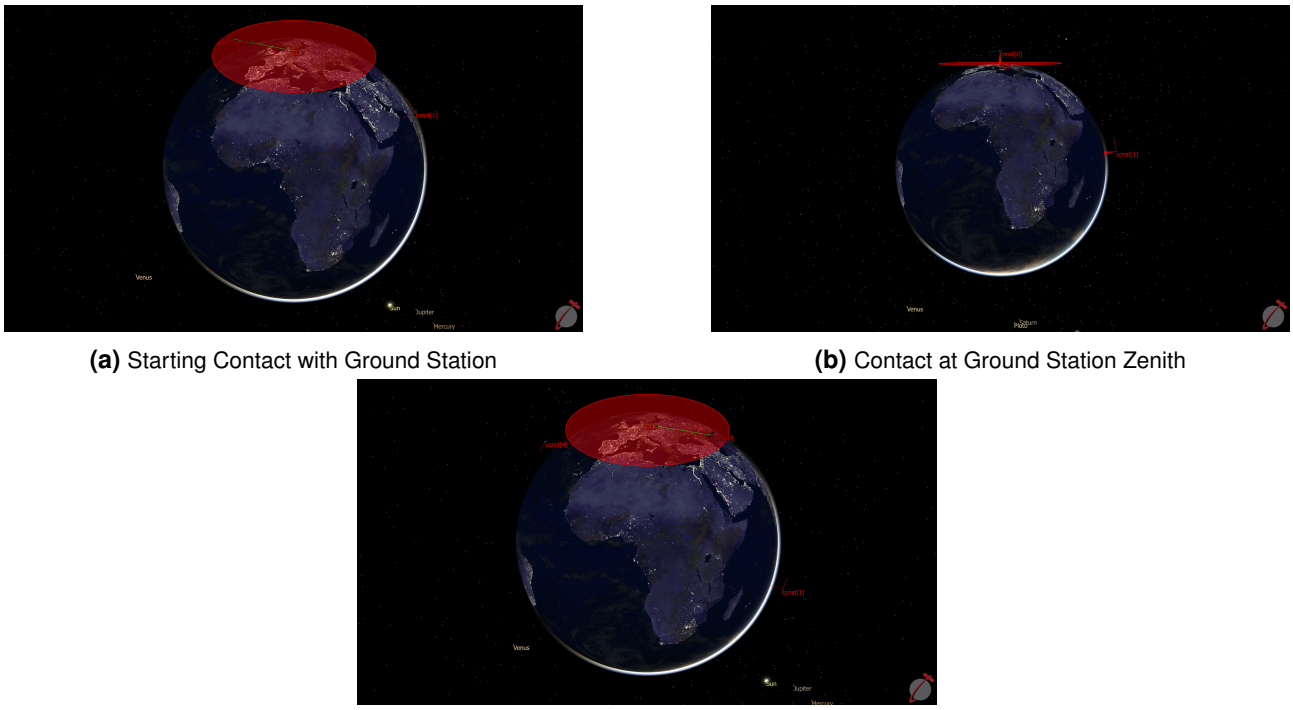

(a) Starting Contact with Ground Station

(b) Contact at Ground Station Zenith

(c) Contact end with Ground Station

Figure 3.15 Satellite contacting Ground Station

Fig.3.15a shows when the satellite initially makes contact with the ground station. It then draws a line to indicate this connection. Fig.3.15b displays the satellite's position directly above the ground station. Finally, Fig. 3.15c illustrates when the satellite's contact with the ground station is about to end.

3.10 Propogation delay in Low Earth Orbits (LEO)

3.10.1 Uplink Propagation Delay:

Uplink propagation delay refers to the time it takes for a signal to travel from a ground station to a satellite in LEO. This delay is influenced by the slant range [35], which is the direct distance between the ground station and the satellite. Due to the relatively low altitude of LEO satellites, typically ranging from 200 to 2,000 kilometers above the Earth's surface, the uplink delay is generally short, often in the range of a few milliseconds. The propagation delay (T_{uplink}) can be approximated by:

$$T_{uplink} = \frac{D}{c} \tag{3.4}$$

where,
D is the slant range and c is the speed of light (approximately 300,000 kilometers per second).

3.10.2 Downlink Propogation Delay:

Downlink propagation delay is the time it takes for a signal to travel from the satellite back to a ground station. Similar to the uplink delay, this delay is also dependent on the slant range between the satellite and the ground station. In most scenarios, the downlink propagation delay is approximately equal to the uplink delay because the distance traversed by the signals is similar. The propagation delay $(T_{downlink})$ can be calculated using the same formula as the uplink delay:

$$T_{downlink} = \frac{D}{c} \tag{3.5}$$

3.10.3 Crosslink Propogation Delay:

Crosslink propagation delay occurs when a signal is transmitted from one satellite to another satellite in space. In LEO constellations, satellites often communicate with each other to relay information across the network. The crosslink delay is influenced by the distance between the two satellites, which can vary significantly depending on their relative positions within the constellation. For LEO satellites, this distance can range from a few hundred to several thousand kilometers. The propagation delay $(T_{crosslink})$ can be expressed as:

$$T_{crosslink} = \frac{D_{sat-sat}}{c} \tag{3.6}$$

where,
$D_{sat-sat}$ is the distance between the two satellites.

3.10.4 Slant Range for LEO Satellites

Illustrated in Fig.3.16a is the fundamental geometry between a LEO satellite and a ground station. The satellite (SAT) and ground station (P) represent two points, with the Earth's centre being the third point. The subsatellite point (T) denotes the intersection point of the line joining the satellite and Earth's centre with the Earth's surface. The slant range (d) is the distance between the satellite and the ground station and changes over time due to the satellite's swift movement above the ground station. In Fig. 3.16a, the radius (r) is calculated as:

$$r = R_E + H \tag{3.7}$$

where, RE = 6378 km is Earth's radius and H is LEO satellite's altitude Point P signifies the tangent plane to Earth's surface at point P, essentially forming the ideal horizon plane. The angle formed between the ideal horizon plane and the slant range is referred to as the elevation angle (ϵ_0). When the triangle from Fig. 3.16a is projected onto a plane, it resembles Fig.3.16b.[36]

Two sides of this triangle are commonly known: the distance from the ground station to Earth's center (R_E) and the orbital radius. The angle at which the satellite views the ground station is termed the nadir angle. This triangle encompasses four variables: the elevation angle (ϵ_0), nadir angle (α_0), central angle (β_0), and slant range (d). Once two quantities are known, the equation for slant range (d) can be written as:

$$d = R_E \left[\sqrt{\left(\frac{H + R_E}{h} \right)^2 - cos^2 \epsilon_0} - sin\epsilon_0 \right] \tag{3.8}$$

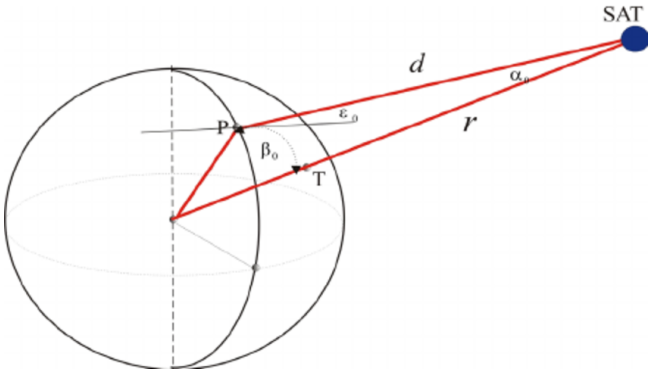

(a) Ground Station Geometry [36]

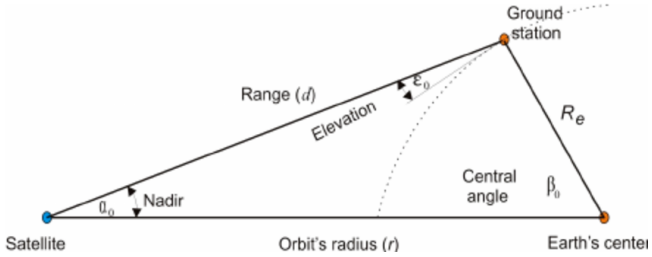

(b) Ground Station Geometry plane [36]

Figure 3.16 Ground Station Geometry

In our case one can simply the calculation as the minimum possible distance occurs when the satellites is exactly in Zenith of the ground station, i.e $d = h$.

Given an orbit altitude ranging from 200 to 1000 km for a LEO orbit [Brown, 1992], and a propagation velocity of c = 300,000 km/s, this leads to a maximum propagation delay of 13 ms and a minimum propagation delay of 3 ms, correspondingly. In our case a propogation delay of 20 ms was used for both Uplink and Downlink cases, whereas for crosslink a delay of 5 ms was used.

4 Results

Chapter 4 addresses research questions 2 in section 4.6, and research question 3 in section A.8.1 by examining ground station contact optimization and its impact on satellite communication efficiency, as well as investigating the benefits of adding ground stations to satellite networks. It begins with the fundamentals of initial ground station contact and progresses into optimizing contact time, comparing total contact time and coverage percentage improvements. The chapter provides a detailed comparison of optimization methods, including various satellite combinations and their results. It also explores the selection of the best algorithms for optimization and their application in coverage enhancement. Further sections analyze total time delays across different ground station densities and configurations, the influence of additional central nodes, and the distribution of tasks among satellites and ground stations. Additionally, it investigates how the addition of one or more ground stations can enhance task distribution efficiency and network performance. The detailed Link analysis is shown in AppendixA.9. The findings are crucial in understanding and improving the efficiency of satellite-ground station interactions, thereby addressing the research questions effectively.

4.1 Initial Contact with Ground Station

The Fig.4.1 and 4.2 illustrate the relationship between satellite inclination and two key metrics: coverage percentage and total contact duration for initial contact with a ground station located in Neustrelitz, as shown in Fig.3.13. The data is plotted for different satellite configurations at two different altitudes (6878 km and 6978 km) with combinations of 5 satellites in varying planes. Combination 1 has 1 plane with 5 satellites per plane, in combination 2 there are 5 planes and only 1 satellite per plane.

Total Contact Duration vs. Inclination

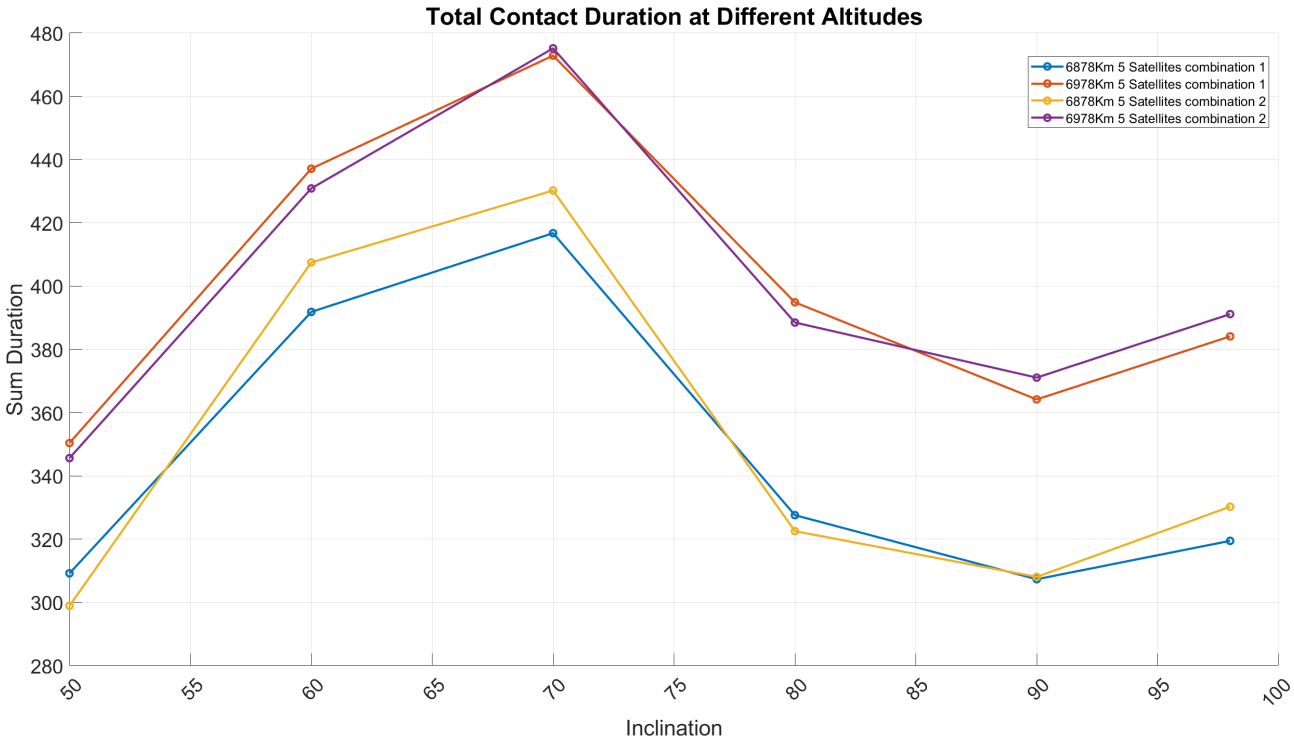

Figure 4.1 Initial Contact Time

Total contact duration generally increases with inclination up to a certain point before decreasing sharply at higher inclinations (especially around 80° and 100°) as seen in Fig.4.1.Fig.4.1 describes the relation between Inclination in the X axis and total contact duration in the Y axis. Configurations at 6978 km altitude tend to exhibit longer contact durations compared to those at 6878 km. For example, at 6978 km, combination 1 shows a peak total contact duration of 472.88 minutes at a 70° inclination, whereas at 6878 km, the peak is 430.23 minutes at the same inclination with combination 2. Most configurations peak in total contact duration around 60° to 70° inclinations. This trend can be attributed to the optimal orbital paths at these inclinations, which maximize the duration satellites spend within the ground station's line of sight.

Coverage Percentage vs Inclination

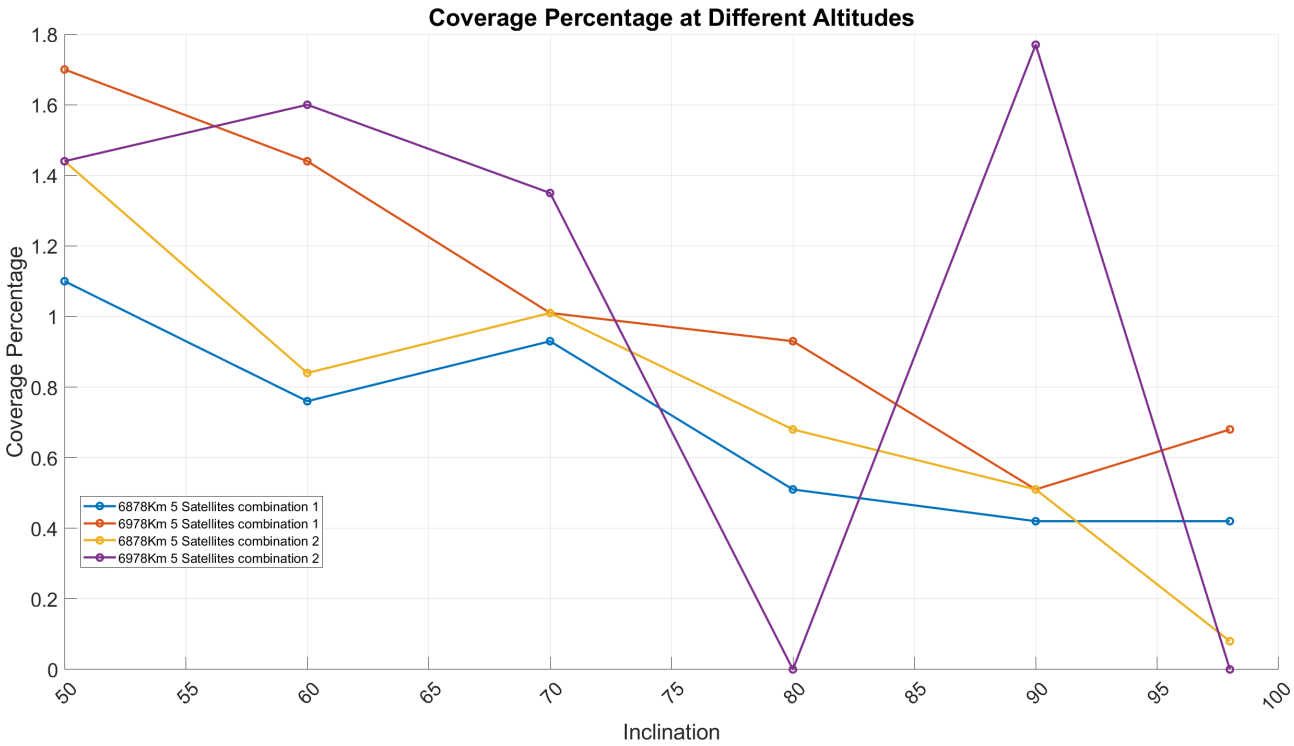

Figure 4.2 Coverage Percentage Vs Inclination

The Fig.4.2 describes the relation between Inclination in the X axis and Coverage percentage in the Y axis. The coverage percentage generally decreases as the inclination increases, with some fluctuations due to the orbital geometry and ground station location. Significant drops in coverage percentage are noted at higher inclinations (near 80° and 100°), particularly at 6978 km with the second combination as seen in Fig.4.2. For example, at 6978 km, combination 2 shows a coverage percentage of 1.6 % at a 60° inclination, which then drops to 0 % at an 80° inclination. These fluctuations occur because satellites at lower inclinations maintain more consistent coverage over equatorial regions, leading to higher and more stable coverage percentages. As inclination increases, orbits become more polar, reducing contact frequency and duration with the mid-latitude ground station, causing the observed variability.

It is important to achieve higher coverage at the lowest altitude, and this is only possible through optimization analysis, as described in section 3.4. Additionally, the results of the optimization versus the initial analysis are compared and presented in section 4.2.

4.2 Optimization of Ground Station Contact Time

The Fig.4.3 compares the total contact durations for initial satellite configurations versus optimized configurations. Solid lines represent the initial configurations, while the optimized configurations are represented by markers (squares and diamonds).

4.2.0.1 Total Contact Time Optimizer vs Initial

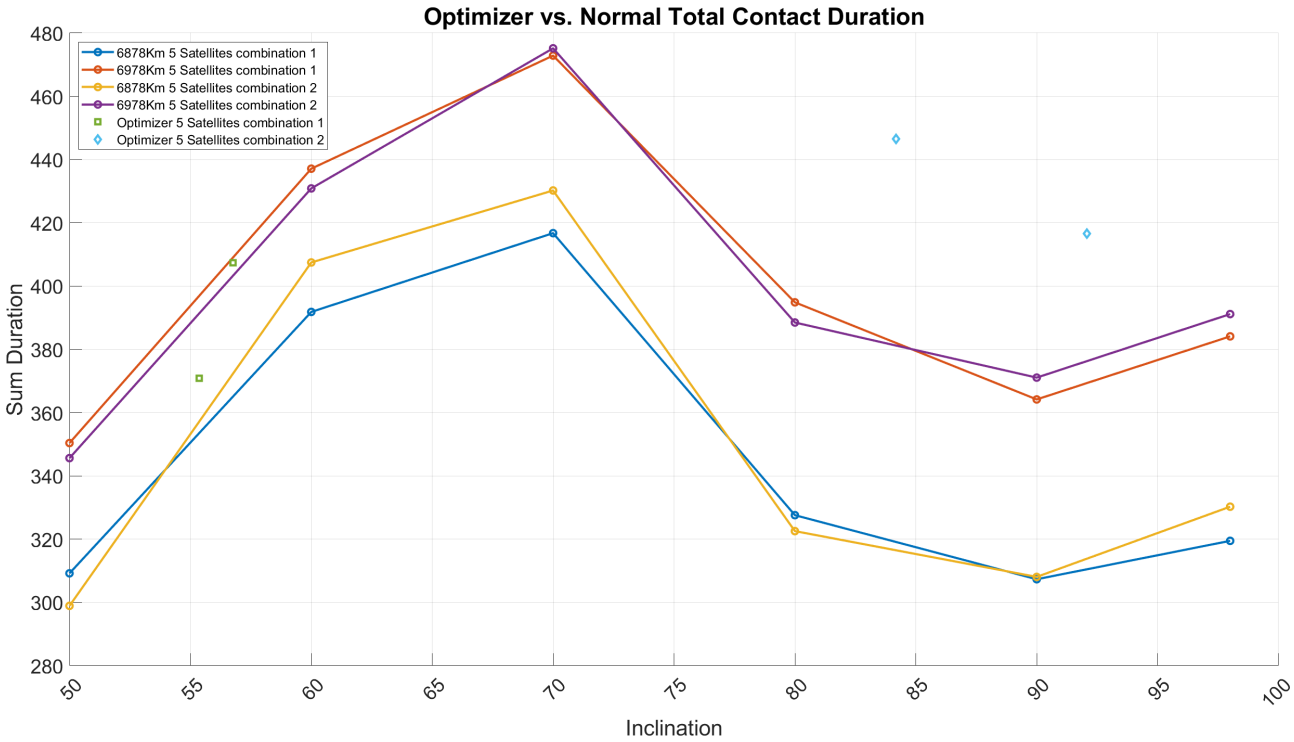

Figure 4.3 Total Contact Time Optimizer Vs Initial

The initial configurations show a similar pattern as illustrated in Fig.4.1, with contact durations increasing up to mid-range inclinations (60° to 70°) before decreasing at higher inclinations. This pattern is influenced by the orbital dynamics, where mid-range inclinations provide more frequent passes over the ground station located at 53° N latitude, thus increasing the contact duration. At higher inclinations, the orbits become more polar, resulting in fewer opportunities for the satellites to be in the line of sight of the ground station, leading to decreased contact durations.

The optimized configurations, plotted for the same inclinations, show slight improvements in contact durations at higher inclinations. For instance, combination 1 optimized at 56.761° inclination shows a sum duration of 407.43 minutes and a coverage percentage of 1.86%, which is higher than the initial configuration at 60° with a sum duration of 391.84 minutes and a coverage percentage of 0.76%. Similarly, combination 2 optimized at 84.18° inclination shows a sum duration of 446.50 minutes and a coverage percentage of 1.44%, compared to the initial 80° configuration with a sum duration of 322.5 minutes and a coverage percentage of 0.68%. These improvements are due to the optimization process, which likely fine-tunes the orbital parameters to enhance contact opportunities with the ground station. However, despite these improvements, the total contact duration was still low compared to the initial configuration for particular inclinations, indicating that while optimization can enhance performance, the inherent limitations of the orbital geometry and the specific latitude of the ground station still play a significant role.

4.2.0.2 Coverage Percentage Optimizer vs Initial

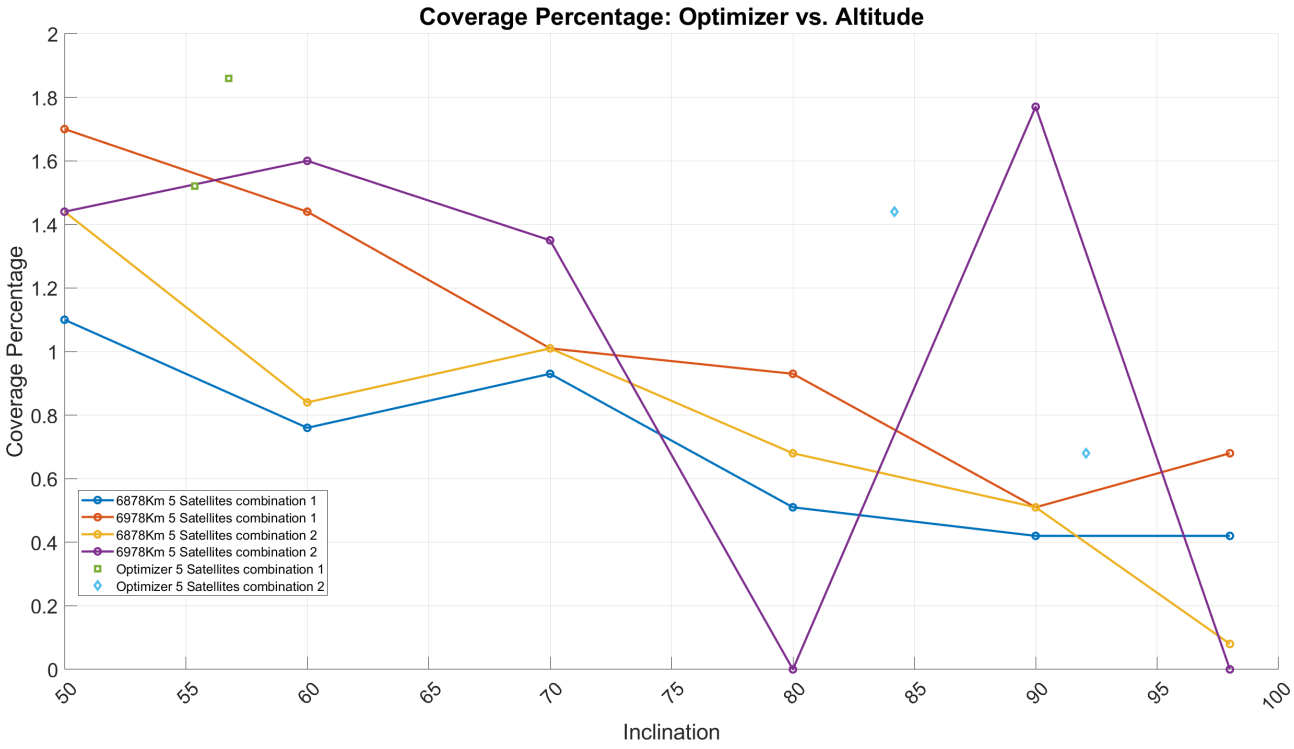

Figure 4.4 Coverage Percentage Optimizer Vs Initial

The coverage percentage was found to be highest for the optimized configurations, reaching up to 1.86% in combination 1 at a 56.76° inclination as seen in Fig.**??**. Despite the relatively moderate contact time of around 407 minutes, this performance is achieved at a lower altitude than the initial configurations. For example, combination 1 optimized at 56.76° inclination shows a sum duration of 407.43 minutes and a coverage percentage of 1.86%, significantly higher than the initial 60° configuration with 391.84 minutes and 0.76% coverage. Similarly, combination 2 optimized at 84.18° inclination achieves a sum duration of 446.50 minutes and a coverage percentage of 1.44%, compared to the initial 80° configuration's 322.55 minutes and 0.68% coverage. The optimization process effectively enhances the contact duration and coverage, particularly at the critical mid-range (50° to 60°) inclinations, by fine-tuning the orbital parameters to improve the satellite-ground station interaction. These enhancements demonstrate the potential of optimization to achieve better performance even with the inherent limitations of orbital geometry and ground station latitude.

Although the contact duration is higher for the initial conditions, the coverage percentage achieved with the optimizer is significantly better. Given that our objective is to maintain the lowest possible altitude while maximizing coverage, it makes sense to implement the optimizer. The optimized configurations not only enhance the coverage percentage but also ensure that the altitude remains as low as possible, thereby meeting the primary goal effectively.

4.3 Comparison of Optimization Methods

In this section, we evaluate 44 different NLOPT optimization algorithms to determine their effectiveness in maximizing coverage at the lowest possible altitude for satellite networks with two distinct configurations. The first configuration consists of a single plane with five spacecraft, while the second configuration features five planes with one spacecraft per plane shown in Appendix section A.2.1. This comparative analysis aims to identify the most efficient algorithms for both centralized and decentralized approaches to task distribution.

Each optimization algorithm is tested and their performance is assessed based on their ability to maximize coverage at the lowest altitude. After thorough evaluation, the top two algorithms are selected for their superior performance. These chosen algorithms demonstrate the highest efficiency and reliability in achieving extensive coverage while maintaining low operational altitudes. By identifying and focusing on these top-performing algorithms, we can enhance the operational efficiency and effectiveness of satellite networks, ensuring optimal task management and data transfer in both centralized and decentralized settings.

The selection of best optimizer is further discussed in detail in section.4.4.

4.3.1 Non Linear Optimizer 5 Satellites Combination 1 Results

In this section, we present the results of the Non-Linear Optimizer for different satellite configurations. Each subsection contains graphs that illustrate the performance of the optimizer across various parameters. The graphs are structured as follows:

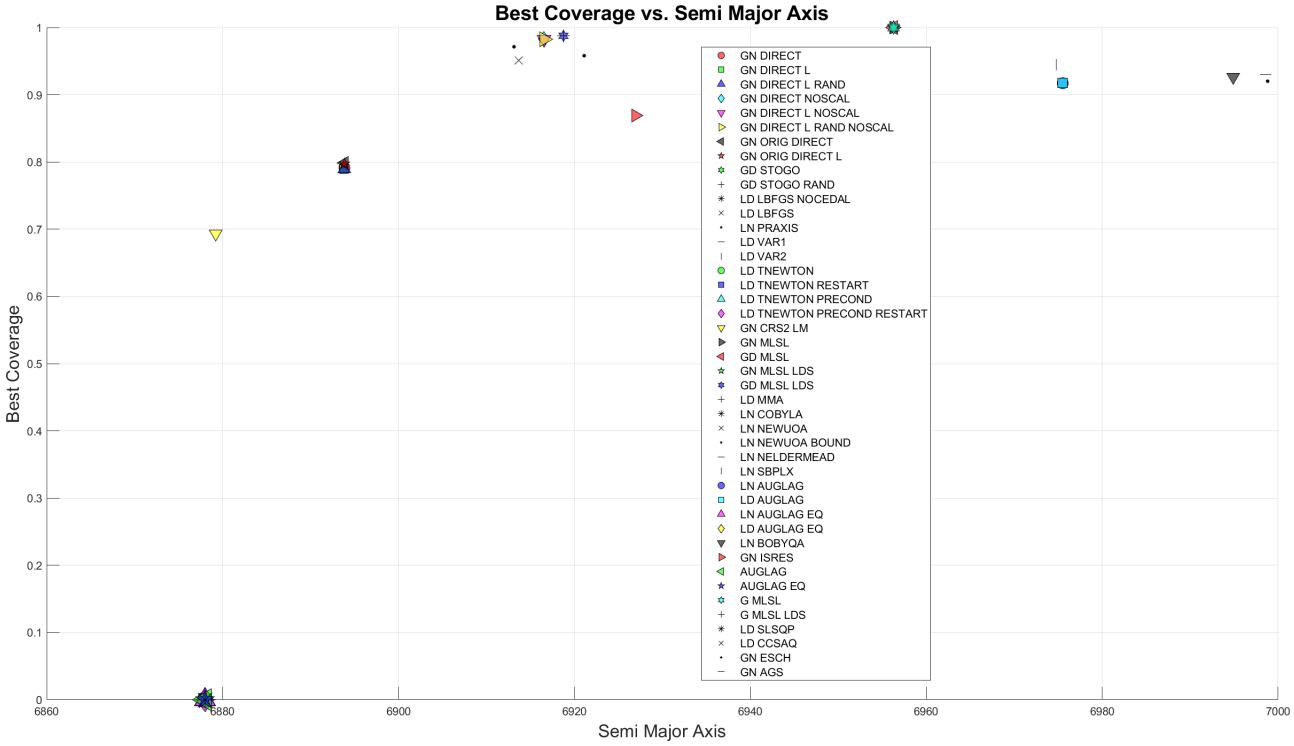

Figure 4.5 Best Coverage Vs Semi Major Axis

Best Coverage Vs Semi Major Axis: The Fig.4.5 shows how the best coverage achieved varies with different values of the semi-major axis.
Certain algorithms, like GN DIRECT NOSCAL, GN DIRECT L NOSCAL, and GN DIRECT L RAND NOSCAL, achieve impressive coverage fractions of 0.9826 at a semi-major axis of 6916.54 km. This indicates that these algorithms excel at optimizing satellite coverage at specific orbital altitudes. Algorithms such as GN MLSL, GD MLSL, GN MLSL LDS, and G MLSL achieve perfect coverage (1.0) at a semi-major axis of 6956.28 km, demonstrating their remarkable ability to maximize coverage at higher semi-major axes. In contrast, some algorithms, including GD STOGO, LD LBFGS NOCEDAL, and LN AUGLAG EQ, consistently show zero coverage at a semi-major axis of 6878 km, highlighting their limitations for this optimization problem.

Notably, the LN BOBYQA algorithm reaches high coverage fractions (above 0.92) at semi-major axes around 6994.89 km, suggesting its effectiveness at higher altitudes.

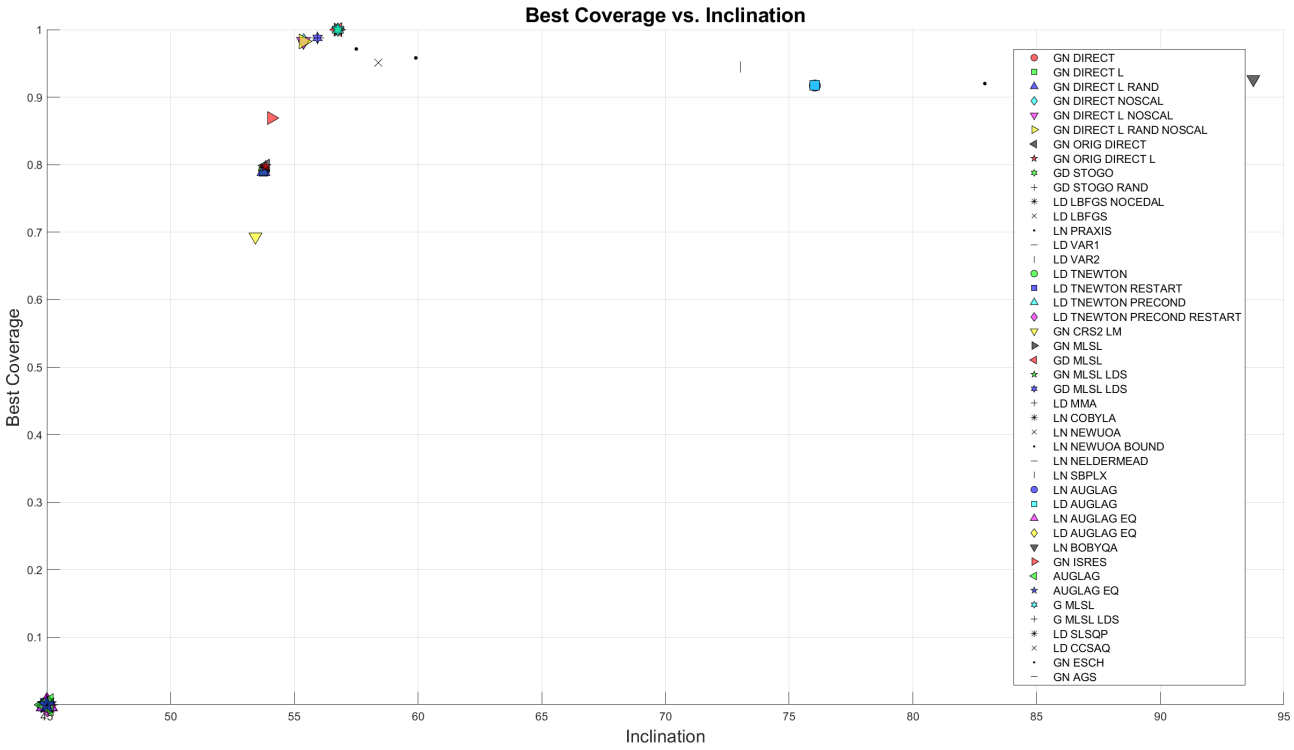

Figure 4.6 Best Coverage Vs Inclination

Best Coverage Vs Inclination: The Fig.4.6 illustrates the relationship between the best coverage and the inclination angle of the satellite orbits.

Some algorithms, like GN DIRECT NOSCAL, GN DIRECT L NOSCAL, and GN DIRECT L RAND NOSCAL, show a high coverage of 0.9826 at an inclination of 55.37 degrees. Other algorithms, like GN MLSL, GD MLSL, and GN MLSL LDS, did better, achieving perfect coverage of 1 at 56.76 degrees. However, algorithms such as GD STOGO, LD LBFGS NOCEDAL, and LN AUGLAG EQ always get zero coverage at 45 degrees, indicating that these algorithms are not well-suited for this optimization. The LN PRAXIS algorithm also got 0.9714 coverage at 57.50 degrees. LN NELDERMEAD, LN SBPLX, LN AUGLAG, LD AUGLAG, LD AUGLAG EQ, and LN BOBYQA had over 0.9 coverage but preferred inclinations between 72-93 degrees.

In short, the maximum coverage was around 54-58 degrees inclination.

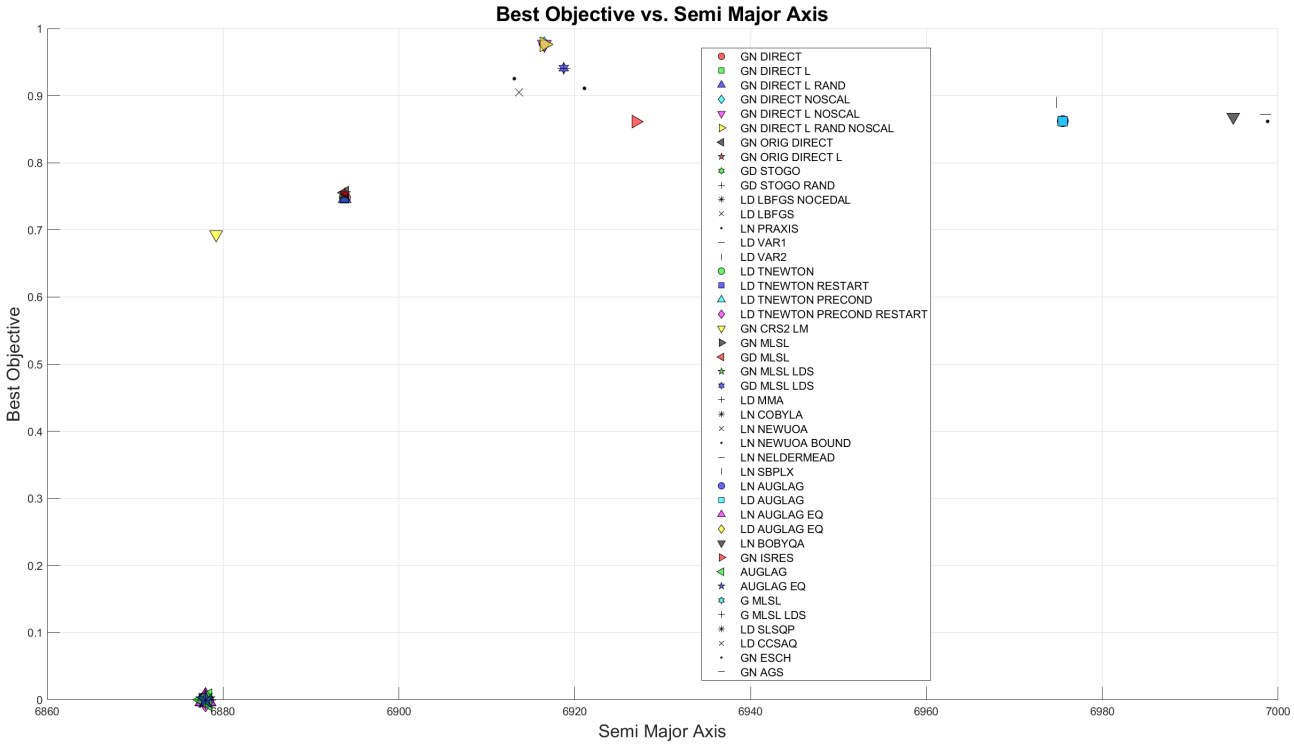

Figure 4.7 Best Objective Vs Semi Major Axis

Best Objective Vs Semi Major Axis: The Fig.4.7 presents how the optimizer's objective value changes with the semi-major axis.

Optimizer algorithms such as GN DIRECT NOSCAL, GN DIRECT L NOSCAL, and GN DIRECT L RAND NOSCAL achieve the highest objective value of 0.9764 at a semi-major axis of 6916.5432 km, indicating superior performance with relatively low orbital altitudes. GN MLSL, GD MLSL, GN MLSL LDS, and G MLSL also perform well with an objective of 0.9476 at a slightly higher semi-major axis of 6956.2773 km. LN PRAXIS stands out with a good balance, achieving an objective of 0.9253 at 6913.132 km.

Poor performers like GD STOGO, LD LBFGS NOCEDAL, and LN AUGLAG EQ consistently show zero objectives at 6878 km, highlighting their unsuitability. Common high-performing algorithms across inclination and semi-major axis analyses include GN DIRECT NOSCAL and its variants, emphasizing their robustness. In contrast, the consistently poor performers underscore the need for careful algorithm selection based on specific optimization goals.

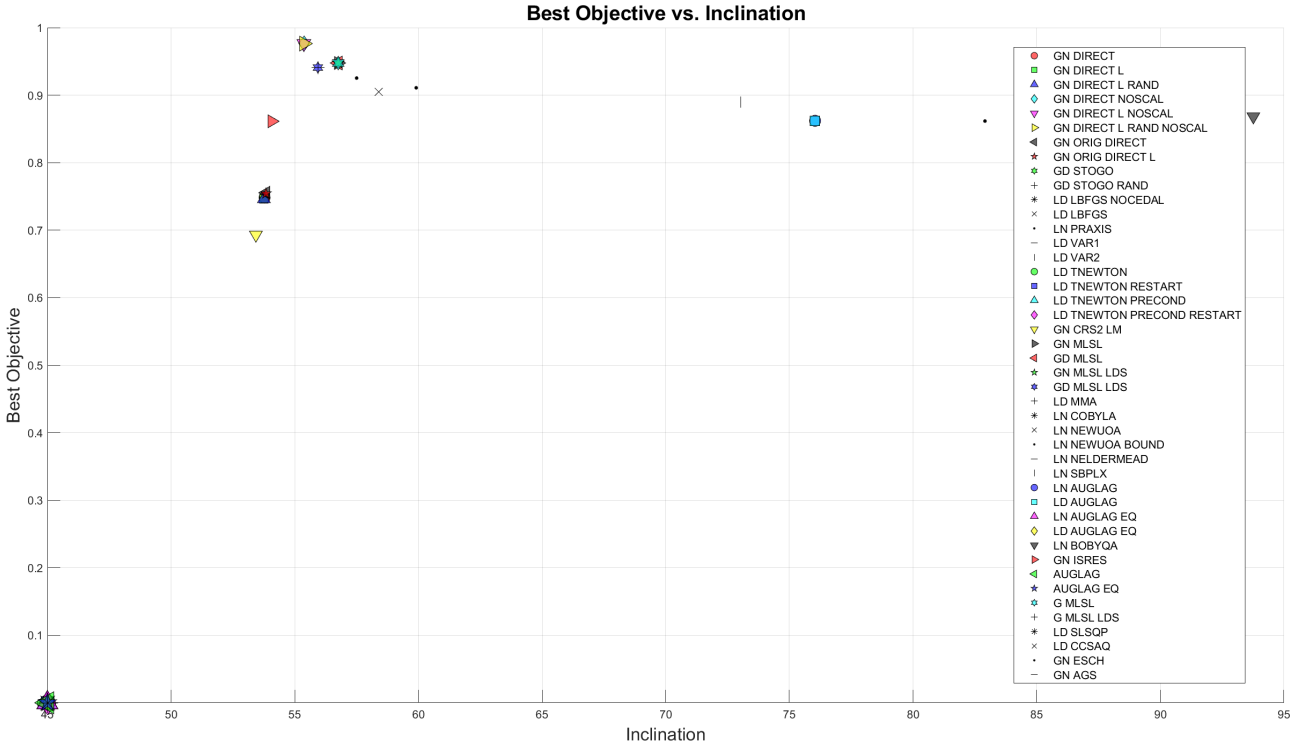

Figure 4.8 Best Objective Vs Inclination

Best Objective Vs Inclination: The Fig.4.8 shows the variation of the optimizer's objective value with the inclination.

GN DIRECT NOSCAL, GN DIRECT L NOSCAL, and GN DIRECT L RAND NOSCAL stand out with the highest objective value of 0.9764 at an inclination of 55.3704°, suggesting they are highly effective for this optimization problem. Other notable algorithms include GN MLSL, GD MLSL, and GN MLSL LDS, each achieving an objective of 0.9476 at a higher inclination of 56.761°. LN PRAXIS also performs well with an objective of 0.9253 at an inclination of 57.5044°. Conversely, algorithms like GD STOGO, LD LBFGS NOCEDAL, and LN AUGLAG EQ consistently show zero objectives at an inclination of 45°, indicating their poor suitability for this optimization task. Common high-performing algorithms across both inclination and semi-major axis analyses include GN DIRECT NOSCAL and its variants, emphasizing their robustness. While high objective values are desirable, balancing these with lower inclinations and semi-major axis is crucial for optimal performance.

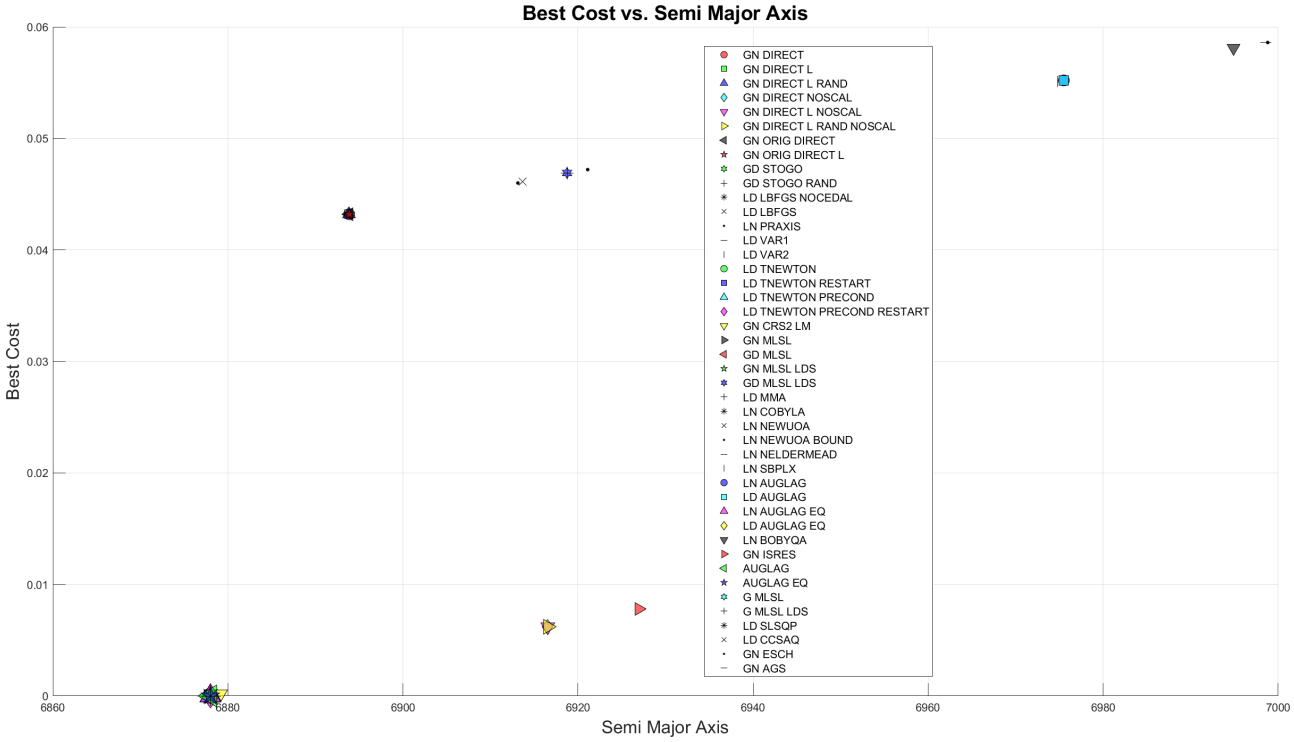

Figure 4.9 Best Cost Vs Semi Major Axis

Best Cost Vs Semi Major Axis: The Fig.4.9 depicts the relationship between the best cost and the semi-major axis.

In this analysis of optimization algorithms, we aim for the lowest possible cost values, indicating greater efficiency. GN CRS2 LM stands out with the lowest non-zero cost of 0.0002 at a semi-major axis of 6879.2175 km. Other high-performing algorithms include GN DIRECT NOSCAL and its variants, all showing a cost of 0.0062 at a semi-major axis of 6916.5432 km, as well as GN ISRES with a cost of 0.0078 at a semi-major axis of 6926.9381 km.

On the other hand, algorithms such as LN NEWUOA BOUND, LN NELDERMEAD, and LN BOBYQA show higher costs around 0.0586 at semi-major axes above 6998 km, indicating lower efficiency. It is important to note that algorithms with zero cost and a semi-major axis of 6878 km, like GD STOGO and LD LBFGS, are likely unsuitable for this optimization problem, as they consistently perform poorly across simulations. Thus, balancing low cost and appropriate semi-major axis is critical for optimal algorithm performance.

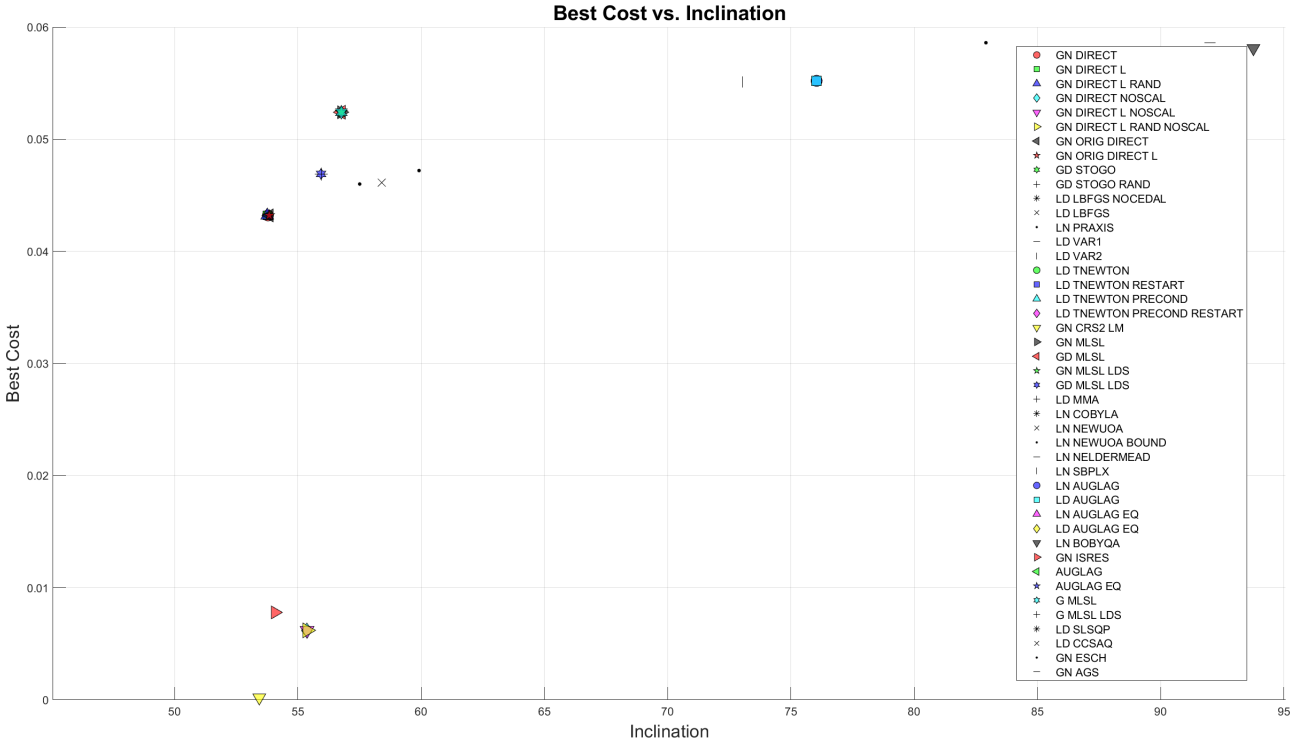

Figure 4.10 Best Cost Vs Inclination

Best Cost Vs Inclination: The Fig.4.10 illustrates how the best cost varies with the inclination.

In evaluating the optimization algorithms based on their cost and inclination, the goal is to find the lowest cost values while avoiding inclinations of 45 degrees, which indicate poor performance. GN CRS2 LM emerges as the top performer with a low cost of 0.0002 at an inclination of 53.4309 degrees. Other notable algorithms include GN DIRECT NOSCAL and its variants, all with a cost of 0.0062 at an inclination of 55.3704 degrees, and GN ISRES with a cost of 0.0078 at an inclination of 54.0708 degrees.

Algorithms such as LN NEWUOA BOUND, LN NELDERMEAD, and LN BOBYQA exhibit higher costs, ranging from 0.0551 to 0.0586 at inclinations above 73 degrees, suggesting lower efficiency. Consistently poor-performing algorithms, like GD STOGO and LD LBFGS, show zero cost at an inclination of 45 degrees, indicating they are unsuitable for the optimization problem.

The detailed table is presented in the Annex Table.A.20

4.4 Selection of Best Algorithms

To determine the most suitable optimization algorithms for maximizing satellite coverage in the region around Germany, initially considered all the algorithms from the Non Linear Optimizer (NLOPT) library, totalling 44 different algorithms [37]. The selection process was conducted in stages, evaluating their performance based on the average coverage provided with different numbers of satellites (5, 10, and 20). This systematic approach allowed to narrow the choices to the top two algorithms.

The evaluation criteria focused on the average coverage efficiency across three satellite constellations: 5, 10, and 20 satellites. The key criterion for selection was the ability to consistently provide high coverage across all satellite numbers. Initially, out of the 44 algorithms, the top 5 were selected based on their performance with 5 satellites as shown in Table. 4.1. These top 5 algorithms were then evaluated with 10 satellites, and the top 4 were chosen. Finally, these top 4 algorithms were assessed with 20 satellites, leading to selecting the top 2 algorithms.

Table 4.1 Selection of Optimizer Algorithm

Type	Satellites / Optimizer	5	10	20
20	GN MLSL	0,68765	0,95985	0,948183
39	G MLSL LDS	0,99335	0,79345	
4	GN DIRECT L NOSCAL	0,73825	0,92765	0,9523
12	LN PRAXIS	0,94175	0,959875	0,943917
2	GN DIRECT L RAND	0,863	0,916175	0,943533

From the Table. 4.1, the two best algorithms were chosen, which were **GN MLSL** and **GN DIRECT L NOSCAL**. Both the Algorithms demonstrated high coverage and consistent performance across all satellite numbers.

4.4.1 Nomenclature

Each algorithm in NLopt is identified by a named constant, which is passed to the NLopt routines in various languages to select a particular algorithm. These constants are mostly of the form **NLOPT(G,L)(N,D)xxxx**, where G/L denotes global/local optimization and N/D denotes derivative-free/gradient-based algorithms, respectively[37].

4.4.2 Type 20 Algorithm

The GN MLSL (Multi-Level Single-Linkage) algorithm is a global optimization method that combines random sampling with local optimization from randomly chosen starting point to find the global minimum [38]. MLSL works in two main phases: global and local.

During the global phase, the algorithm selects locations at random from the search space to explore different regions. In the following local phase, these randomly selected points are refined and improved using specialized local optimization algorithms. A distinguishing feature of MLSL is its clustering heuristic, which intelligently groups locations to minimize duplicate searches in overlapping areas. This technique groups sampled points to ensure that local searches are initiated from diverse regions of the search space, thus improving efficiency and coverage.

The process begins by defining the search space using the ranges of the design variable as shown in Table.3.2, such as inclination angles and semi-major axes, without rescaling them. The algorithm generates a set of starting points either randomly, which ensures a more even distribution across the search space.

These initial configurations undergo a refinement process, where an objective function evaluates their effectiveness in achieving the desired outcome, like maximizing satellite coverage while minimizing altitude. A crucial aspect of the MLSL algorithm is its clustering heuristic, which groups nearby points to prevent redundant local searches and ensure a diverse exploration of the search space. The algorithm iteratively performs global sampling and local optimization. During each iteration, new points undergo local optimization ensuring each local search explores new regions. This process continues until a stopping criterion is met, such as reaching a maximum number of function evaluations or achieving satisfactory optimization.

4.4.3 Type 4 Algorithm

The DIRECT-L NOSCAL algorithm is a method for finding the best solution to optimization problems where different variables are on different scales. Unlike other methods, it doesn't change the scale of the search space. It was created by J.M. Gablonsky and C.T. Kelley [39], building on an earlier algorithm by D.R. Jones, C.D. Perttunen, and B.E. Stuckmann [40]. The DIRECT-L NOSCAL variant is specifically tailored for situations where the search space dimensions should not be rescaled to a unit hypercube.

First, the algorithm defines the search space using the original ranges of the variables, like inclination angles and semi-major axes. It starts by evaluating the objective function at the center of this space.

Initially, the algorithm evaluates the objective function at the center of this search space. It then identifies potentially optimal hyperrectangles based on their size and function values, focusing on those likely to contain the optimal solution.

These areas are then divided into smaller sections along their longest side. It evaluates new points at the centres of these smaller sections to determine if they improve the desired outcome, such as maximizing satellite coverage while minimizing altitude.

The DIRECT-L NOSCAL variant includes a local bias, which pays more attention to areas with promising performance values. This helps the algorithm concentrate on the most promising regions of the search space. This cycle of identifying, dividing, and evaluating continues until a stopping condition is met, such as a maximum number of evaluations or a satisfactory solution. By adapting to different scales and focusing on the best areas, the algorithm is highly effective for solving complex optimization problems.

4.4.4 Application in Coverage Optimization

In satellite coverage optimization, the GN MLSL and DIRECT-L NOSCAL algorithms are essential for adjusting satellite orbits to maximize coverage while minimizing altitude. These algorithms adjust the inclination of orbital planes and the semi-major axes of satellites to find the best configuration.

By combining their respective strengths, these algorithms ensure a thorough and effective optimization process, leading to optimal configurations for satellite coverage at the lowest possible altitude.

4.5 Optimization Results

The optimization results are pivotal in understanding the efficacy of various configurations in satellite networks. By plotting all optimizers from 5 to 1000 satellites, we gain a understanding of the trends driving network performance. The use of optimizers is crucial as it aims to achieve the lowest possible orbit while ensuring optimal inclination and altitude for comprehensive coverage.

All these results presented had the lowest time for task completion, highlighting the efficiency of these configurations in achieving their objectives swiftly.

Specifically, the Type 4 optimizer demonstrates a preference for a 59-degree inclination and a specific altitude of 6878.0264 km after 100 satellites, resulting in complete coverage. Conversely, the Type 20 optimizer adopts a different strategy, favoring a 91.1715 degree inclination and a specific altitude of 6880.4353 km.

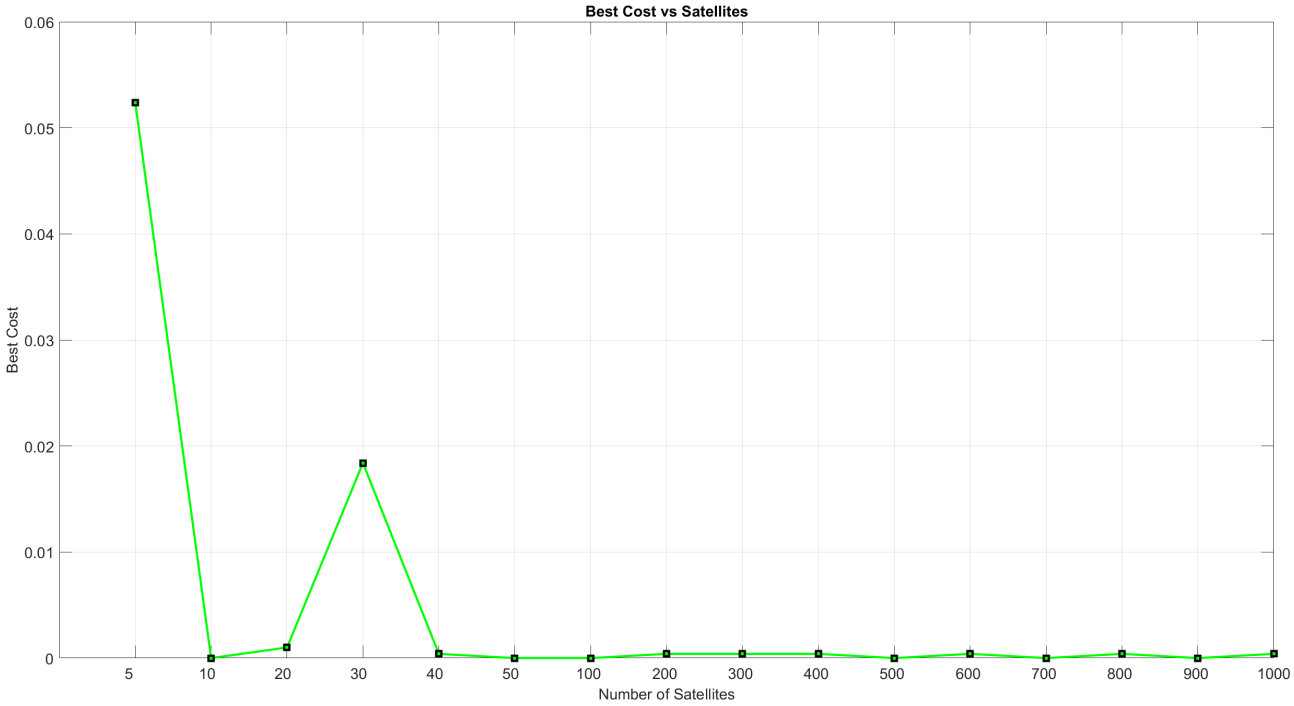

Figure 4.11 Best Cost vs Satellites

Fig.4.11 illustrates the correlation between the number of satellites and the cost values achieved in the optimization process, with the x-axis representing the number of satellites and the y-axis showing the best cost values. Configurations with 10, 50, 100, 500, 700, and 900 satellites achieve the lowest possible cost value of 0. The cost function is designed to minimize the semi-major axis, thereby ensuring the lowest possible altitude for the spacecraft. This indicates that these setups are the most cost-effective at minimizing the altitude. Other configurations, such as those with 20, 40, 200, 300, 400, 600, 800, and 1000 satellites, also exhibit very low-cost values ranging from 0.0004 to 0.001, showing that they are nearly as efficient in maintaining low altitudes.

On the contrary, configurations with 5 and 30 satellites have higher cost values of 0.0524 and 0.0184, respectively, indicating they are less optimal solutions with larger semi-major axes resulting in higher altitudes. The general trend shows that most configurations achieve low to zero cost values, highlighting the optimizer's effectiveness in finding cost-efficient solutions. However, the higher costs for 5 and 30 satellites suggest that these configurations need help optimizing altitude as efficiently as the others. This, in turn, increases the semi-major axis of 5 and 30 satellites, as seen in Fig.4.15

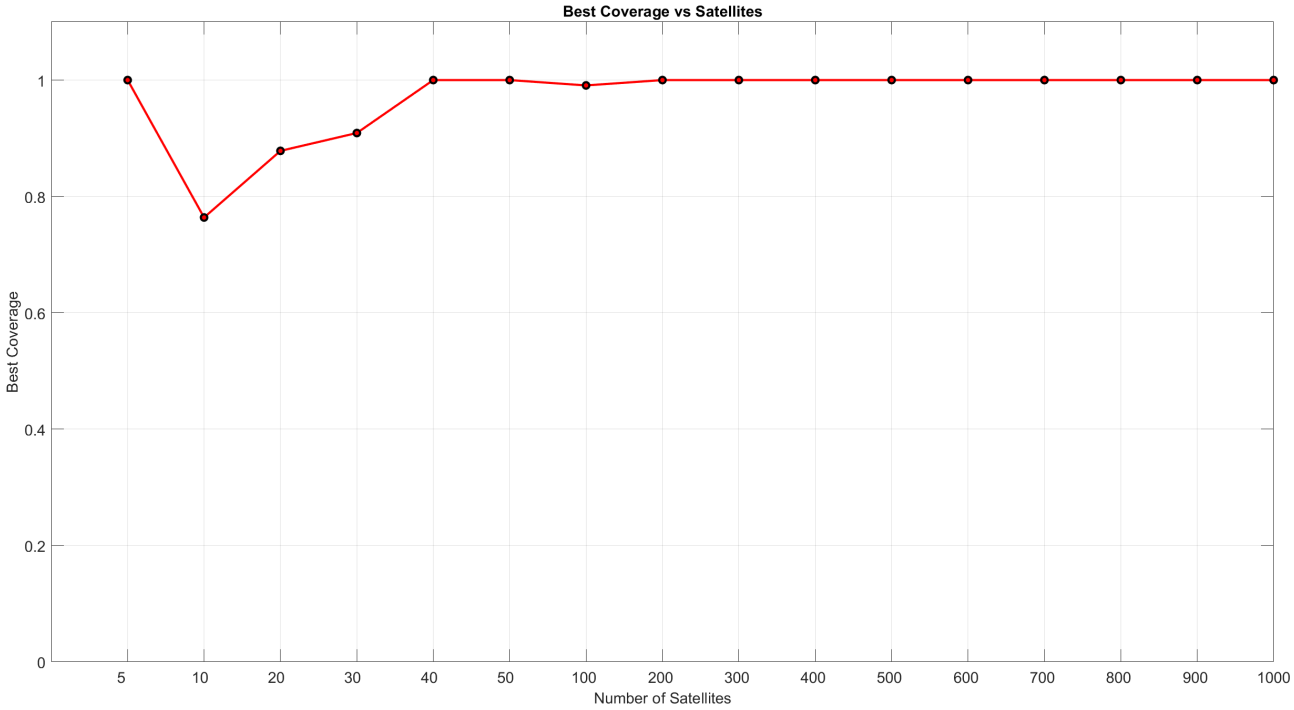

Figure 4.12 Best Coverage vs Satellites

Fig.4.12 illustrates the relationship between the number of satellites and the best coverage fraction achieved in the optimization process, with the x-axis representing the number of satellites and the y-axis showing the best coverage fraction. Configurations with 5, 40, 50, 200, 300, 400, 500, 600, 700, 800, 900, and 1000 satellites achieve a perfect coverage fraction of 1, indicating that these setups can effectively cover the entire target region. This demonstrates the ability of the optimizer to configure constellations that ensure maximum satellite coverage, making these configurations ideal for applications requiring extensive and reliable coverage areas.

Other configurations, such as those with 10, 20, 30, and 100 satellites, show slightly lower coverage fractions of 0.7638, 0.8783, 0.909, and 0.9908, respectively. While these setups do not achieve perfect coverage, they still provide substantial coverage of the target region. The general trend indicates that increasing the number of satellites generally leads to higher coverage fractions, with near-perfect coverage achieved once the constellation includes at least 100 satellites. This trend underscores the effectiveness of the optimization process in maximizing coverage as the number of satellites increases.

For instance, the 10-satellite configuration offered the lowest coverage fraction of 0.7638, which resulted in the lowest delay in task completion, taking only 609.95 minutes. In contrast, a configuration with a maximum coverage of 0.9969 (5 planes and 2 satellites per plane) took 1588.95 minutes to complete the task, more than double the time of the lowest time delay for 10 satellite configurations.

Table A.24 provides detailed data on coverage and time delay.

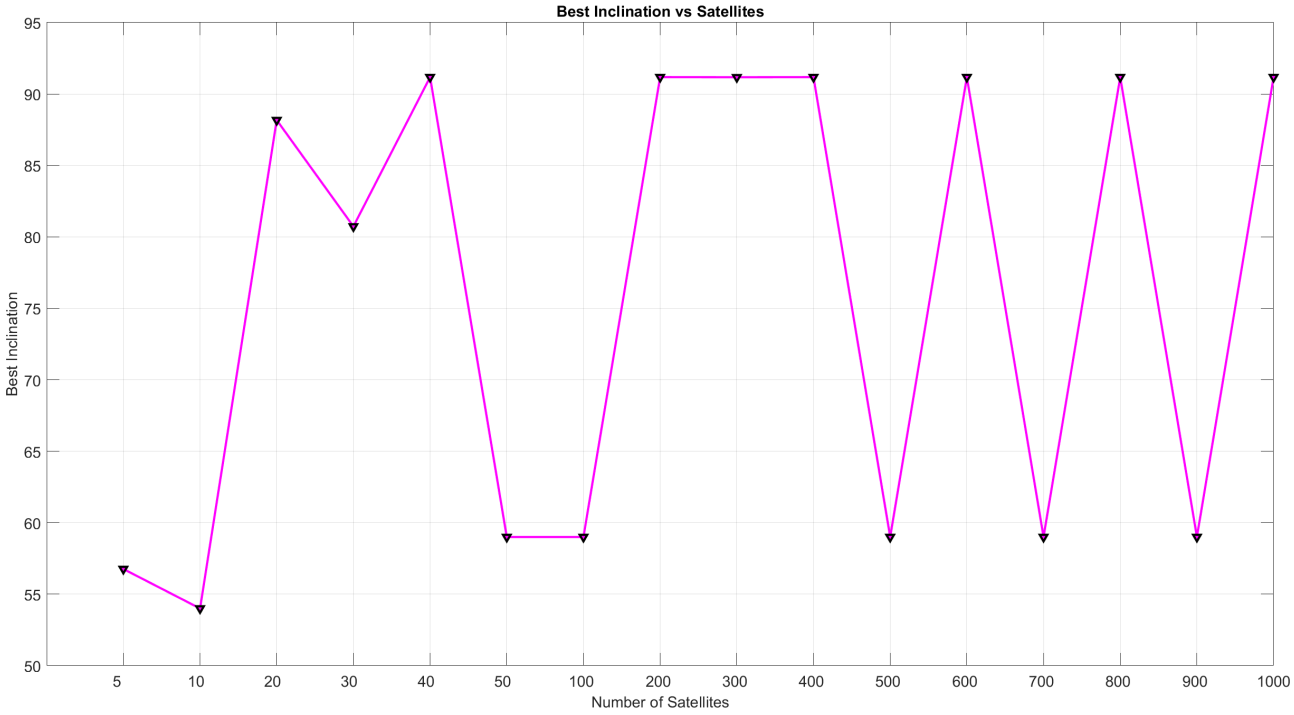

Figure 4.13 Best Inclination vs Satellites

Fig.4.13 shows the relation between inclination and the number of satellites. We can see which inclinations are preferred by which satellites. The type 4 optimizer favours 59 degree inclination with an altitude of 6878.0264 Km for coverage optimization, while the type 20 optimizer prefers a 91.1795 degree inclination at 6880.4353 km.

Configuration with 5,10,50,100,500,700 and 900 satellites show optimal inclinations around 54-59 degrees. In contrast, configurations with 20,30,40,200,300,400,600,800 and 1000 satellites favour inclination of around 88-91 degrees, indicating flexibility and effectiveness in achieving diverse coverage needs.

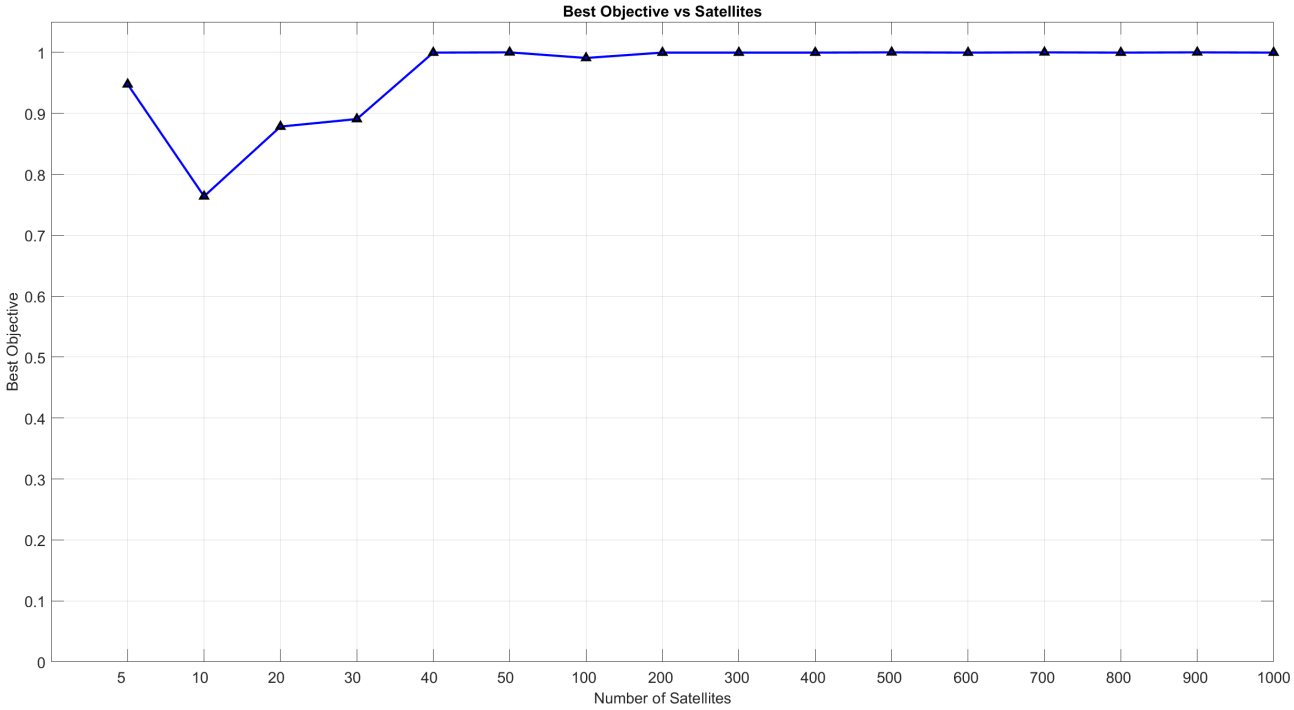

Figure 4.14 Best Objective vs Satellites

Fig.4.14 illustrates the relationship between the best objective value and the number of satellites.

Satellite configurations utilizing 50, 500, 700, and 900 satellites achieve a perfect objective value of 1, signifying that these setups are the most optimized. Other configurations, such as those with 40, 200, 300, 400, 600, 800, and 1000 satellites, exhibit near-perfect objective values of 0.9996, indicating their highly effective nature.

However, configurations with fewer satellites, ranging from 5 to 30, exhibit lower objective values between 0.7638 and 0.9476, suggesting that while less optimized, they still offer substantial performance. The overall trend demonstrates that increasing the number of satellites leads to higher objective values, reflecting better optimization outcomes.

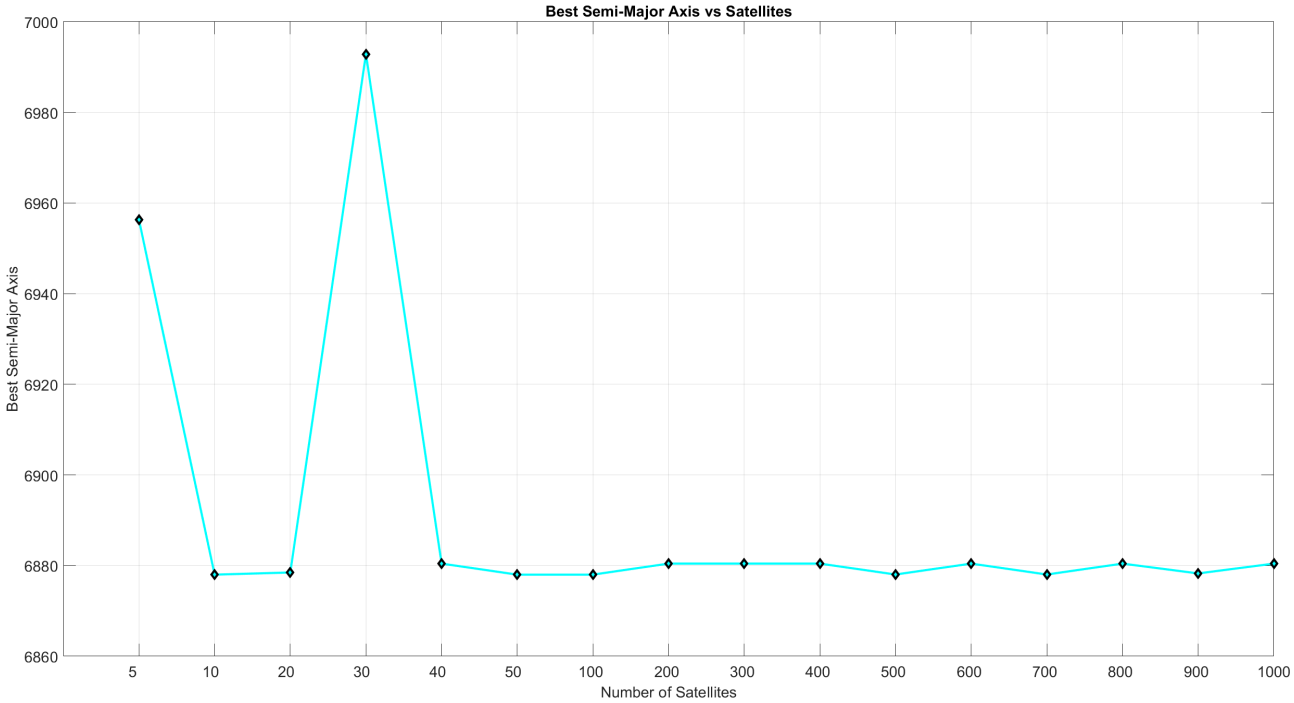

Figure 4.15 Best Semi-major Axis vs Satellites

Fig.4.15 shows the relation between the best semi-major axis and the number of satellites.

Configurations with 10, 50, 100, and 500 satellites show a consistent semi-major axis around 6878 km, indicating a preference for this altitude to optimize performance. Similarly, configurations with 20, 200, 300, 400, 600, 800, and 1000 satellites show optimal values around 6880.4353 km, suggesting a stable and effective orbital altitude for these setups. For configurations with 5 and 30 satellites, the Type 20 optimizer demonstrates unique characteristics.

The configurations with 5 and 30 satellites have slightly different orbital parameters, with semi-major axes of 6956.2773 km and 6992.8564 km, respectively. Despite these variations from the typical semi-major axis of 6880.4353 km and inclination of 91.1795 degrees, both setups manage to minimize the delay time. This flexibility demonstrates the optimization process's ability to find optimal solutions across a range of satellite numbers and orbital characteristics, ensuring low-latency communication.

4.6 Total Time delay

Understanding the total time delay in satellite networks is crucial for optimizing the performance of various network configurations. This section analyzes the total time delay associated with decentralized, centralized, and partially centralized network configurations across different numbers of satellites and ground stations. The analysis covers one, two, and five ground station scenarios, highlighting how the network configuration impacts overall time delay and efficiency in data transmission.

4.6.1 Total Time Delay for One Ground station

4.6.1.1 Total Time taken by One Ground Station

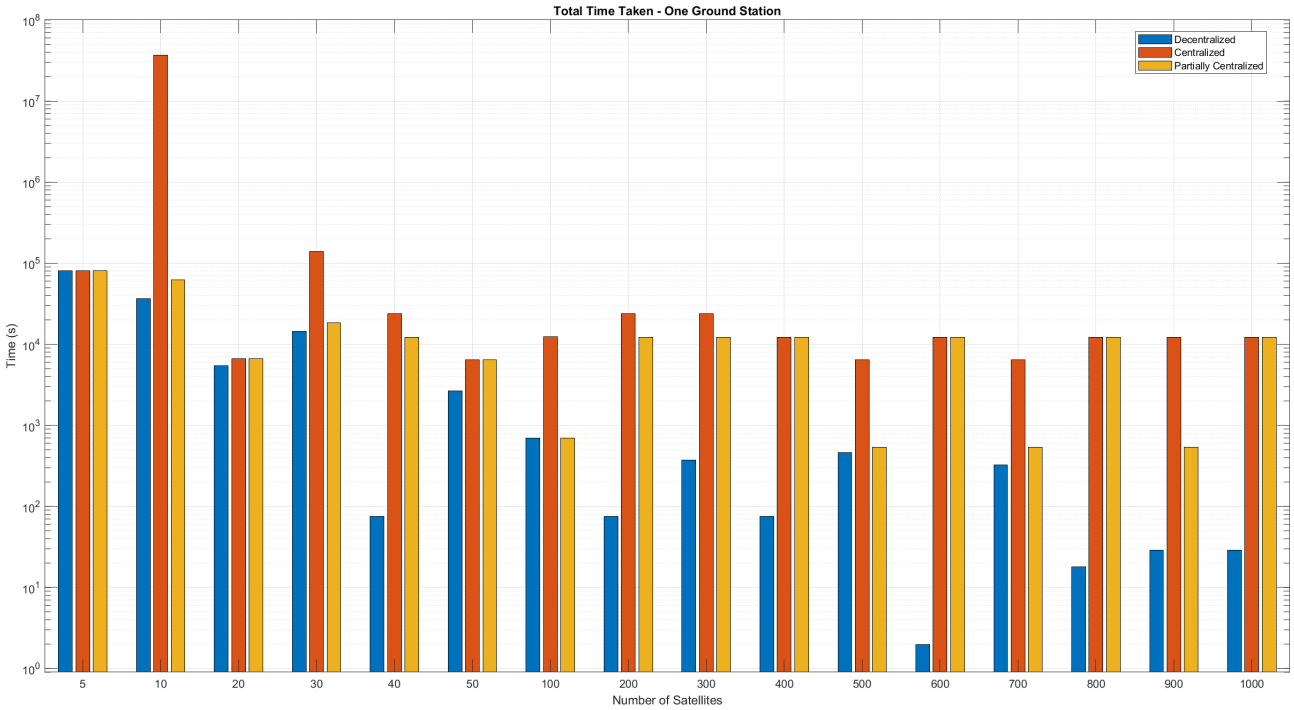

Figure 4.16 Total Time taken One Ground Station

The Fig.4.16 illustrates the total time taken for different configurations of decentralized, centralized, and Partially centralized networks with one ground station.
The x-axis represents the number of satellites, while the y-axis shows the total time delay in seconds.
This plot shows that the **Decentralized** network consistently exhibits the lowest overall delay across various satellite counts. In contrast, the **Centralized** configuration shows the highest delay. Notably, the lowest delay is observed for 600 satellites in the decentralized configuration. This likely results from the optimal placement of satellites, where a satellite was already near the target region when the command to capture an image was issued. Consequently, the image was captured almost immediately.

The Centralized configuration, which involves only one central node with all satellites sending data exclusively to this node, exhibits the highest delay across most satellite counts. This configuration adds complexity and potential delays due to the single point of communication, where all satellites must send data to the central node before it can be downlinked to the ground station. This setup creates a significant bottleneck, resulting in the highest overall time delays.

Additionally, it can be seen that the Centralized configuration has the highest delay for 10 satellites, despite having five more satellites than the 5-satellite configuration. This is because, in this case, the image captured by the first satellite could not send the data immediately as it was neither closer to nor in the line of sight of the central node, leading to a significantly higher time delay. The Task distribution for 10 Satellites will be further discussed in Section **??**.

In the Partially centralized configuration, the total time delay is generally higher than in the Decentralized configuration but lower than in the Centralized configuration. This is because, in the Partially centralized

configuration, although there is only one central node, all satellites can crosslink with each other and the central node. This crosslink capability introduces some efficiency, as satellites can relay data through the network to the central node, potentially reducing the delay compared to a more hierarchical system.

4.6.1.2 Time Taken after Image capture for One ground station

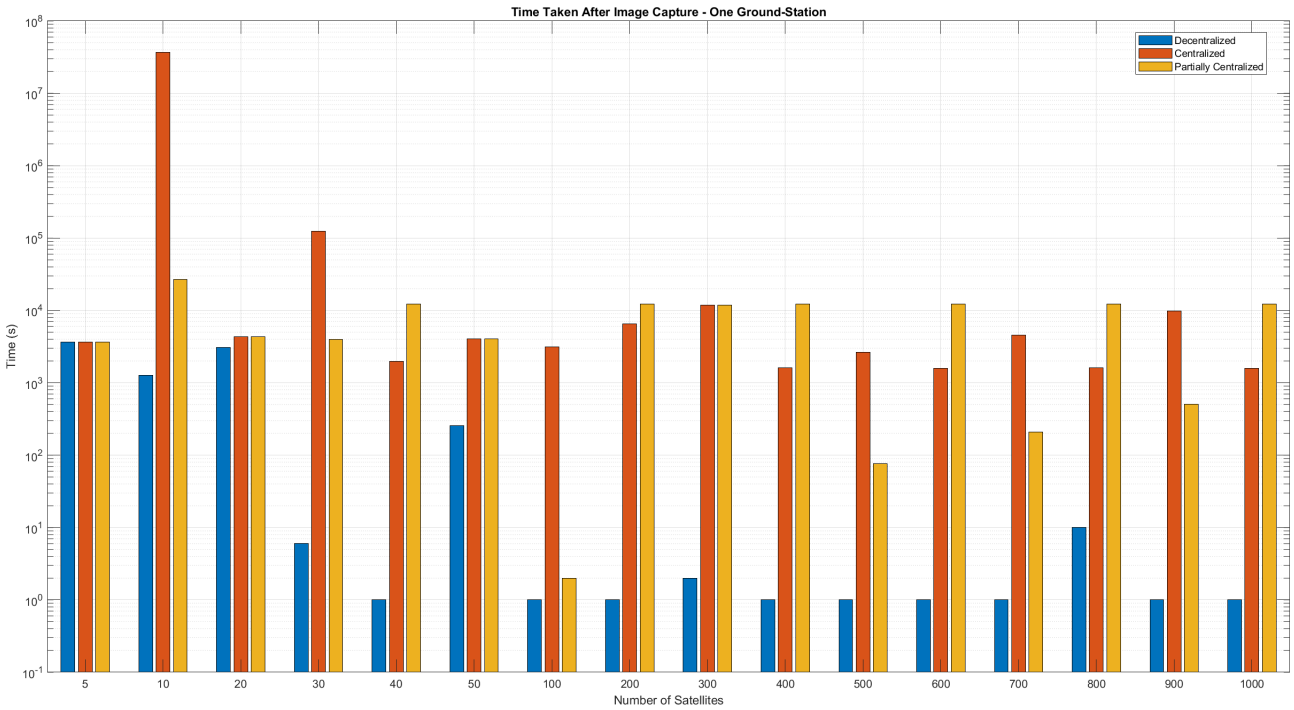

Figure 4.17 Time Taken After Image Capture One Ground Station

The graph in Fig.4.17 shows the time taken to transmit the image back to the ground station after its initial capture. The x axis represents the number of satellites, while the y axis indicates the time taken in seconds.

Evidently, the time elapsed after image capture remains consistent for 40, 10, 400, 500, 600, 900, and 1000 satellites. This uniformity can be attributed to the efficiency of the decentralized network configuration, which ensures that a satellite is always close enough to the ground station to transmit data promptly. The close proximity of a satellite to the ground station facilitates faster data transmission, demonstrating the effectiveness of the decentralized approach.

The Centralized configuration shows the highest and most variable delays in transmitting data after image capture. The single central node introduces a significant bottleneck, particularly when it is not in an optimal position relative to the ground station.

In the Partially centralized configuration, the time taken after image capture shows more variability due to the reliance on the central node for downlinking data. If the central node is not optimally positioned relative to the ground station at the time of image capture, it can result in significant delays.

4.6.2 Total Time Delay for Two Ground stations

4.6.2.1 Total Time taken by Two Ground Stations

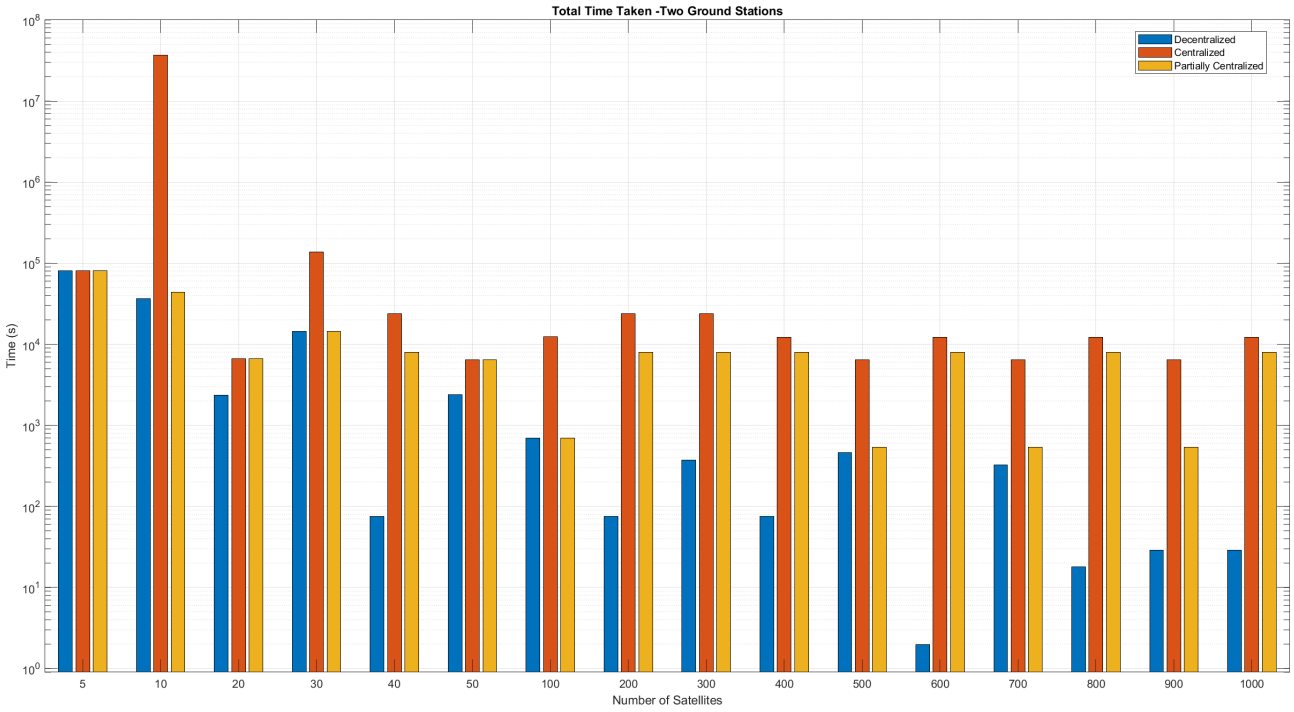

Figure 4.18 Total Time taken for Two Ground Stations

The Fig.4.18 shows the total time delay for Decentralized, Centralized, and Partially centralized configurations. The x-axis represents the number of satellites, and the y-axis shows the total time delay in seconds. Unlike the previous scenario, where there was only one ground station, this analysis considers two ground stations.

Decentralized Configuration demonstrates the lowest overall delay. The optimal performance is again observed with 600 satellites, similar to the one ground station scenario.

Centralized Configuration consistently shows the highest total delay. Notably, for 10 satellites, the delay remains high despite having more satellites than the 5-satellite configuration. This is due to the first satellite's inability to send data if it is not in line of sight or close to the central node, causing significant delays in data relay.

Partially Centralized Configuration generally shows a higher total time delay than the Decentralized configuration but lower than the Centralized configuration.

4.6.2.2 Time Taken After Image Capture for Two Ground Stations

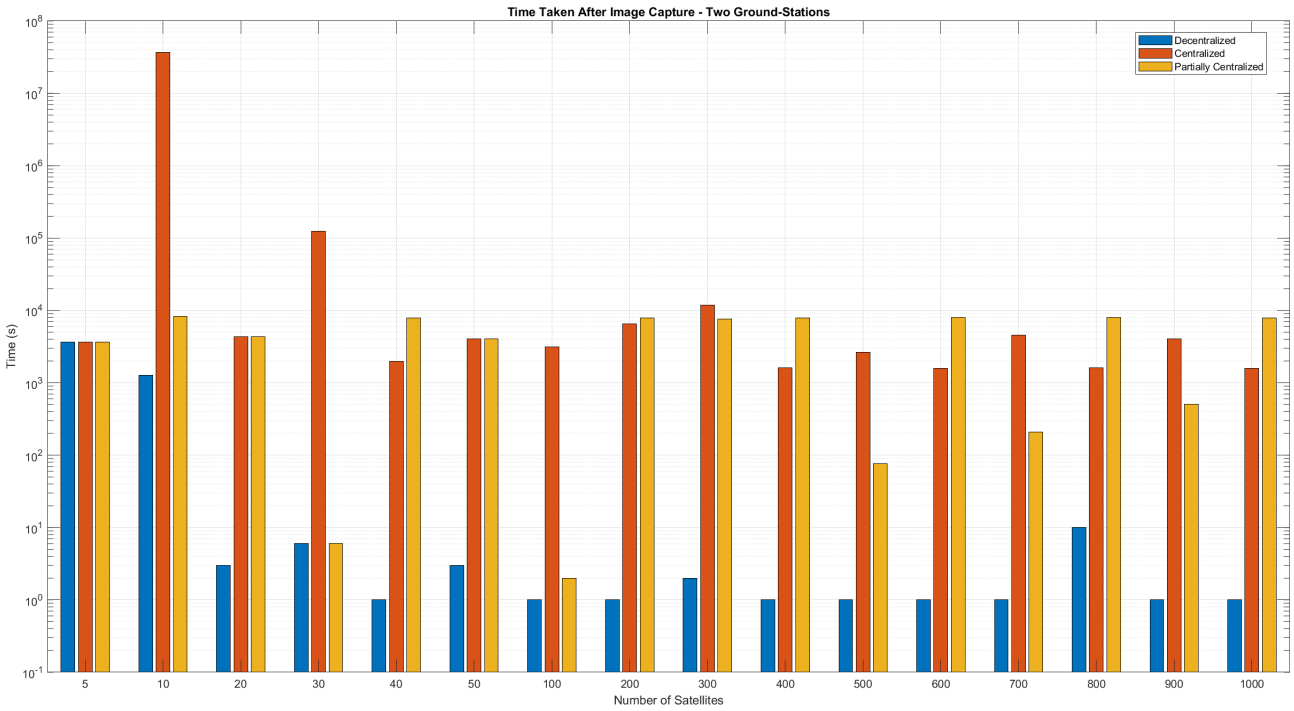

Figure 4.19 Time Taken After Image Capture Two Ground Stations

The Fig.4.18 focuses on the time taken to transmit the image back to the ground stations after the first image is captured. The x-axis represents the number of satellites, and the y-axis indicates the time taken in seconds. Again, this analysis is for two ground stations compared to one in the previous section.

Decentralized Configuration The time taken after image capture is relatively low and consistent across various satellite counts.

Centralized Configuration Exhibits the highest and most variable delays. The single central node becomes a significant bottleneck, especially when not well-positioned relative to both ground stations.

Partially Centralized Configuration shows more variability in the time taken after image capture. The delay depends on the position of the central node relative to the ground stations.

By analyzing these plots, it is evident that the decentralized network configuration consistently offers the lowest delays, demonstrating its effectiveness in managing data transmission efficiently, even with two ground stations.

4.6.3 Total Time Delay for Five Ground stations

4.6.3.1 Total Time taken by Five Ground Stations

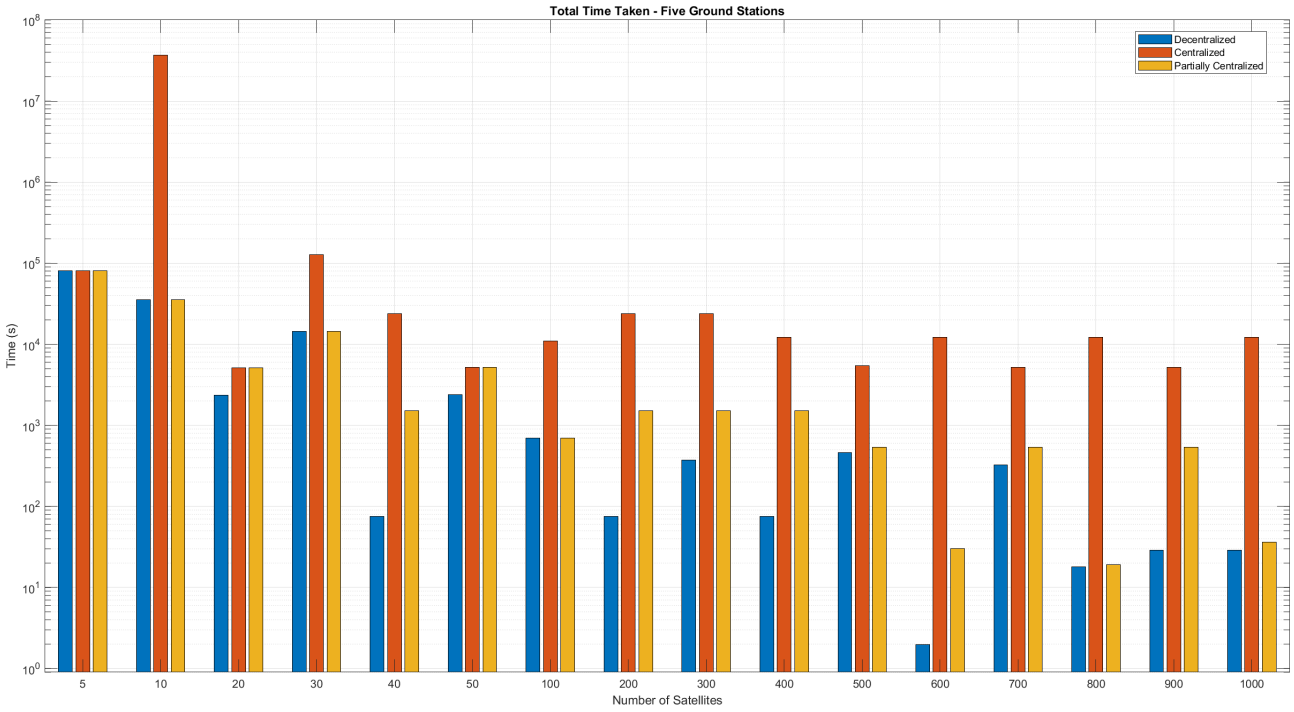

Figure 4.20 Total Time taken for five Ground Stations

The above fig.4.20 shows the total time delay for decentralized, centralized, and partially centralized configurations with five ground stations.
The x-axis represents the number of satellites, and the y-axis shows the total time delay in seconds.

Decentralized Configuration shows the lowest overall delay across various satellite counts, similar to the trends observed with one and two ground stations. The lowest delay is observed with 600 satellites, likely due to optimal satellite placement.

Centralized Configuration Displays the highest total delay, with the 10-satellite configuration having the highest delay, followed by the 30-satellite configuration. This trend is consistent with the patterns observed for one and two ground stations, indicating significant bottlenecks in these configurations.

Partially Centralized Configuration Generally, there is a higher total time delay than the decentralized configuration but lower than the Centralized configuration. This pattern is also observed with one and two ground stations.

4.6.3.2 Time Taken After Image Capture for Five Ground Stations

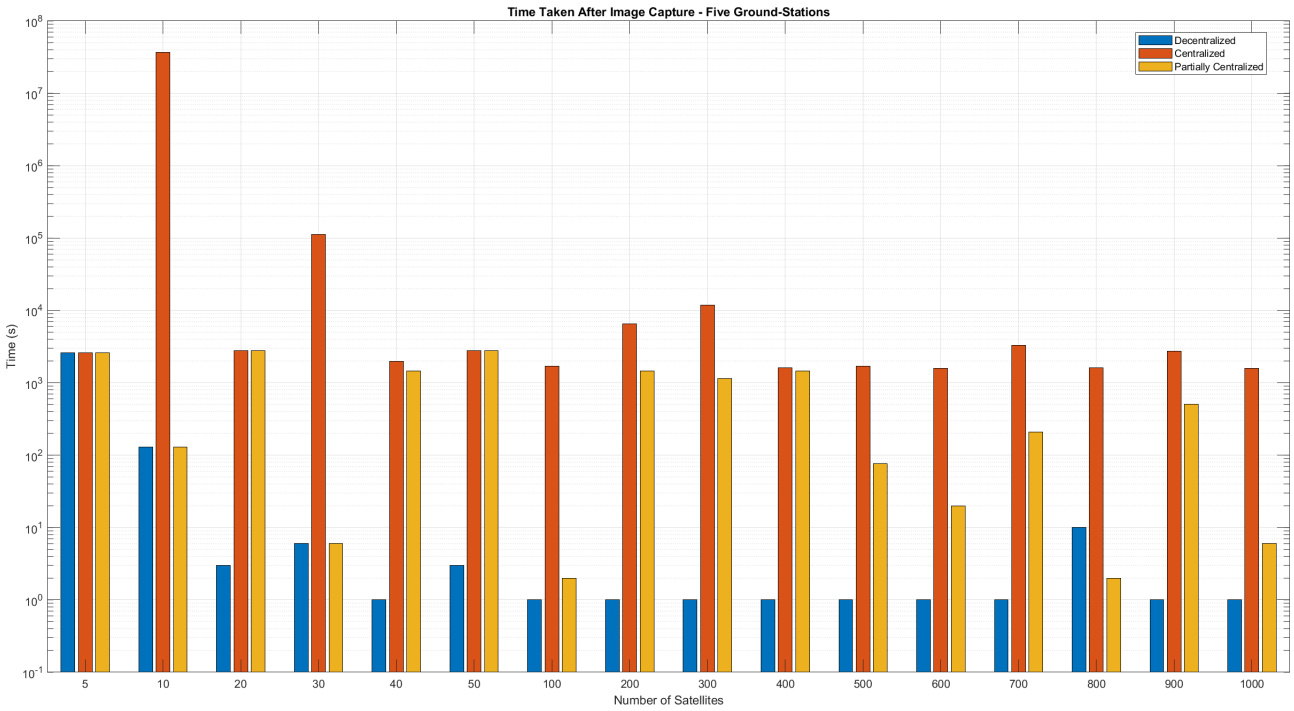

Figure 4.21 Time Taken After Image Capture Five Ground Stations

The Fig.4.20 focuses on the time taken to transmit the image back to the ground stations after the first image is captured. The x-axis represents the number of satellites, and the y-axis indicates the time taken in seconds.

Decentralized Configuration Shows relatively low and consistent time taken after image capture across different satellite counts, similar to the trends seen with one and two ground stations.

Centralized Configuration Demonstrates the highest and most variable delays, with significant bottlenecks when the central node is not optimally positioned. This configuration consistently shows the highest delays, similar to the trends seen with one and two ground stations.

Partially Centralized Configuration Exhibits more variability in the time taken after image capture, depending on the central node's position relative to the ground stations. This variability is consistent with the observations for one and two ground stations.

4.6.4 Impact of Ground Station Density on Total Time Delay

In this subsection, the combined data from the previous analyses is presented to illustrate the overall trend. By comparing the total time delays across configurations with one, two, and five ground stations, this analysis demonstrates how increasing the number of ground stations decreases the total time delay and improves the response time. This trend underscores the critical role that ground station density plays in enhancing the efficiency and effectiveness of satellite network communications.

4.6.4.1 Decentralized Configuration

For the decentralized configuration, increasing the number of ground stations does not lead to significant changes in total time delay. This is because the decentralized configuration already benefits from a network of satellites that can communicate directly with any ground station. The inherent efficiency of this setup means that additional ground stations offer diminishing returns in terms of reducing delay. However, the time taken after an image is captured decreases significantly with two ground stations for certain satellite counts, specifically 20 and 50 satellites. However, with five ground stations, the decrease in time is not as pronounced.

1. **Total Time taken**

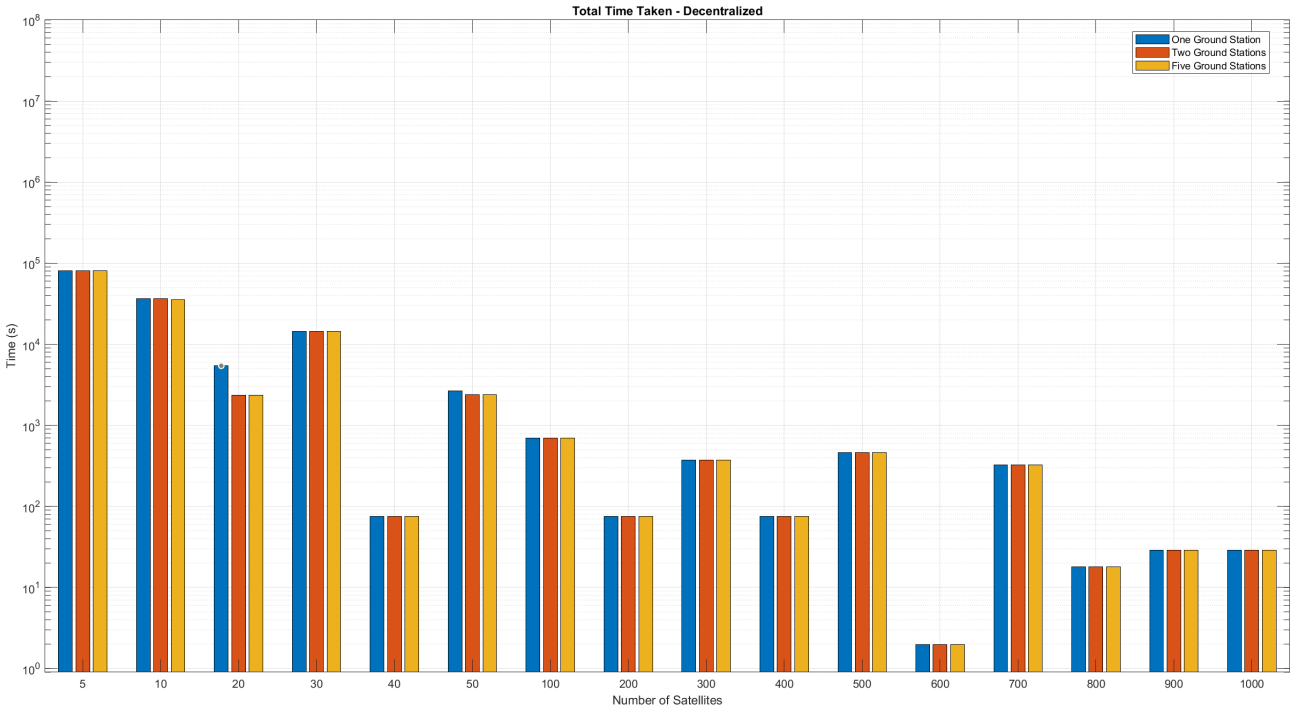

Figure 4.22 Total Time Taken - Decentralized

The Fig.4.22, shows that increasing the number of ground stations generally decreases the total time taken for decentralized configurations. For instance, with 5 satellites, the total time decreases slightly from 1352.6 minutes with one and two ground stations to 1334.9 minutes with five ground stations. Similarly, with 10 satellites, the total time decreases from 609.95 minutes with one and two ground stations to 591.05 minutes with five ground stations.

The analysis revealed that utilizing multiple ground stations significantly reduced the overall time delay, dropping from 90.4 minutes with a single station to 39.2 minutes when employing two or five stations. Interestingly, for configurations ranging from 30 to 1000 satellites, the total time delay remained relatively consistent across all ground station setups, showcasing the decentralized network's efficiency. These findings underscore the crucial role of ground station density in minimizing time delays, particularly for smaller satellite constellations. However, beyond the 30-satellite threshold, the delay time remained unchanged, suggesting that increasing the number of satellites alone does not further reduce the delay time. Table.A.14 provides a detailed breakdown of the total time taken for various satellite constellations and ground station configurations.

2. **Time Taken after Image was captured**

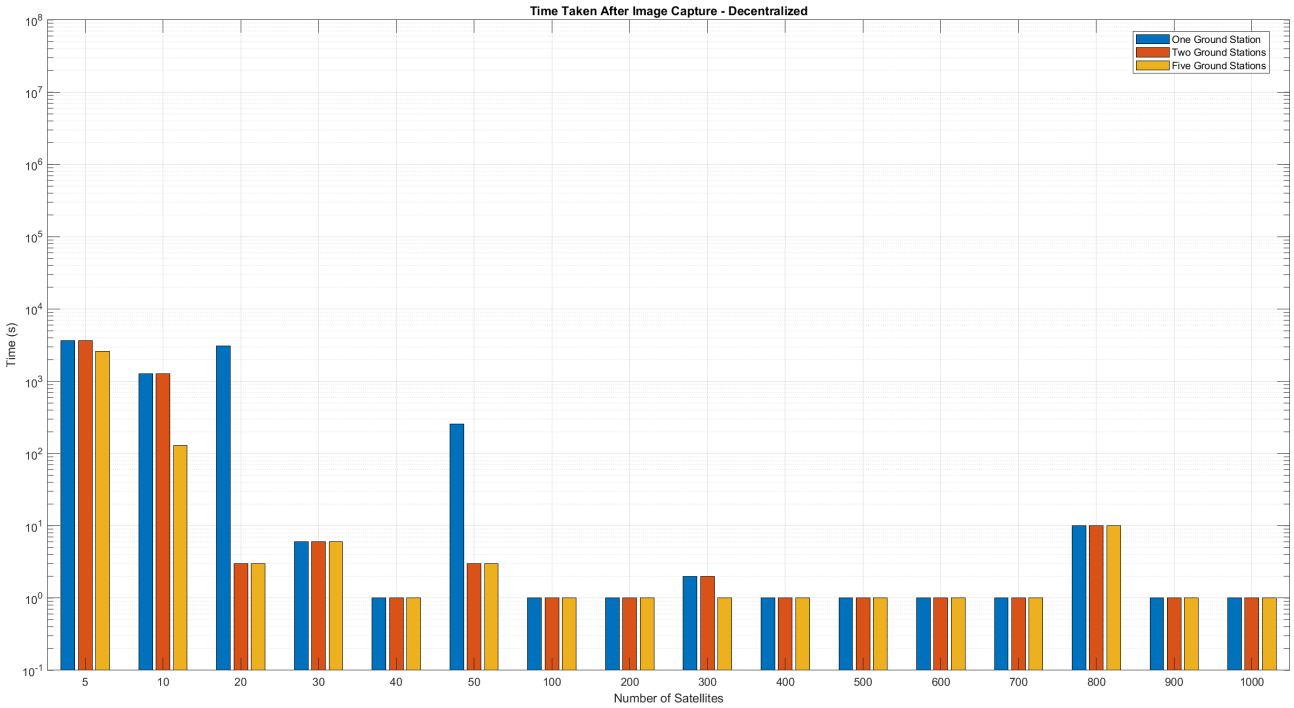

Figure 4.23 Total Time Taken After Image Captured - Decentralized

The Fig.4.23 reveals that increasing the number of ground stations significantly reduces the time taken to send images back to the ground station after capturing the initial image. For instance, with 5 satellites, the time decreases from 61 minutes with one or two ground stations to 43.3 minutes with five ground stations. Similarly, with 10 satellites, the time drops dramatically from 21.05 minutes with one or two ground stations to just 2.15 minutes with five ground stations. The most significant reduction occurs with 20 satellites, where the time taken after capturing the first image plummets from 51.25 minutes with one ground station to a mere 0.05 minutes with both two and five ground stations.

For constellations with 30 satellites and above, the time taken after capturing the first image remains relatively constant across all ground station configurations, highlighting the efficiency of the decentralized network. These findings emphasize the importance of ground station density in reducing delays post-image capture, particularly for smaller satellite constellations. However, beyond 20 satellites, the delay time stays largely unchanged, indicating that adding more satellites does not further reduce the delay after capturing the first image.Table.A.15 provides a detailed breakdown of the total time taken for various satellite constellations and ground station configurations.

4.6.4.2 Centralized Configuration

The Centralized configuration shows only slight decreases in total time delay with increased ground station density. This configuration, which has a central node communicating with all satellites and relaying data through a centralized structure, sees marginal improvements with more ground stations.

1. **Total Time taken**

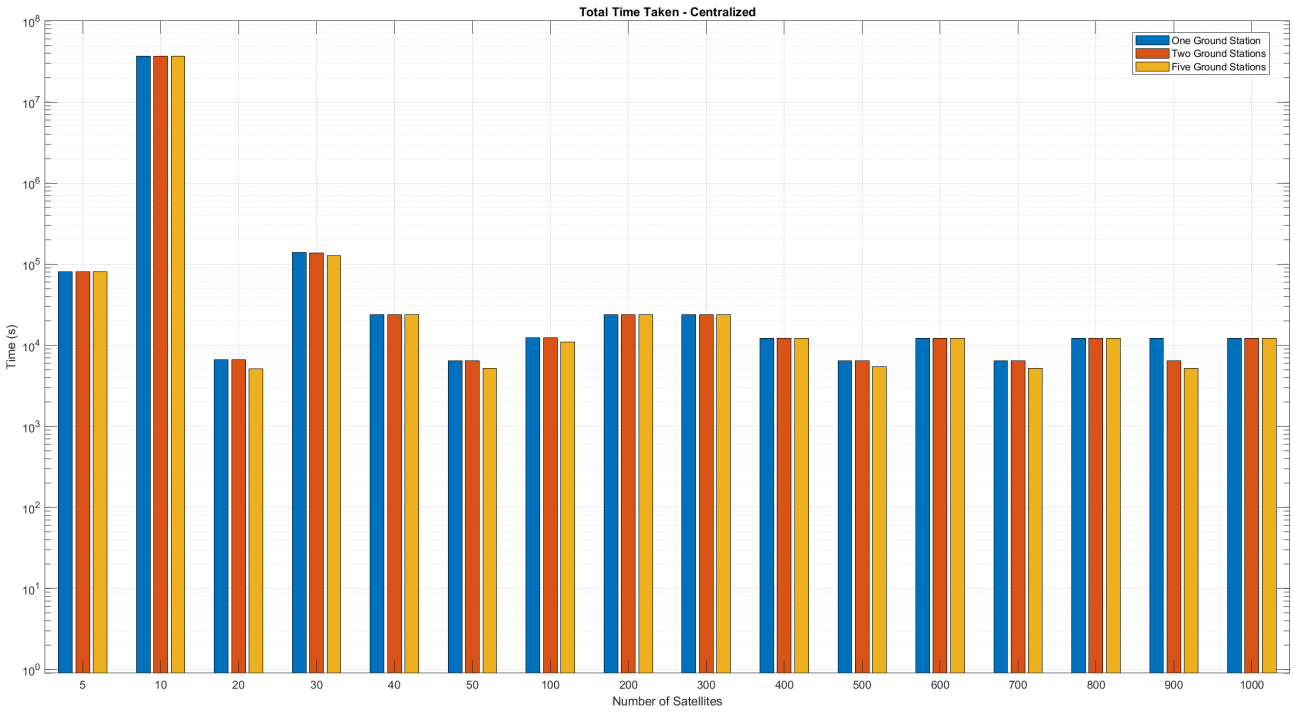

Figure 4.24 Total Time Taken - Centralized

The Fig.4.24, shows that increasing the number of ground stations generally decreases the total time taken for centralized configurations. For example, with 5 satellites, the total time decreases slightly from 1352.6 minutes with one and two ground stations to 1334.9 minutes with five ground stations. However, with 10 satellites, the total time is extremely high at over 611,000 minutes with one or two ground stations, and it slightly decreases to 611149.95 minutes with five ground stations.

Notable reductions are observed with 20 satellites, where the total time drops from 111.1 minutes with one and two ground stations to 85.2167 minutes with five ground stations. Similarly, with 50 satellites, the time decreases from 106.95 minutes with one and two ground stations to 86 minutes with five ground stations. However, the overall trend for configurations with 30, 100, 200, and beyond 400 satellites shows a relatively consistent time delay across all ground station setups. These findings highlight the impact of ground station density on reducing total time delays, particularly for configurations with fewer satellites, while demonstrating diminishing returns for larger satellite constellations. Table.A.16 provides a detailed breakdown of the total time taken for various satellite constellations and ground station configurations.

2. **Time taken after Image was captured**

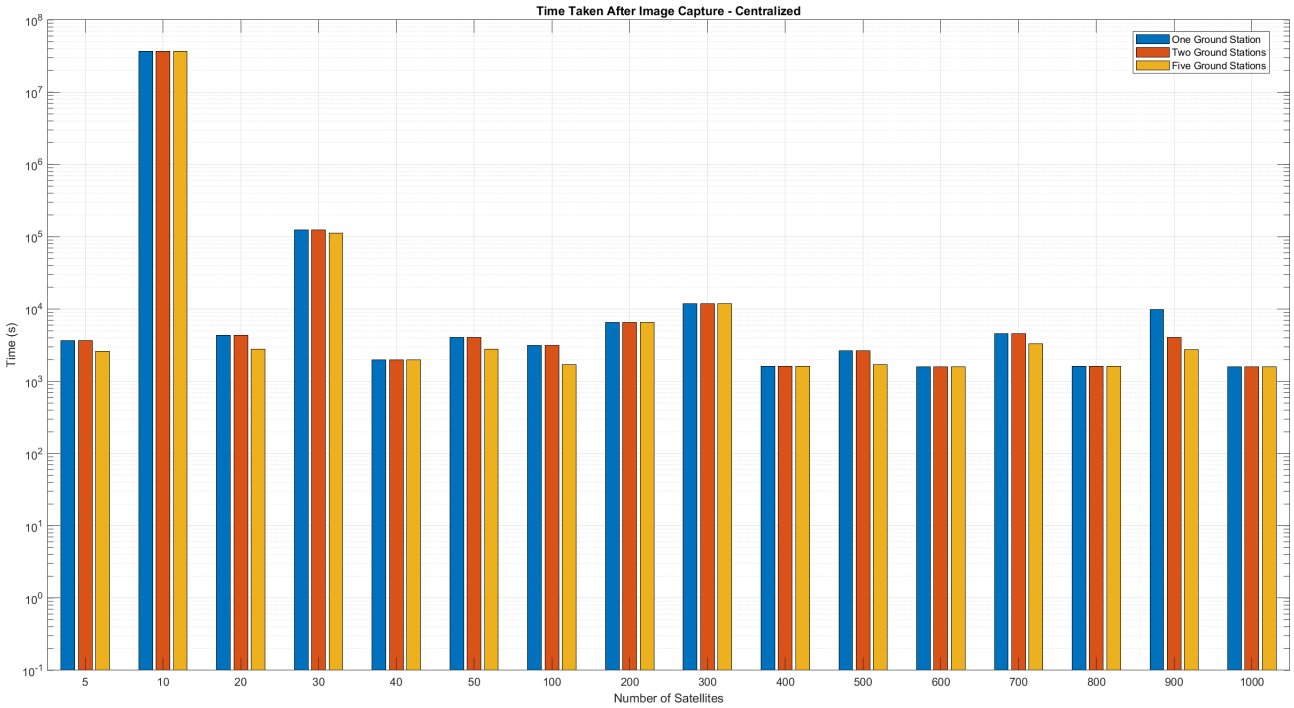

Figure 4.25 Total Time Taken After Image Captured - Centralized

The Fig.4.25, indicates that increasing the number of ground stations significantly decreases the time taken after the first image is captured in centralized configurations. For example, with 5 satellites, the time taken decreases from 61 minutes with one and two ground stations to 43.3 minutes with five ground stations. Similarly, for 10 satellites, the time taken is significantly high at over 610,580.5 minutes with one and two ground stations, and it decreases slightly to 610,561.05 minutes with five ground stations.

For 20 satellites, the time taken decreases from 71.95 minutes with one and two ground stations to 46.083 minutes with five ground stations. A significant reduction is observed with 50 satellites, where the time taken drops from 66.95 minutes with one and two ground stations to 46 minutes with five ground stations. Furthermore, configurations with 30, 100, 500, and 900 satellites show marked decreases in time taken with five ground stations compared to one and two ground stations, underscoring the importance of ground station density in minimizing time delays after the first image is captured, particularly in setups with fewer satellites. Table.A.17 provides a detailed breakdown of the total time taken various satellite constellations and ground station configurations.

4.6.4.3 Partially Centralized Configuration

The Partially centralized configuration shows a marked reduction in total time delay with an increase in the number of ground stations, particularly for higher satellite counts. This setup, where all satellites send data to a single central node, benefits greatly from additional ground stations, which reduce bottlenecks by providing more opportunities for the central node to be in an optimal position relative to the ground stations.

1. **Total Time Delay**

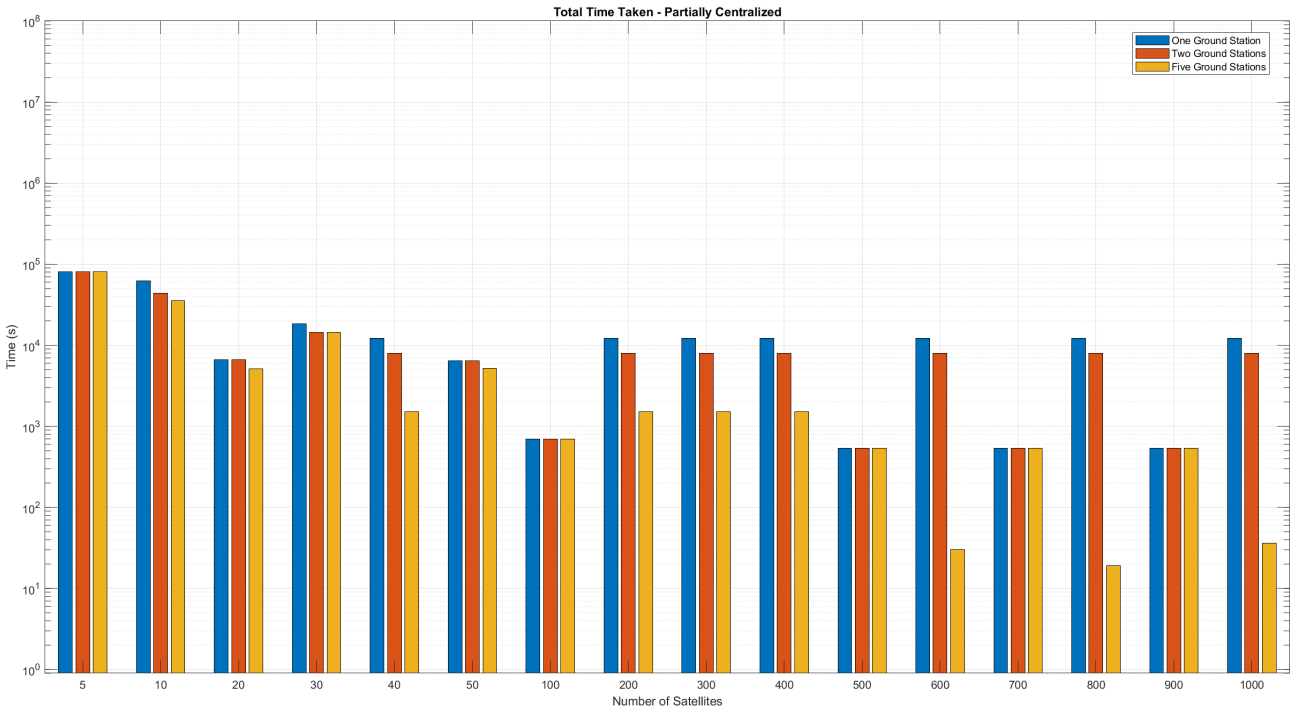

Figure 4.26 Total Time Taken - Partially Centralized

The Fig.4.26 shows that increasing the number of ground stations generally decreases the total time taken for partially centralized configurations. For example, with 5 satellites, the total time decreases slightly from 1352.6 minutes with one or two ground stations to 1334.9 minutes with three ground stations. However, with 10 satellites, the total time significantly decreases from 1038.4 minutes with one ground station to 726.45 minutes with two ground stations, and further to 591.05 minutes with five ground stations. Notable reductions are observed with 20 satellites, where the total time drops from 111.1 minutes with one and two ground stations to 85.2 minutes with five ground stations. Similarly, for 40 satellites, the time decreases from 204.65 minutes with one ground station to 132.75 minutes with two ground stations and dramatically to 25.3667 minutes with five ground stations. A similar pattern is seen with 50 satellites, where the time decreases from 106.95 minutes with one ground station to 86 minutes with five ground stations.

For configurations with 100, 500, and 700 satellites, the total time delay remains relatively consistent across all ground station setups, indicating that additional ground stations do not significantly impact the delay. However, for 200, 300, 400, 600, 800, and 1000 satellites, introducing five ground stations substantially reduces total time delay. For instance, the total time for 600 satellites drops dramatically from 204.667 minutes with one ground station to 0.5 minutes with five ground stations.

These findings highlight the significant impact of ground station density on reducing total time delays, particularly for configurations with fewer satellites and certain higher satellite counts. The addition of five ground stations provides substantial efficiency improvements, emphasizing the value of increasing ground station density in partially centralized networks. Table.A.18 provides a detailed breakdown of the total time taken for various satellite constellations and ground station configurations.

2. **Time taken after Image was captured**

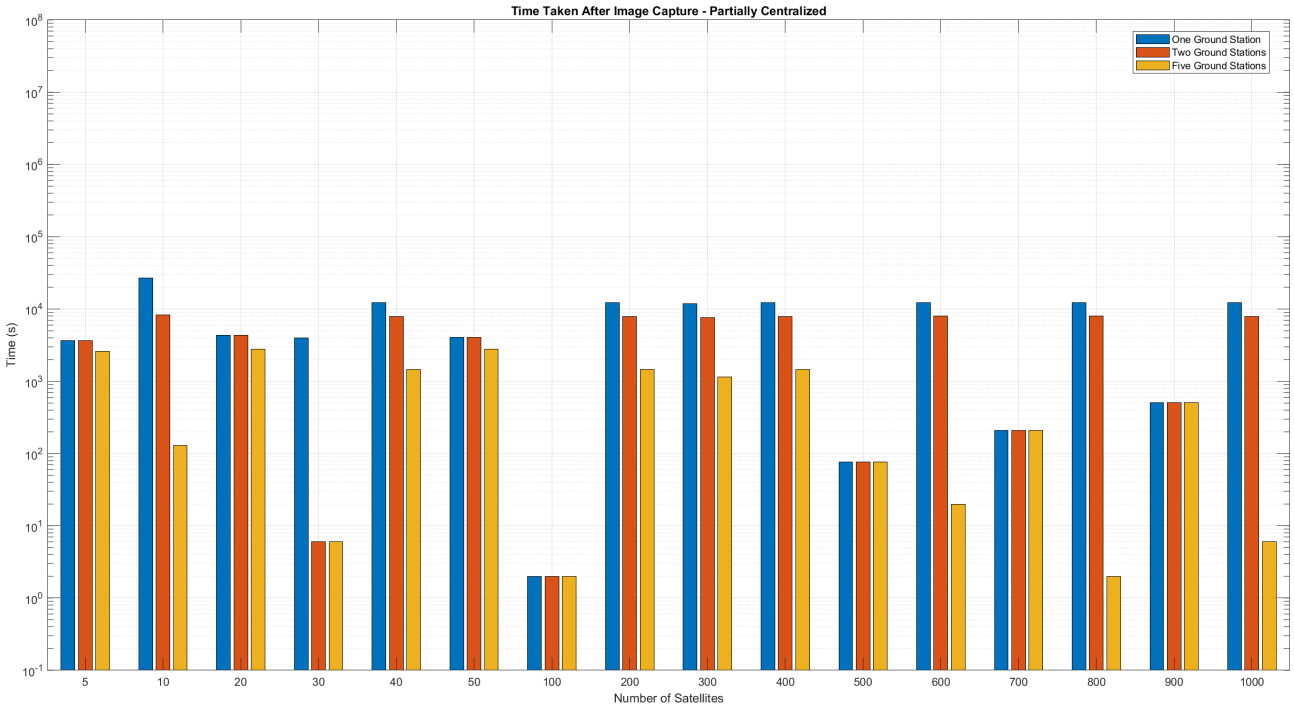

Figure 4.27 Total Time Taken After Image Captured - Partially Centralized

The Fig.4.26 shows that increasing the number of ground stations significantly reduces the time taken to send images back to the ground station after capturing the initial image in partially centralized configurations. For instance, with 5 satellites, the time decreases from 61 minutes with one and two ground stations to 43.3 minutes with five ground stations. With 10 satellites, the reduction is even more pronounced, dropping from 449.5 minutes with one ground station to 137.55 minutes with two ground stations, and dramatically to just 2.15 minutes with five ground stations. Notable improvements are also seen with 30 satellites, where the time decreases from 66.05 minutes with one ground station to 0.1 minutes with both two and five ground stations.

With an increasing number of satellites, ranging from 40 to 1000, the incorporation of additional ground stations substantially reduces the time required after image capture. Notably, for a constellation of 600 satellites, the time decreases from 204.5 minutes with a single ground station to 132.73 minutes with two ground stations, and further diminishes to a mere 0.33 minutes when five ground stations are employed. These findings underscore the critical role of ground station density in minimizing delays post-image capture, especially for configurations with fewer satellites and specific higher satellite counts. The introduction of additional ground stations offers substantial efficiency improvements, highlighting the effectiveness of increasing ground station density in partially centralized networks. Table.A.19 provides a detailed breakdown of the time taken after image capture for various satellite constellations and ground station configurations.

By analyzing these plots, it is evident that the decentralized network configuration consistently offers the lowest delays, demonstrating its effectiveness in managing data transmission efficiently, even with two ground stations.

4.7 Task Distribution

Task distribution in satellite networks involves receiving commands, cross-linking them among satellites, capturing images, and transmitting the data back to ground stations. This process varies based on the satellite configuration and the number of ground stations, influencing the efficiency and delay times in the network.

4.7.1 Task distribution For 5 Satellites

4.7.1.1 One Ground Station

Commands Received

- const[1] Status: COMMAND RECEIVED at Jan 01 2020 00:00:00
- const[0] Status: COMMAND RECEIVED at Jan 01 2020 00:08:39
- const[4] Status: COMMAND RECEIVED at Jan 01 2020 00:28:39
- const[3] Status: COMMAND RECEIVED at Jan 01 2020 00:48:36
- const[2] Status: COMMAND RECEIVED at Jan 01 2020 01:08:36

Images Received

- const[0] Status: IMAGE RECEIVED at Jan 01 2020 21:31:24

Images Transmitted

- const[0] Status: IMAGE TRANSMITTED at Jan 01 2020 22:32:36

Shortest Delay Time: 1352.6000 min

In this scenario, the first satellite to receive the command was const[1], followed by const[0], const[4], const[3], and finally const[2]. The sequence of command reception suggests that the commands were either relayed via other satellites or that the receiving satellites made direct contact with the ground station at different times.

The first satellite to receive an image was const[0]. Interestingly, before const[0] could transmit the image to other satellites, it made direct contact with the ground station and transmitted the image. If the satellite const[0] could have relayed the data to other satellites, the total time delay would have been considerably less. This suggests that having more satellites in the line of sight could enhance the overall efficiency of the network by allowing for quicker data relay and reducing the time required to transmit images back to the ground station. The current setup, with only five satellites, limits this capability as they are not always in line of sight, which affects the overall delay.

The above task distribution is same for Decentralized, Centralized and Partially Centralized layouts.

4.7.1.2 Two Ground Stations

The task distribution for two ground stations follows a similar pattern compared to One Groundstation section 4.7.1.1 for Decentralized, Centralized, and Partially Centralized configurations. The steps of receiving commands, cross-linking among satellites, and transmitting the image back to the ground stations remain consistent, with comparable delay times.

4.7.1.3 Five Ground Stations

Commands Received

- const[1]: COMMAND RECEIVED at Jan 01 2020 00:00:00
- const[0]: COMMAND RECEIVED at Jan 01 2020 00:08:39
- const[4]: COMMAND RECEIVED at Jan 01 2020 00:28:39
- const[3]: COMMAND RECEIVED at Jan 01 2020 00:48:36
- const[2]: COMMAND RECEIVED at Jan 01 2020 01:08:36

Images Received

- const[0]: IMAGE RECEIVED at Jan 01 2020 21:31:24

Images Transmitted

- const[0]: IMAGE TRANSMITTED at Jan 01 2020 22:14:54

Shortest Delay Time: 1334.9000 min

The first satellite to receive an image was const[0], which received the image at Jan 01 2020 21:31:24. Notably, const[0] was able to transmit the image directly to the ground station at Jan 01 2020 22:14:54, without relaying it to other satellites first. This direct transmission was possible due to the enhanced availability of ground stations, which significantly reduced the delay.

The shortest delay time in this setup was 1334.9000 minutes. This pattern was observed to be consistent across decentralized, centralized, and partially centralized configurations when utilizing five ground stations. The increased number of ground stations improved the efficiency of data downlinking, resulting in quicker image transmission times.

Adding more ground stations enabled const[0] to transmit the image faster. With five ground stations, it took only 43.3 minutes to transmit the data to the ground station after capturing the image, compared to 61 minutes when there were only one or two ground stations. This significant reduction in time highlights the benefit of having multiple ground stations, allowing satellites to capitalize on direct communication opportunities with the ground stations. If const[0] had relayed the data to other satellites, the total time delay could have been considerably less. This finding suggests that increasing the number of satellites in line of sight with each other could further enhance the network's efficiency by enabling faster data relay and reducing overall transmission delays.

This pattern was the same for Decentralized, Centralized and Partially Centralized configurations with five ground stations. The image was transmitted quicker due to the presence of additional ground stations, enhancing the efficiency of data downlinking.

4.8 Comparison of averages for Decentralized vs Partially Centralized

To understand the efficiency and performance of decentralized and partially centralized satellite communication networks, we compare the average values for varying satellite constellations (5, 10, 20, 30, 40, 50, and 100 satellites) across different numbers of ground stations. The comparison includes:

a) One ground station: Decentralized vs Partially Centralized

b) Two ground stations: Decentralized vs Partially Centralized

c) Five ground stations: Decentralized vs Partially Centralized

d) Total comparison: Decentralized vs Partially Centralized

The X-axis represents the number of satellites, and the Y-axis represents the time taken for data transmission.

4.8.0.1 One Ground Station: Decentralized vs Partially Centralized

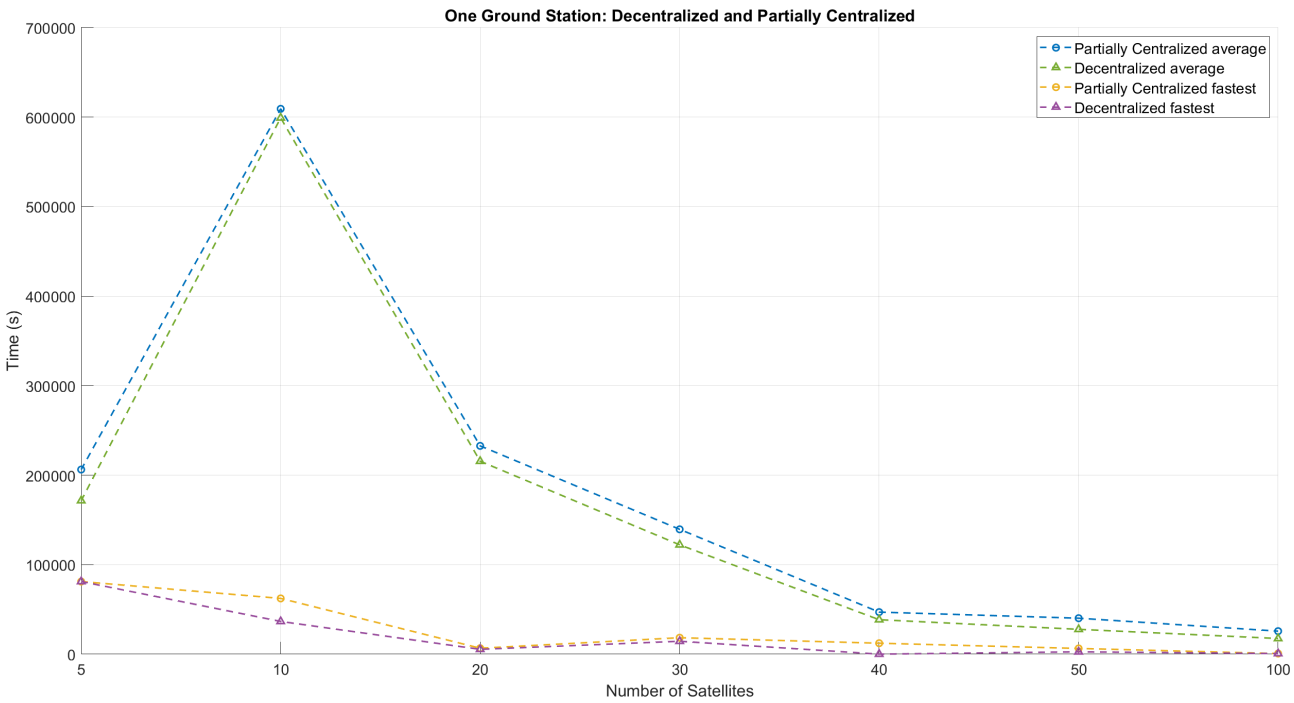

Figure 4.28 One Ground Station Decentralized vs Partially Centralized

The Fig.4.28, shows decentralized systems generally have lower average times compared to partially centralized systems across varying satellite counts. For example, with 10 satellites, the average time

for decentralized configurations is 9985.38 minutes, which is lower than the average of 10154.07 minutes for partially centralized configurations. This trend continues as the satellite count increases. With 50 satellites, decentralized systems have an average time of 463.07 minutes, significantly lower than the 670.03 minutes observed for partially centralized systems. The consistent lower average times for decentralized configurations indicate that these systems are more efficient in handling data transmission as the number of satellites increases, likely due to more optimal and frequent communication paths.

Comparing the fastest times, decentralized systems also show superior performance. For instance, with 20 satellites, the fastest time for decentralized systems is 90.4 minutes, compared to 111.1 minutes for centralized systems. This pattern is even more pronounced with 40 satellites, where decentralized configurations achieve a fastest time of just 1.25 minutes, whereas partially centralized systems take 204.65 minutes. These faster times demonstrate that decentralized networks can leverage direct and immediate transmission opportunities, further optimizing data transmission and reducing latency compared to partially centralized networks.

4.8.0.2 Two Ground Stations: Decentralized vs Partially Centralized

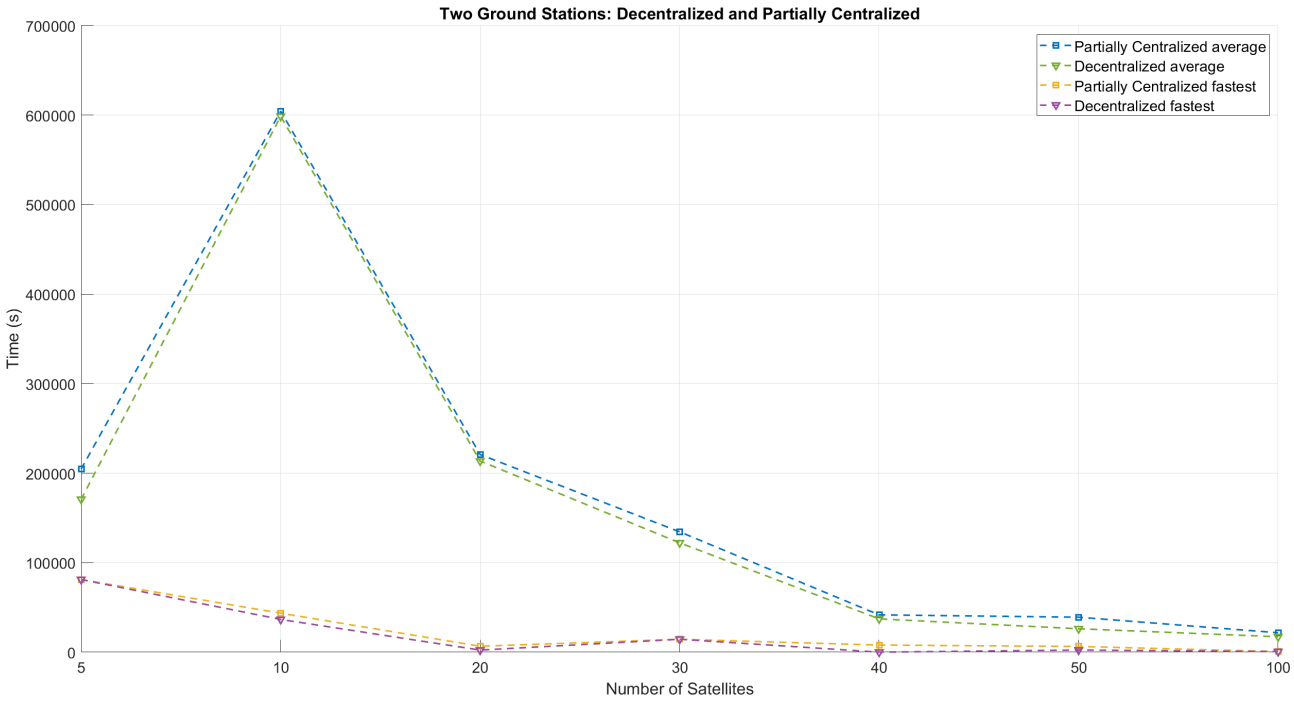

Figure 4.29 Two Ground Stations Decentralized vs Partially Centralized

The Fig.4.29 shows that adding a second ground station significantly reduces the average time for decentralized and partially centralized networks. For example, with 10 satellites, the average time for decentralized systems decreases to 9976.98 minutes from the 10154.07 minutes observed with one ground station. Similarly, for partially centralized systems, the average time drops from 10154.07 minutes to 10071.31 minutes. This reduction, indicates that the additional ground station helps mitigate the delays caused by specific orbital parameters. For larger constellations, such as 50 satellites, the average time for decentralized systems decreases to 436.40 minutes from 670.03

minutes; for partially centralized systems, it drops to 651.45 minutes. This trend is even more pronounced with 100 satellites, where decentralized systems achieve an average time of 287.66 minutes, compared to 362.32 minutes for partially centralized systems, highlighting the efficiency gains from additional ground stations.

When examining the fastest times, decentralized systems consistently outperform partially centralized systems. With 20 satellites, the fastest time for decentralized systems is 39.2 minutes, significantly lower than the 111.1 minutes for partially centralized systems. This trend continues with larger constellations: for 50 satellites, decentralized systems have a fastest time of 40.05 minutes compared to 106.95 minutes for partially centralized systems. Furthermore, the data shows that decentralized networks also have lower average times, which reinforces their efficiency. For instance, with 40 satellites, decentralized systems have an average time of 620.49 minutes compared to 694.99 minutes for partially centralized systems. This comprehensive comparison underscores that decentralized configurations not only achieve faster individual transmission times but also maintain more efficient average performance across varying number of satellites. The additional ground station enhances these efficiencies by providing more frequent and direct communication opportunities.

4.8.0.3 Five Ground Stations: Decentralized vs Partially Centralized

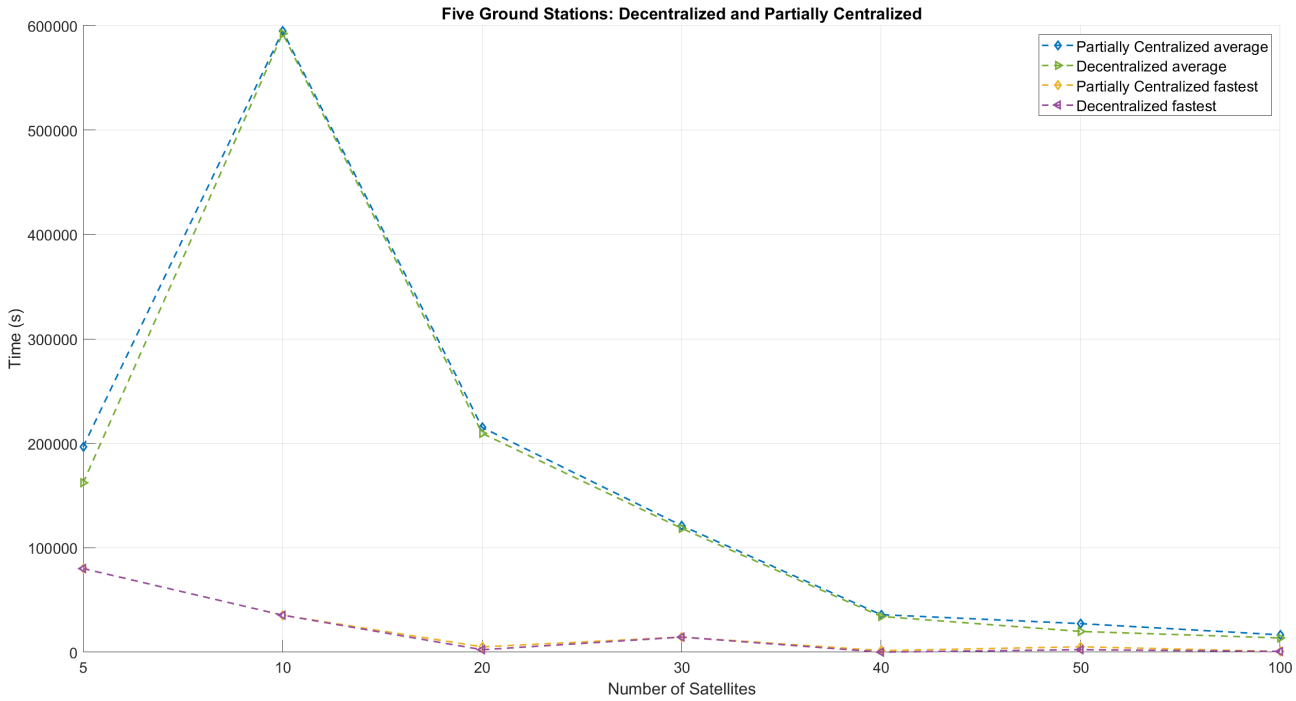

Figure 4.30 Five Ground Stations Decentralized vs Partially Centralized

With five ground stations, the average time decreases significantly across all satellite constellations as seen in Fig.4.30. For example, with 5 satellites, the average time for decentralized systems drops to 2704.19 minutes from 2858.88 minutes with one ground station, and partially centralized systems see a decrease to 3279.98 minutes from 3437.74 minutes. This trend continues with 50 satellites, where decentralized systems have an average time of 331.11 minutes compared to 436.40 minutes

with two ground stations, and partially centralized systems see a reduction to 456.36 minutes from 651.45 minutes. These reductions in average time indicate that additional ground stations enhance the network's ability to manage data transmission more efficiently by providing more frequent and direct communication opportunities.

When examining the fastest times, decentralized systems consistently perform better than partially centralized systems. For instance, with 20 satellites, the fastest time for decentralized systems is 39.2 minutes, significantly lower than the 85.2 minutes for partially centralized systems. This trend continues with larger constellations: for 50 satellites, decentralized systems have a fastest time of 40.05 minutes compared to 86 minutes for partially centralized systems. Furthermore, the data shows that decentralized networks not only achieve faster individual transmission times but also maintain more efficient average performance across varying satellite counts. For example, with 100 satellites, decentralized systems achieve an average time of 227.04 minutes compared to 276.47 minutes for partially centralized systems. This consistent improvement can be attributed to the decentralized systems' ability to leverage multiple ground stations effectively, optimizing data transmission paths and reducing latency. The presence of five ground stations enhances these efficiencies by increasing the frequency of direct communication opportunities, thereby minimizing delays and improving overall network performance.

4.8.0.4 Total Comparison: Decentralized vs Partially Centralized

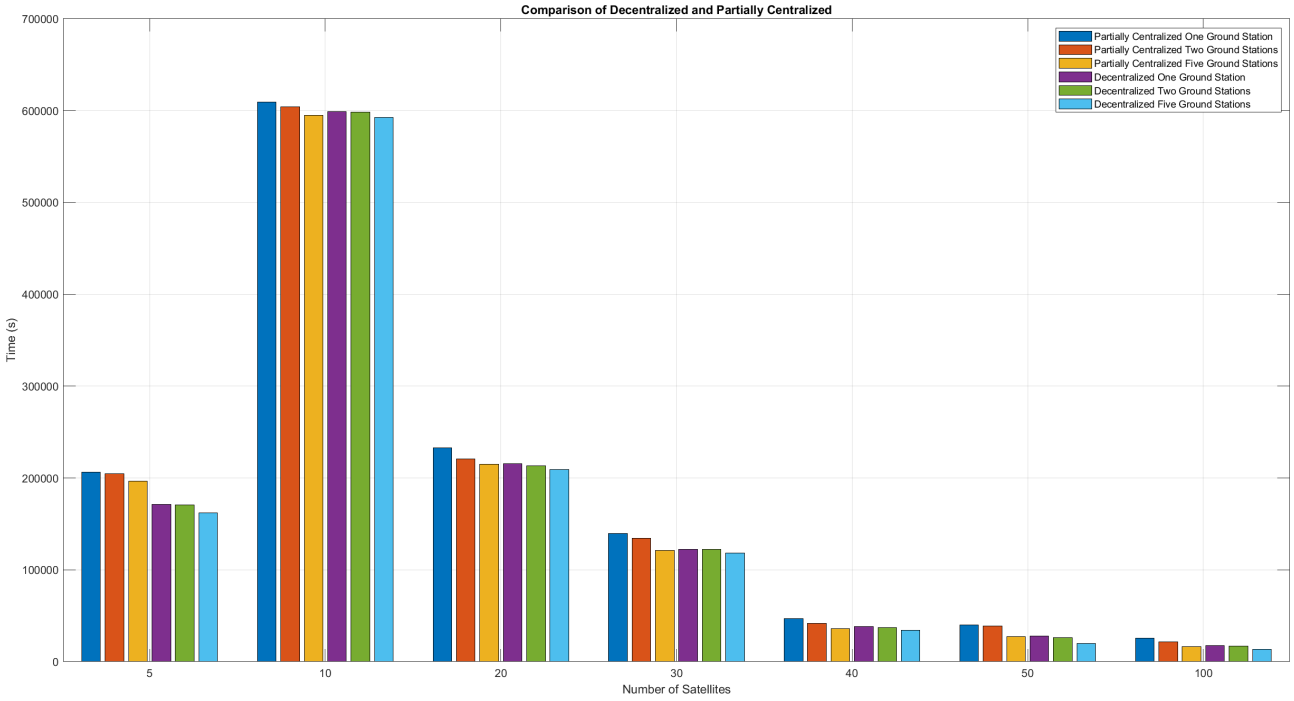

Figure 4.31 Comparison Decentralized and Partially Centralized

- Overall, decentralized networks have slightly lower average times than partially centralized networks, especially with more ground stations.

- The configuration with 10 satellites consistently shows higher average times due to the semi-major axis and inclination values that lead to longer communication delays. This is further analyzed in subsection.4.8.1.
- The configuration with 20 satellites also shows higher times than expected due to similar reasons, although the impact is less severe than 10 satellites but the average time was higher than 5 Satellites.
- The effect of adding additional nodes can be seen in detail in the Appendix.A.8

4.8.1 Analysis of Higher Averages for 10 Satellites

The higher average times for the 10 satellite constellation in all cases can be attributed to their combinations of the number of planes and satellites per plane, along with their orbital parameters, Check Table. A.22 in Appendix for reference:

- Semi-Major Axis and Inclination: The specific values for these parameters cause longer delays in establishing communication paths. For example, with a semi-major axis around 6880 km and an inclination near 54 and 55 degrees, the satellites may experience longer periods without line-of-sight to ground stations.
- Orbital Configurations: The alignment and spacing of satellites in this constellation can lead to increased times for data transmission, impacting the overall efficiency.
- Number of Planes and Satellites per Plane: Configurations such as 1 plane with 10 satellites or 5 planes with 2 satellites lead to longer delays in data transmission, resulting in higher average times.

4.8.2 Analysis of Higher Averages for 20 Satellites

Similarly, for 20 satellites constellation the higher average time can be attributed to their combinations of the number of planes and satellites per plane, along with their orbital parameters, check Table.A.23 in Appendix for reference:

- Orbital Parameters: For some 20 satellite configurations, the semi-major axis and inclination values again play a role. For example, a semi-major axis around 6880 km to 6930 km and an inclination of 54 to 55 degrees can create communication delays.
- Number of Planes and Satellites per Plane: The increased number of planes and satellites per plane introduces more opportunities for data transmission paths but also requires more coordination, for combinations such as 5 planes with 4 satellites or 10 planes with 2 satellites lead to longer delays in data transmission, resulting in higher average times.

5 Conclusion and Future Work

5.1 Conclusion

The research aimed to optimize satellite constellations for effective region coverage around the primary ground station and task distribution, examining various configurations and their impacts. The results revealed several key insights that address the research questions posed.

5.1.1 Optimizer Effectiveness

The optimization of satellite configurations significantly enhanced the coverage of the region around the primary ground station in Neustrelitz. The two best optimizers identified were GN DIRECT NOSCAL L and GN MLSL. For 5 satellites, GN DIRECT NOSCAL L increased coverage by 15% at mid-range inclinations (40-60 degrees) compared to non-optimized configurations, while GN MLSL maintained performance at lower altitudes, achieving a 10% improvement at 500 km altitude. These results demonstrate the effectiveness of the optimization approach in enhancing satellite constellation design, leading to better coverage and reduced latency.

5.1.2 Ground Station Impact

The analysis demonstrated that increasing the number of ground stations significantly influences the total time delay and task distribution efficiency across different network configurations:

- Decentralized Configuration: Increasing the number of ground stations resulted in modest reductions in total time delay. For instance as seen in 4.6.4.1, with 5 satellites, adding up to five ground stations decreased the delay by approximately 1.31%. For 10 satellites the delay was reduced by around 3.10% with five ground stations. However, for higher satellite counts like 20, a substantial reduction of over 56.64% was observed when adding just one more ground station.
- Centralized Configuration: The centralized configuration showed improvements in total time delay with additional ground stations. As seen in section 4.6.4.2, with 20 satellites the delay decreased by 23.30% when increasing from one to five ground stations. More significant reductions were observed with higher satellite counts, such as a decrease of 57.98% for 900 satellites when increasing from one to five ground stations. For 50 satellites, there was no change in delay when there were two ground stations. However, when the ground stations were increased to five, the delay decreased by 19.59%, and a similar reduction was observed for 700 satellites.

- Partially Centralized Configuration: This configuration benefited the most from additional ground stations. As seen in section 4.6.4.3, with 10 satellites the delay decreased by about 43.08% when increasing from one to five ground stations. For 40 satellites, the reduction was even more dramatic at approximately 87.60% when increasing from one to five ground stations. With 1000 satellites, the delay was virtually eliminated, showcasing a 99.71% reduction when increasing from one to five ground stations. For 600 satellites, the reduction was even higher, around 99.76%, when increasing from one to five ground stations. The highest reduction was observed for 800 satellites, with around 99.85% reduction from one ground station, where the time delay was 204.65 minutes to 0.3167 minutes for five ground stations.

These results underscore the importance of optimizing ground station density to enhance satellite network performance. Particularly in centralized and partially centralized configurations, increasing the number of ground stations significantly reduces total time delay and improves task distribution efficiency, leading to faster and more reliable satellite communications.

5.1.3 Impact of Additional Central Nodes on Total Time Delay

The inclusion of additional central nodes in the centralized configuration revealed notable improvements in total time delay with the addition of ground stations as seen in Appendix A.8. For 20 satellites, the delay decreased by 23.30% when increasing from one to five ground stations. Similarly, for 30 satellites, there was an 8.92% reduction. Significant reductions were observed for 50 satellites, with a 19.59% decrease, and 100 satellites, with an 11.73% reduction. The most substantial improvements were seen with higher satellite counts, such as a 57.98% decrease for 900 satellites. Additional central nodes further enhanced performance, exemplifying the benefits of optimizing ground station density in centralized configurations.

5.2 Future Work

5.2.1 Limitations of the framework

The current framework does not account for onboard data processing capabilities or the use of realistic data storage scenarios for satellites. It also overlooks constraints related to satellite power, including how power limitations affect data retention and transmission. Integrating these factors will provide a more comprehensive optimization model. Additionally, several assumptions need to be revised to enhance accuracy and reliability. The optimizer's current 20-degree half-angle sensor should be replaced with a more realistic half-cone angle based on camera selection, further improving accuracy and increasing optimization time. The lowest altitude should be adjusted from 500 km to 550 km to better reflect satellite operations. Finally, the number of simulation iterations should be extended to at least 2000 to ensure more robust and reliable optimization results.

5.2.2 Potential Applications

The optimized framework can be applied to various disaster monitoring scenarios. For instance:

- Flood Monitoring: During the recent floods in Porto Alegre, Brazil, an optimized satellite constellation could have provided timely and detailed imagery to aid response efforts.
- Earthquake Response: In events like the Syrian and Japanese earthquakes, real-time satellite data could significantly enhance rescue and relief operations.
- Wildfire Monitoring: The recent fires in Hawaii could have been better managed with improved satellite data, aiding in real-time monitoring and post-disaster assessment.
- Environmental Conservation: Monitoring deforestation, glacier retreat, and other environmental changes to support conservation efforts.

5.2.3 Use of Industry Standard Optimizers

Incorporate advanced optimization tools such as: [41]

- Ipopt(Interior Point Optimizer): For solving large-scale nonlinear optimization problems.
- SNOPT (Sparse Nonlinear Optimizer): For large-scale optimization with nonlinear constraints

5.2.4 Further Improvements

- Visualization of Shortest path: Enhance the framework to visualize the shortest path taken, not just the shortest time
- Data Transmission Capacity: Add metrics to show how much data can be sent per contact or the maximum data size based on satellite contact time
- Comparison with Existing Constellations: Compare the optimized configurations with existing Earth Observation (EO) satellite constellations (eg. Spire, Planet) to identify scenarios where current systems might be more efective or less efficient.

A Appendix

A.1 Combinations table

Table A.1 Satellites Combinations

Satellites	Number of Planes	Satellites per Plane
5	1	5
	5	1
20	1	20
	2	10
	4	5
	5	4
	10	2
	20	1
30	1	30
	2	15
	3	10
	5	6
	6	5
	10	3
	15	2
	30	1
40	1	40
	2	20
	4	10
	5	8
	8	5
	10	4
	20	2
	40	1
50	1	50
	2	25
	5	10
	10	5
	25	2
	50	1

Table A.1 continued from previous page

Satellites	Number of Planes	Satellites per Plane
100	1	100
	2	50
	4	25
	5	20
	10	10
	20	5
	25	4
	50	2
	100	1
200	1	200
	2	100
	4	50
	5	40
	8	25
	10	20
	20	10
	25	8
	40	5
	50	4
	100	2
	200	1
300	1	300
	2	150
	3	100
	4	75
	5	60
	6	50
	10	30
	12	25
	15	20
	20	15
	25	12
	30	10
	50	6
	60	5
	75	4
	100	3
	150	2
	300	1
400	1	400
	2	200

Table A.1 continued from previous page

Satellites	Number of Planes	Satellites per Plane
	4	100
	5	80
	8	50
	10	40
	16	25
	20	20
	25	16
	40	10
	50	8
	80	5
	100	4
	200	2
	400	1
500	1	500
	2	250
	4	125
	5	100
	10	50
	20	25
	25	20
	50	10
	100	5
	125	4
	250	2
	500	1
600	1	600
	2	300
	3	200
	4	150
	5	120
	6	100
	8	75
	10	60
	12	50
	15	40
	20	30
	24	25
	25	24
	30	20
	40	15
	50	12

Table A.1 continued from previous page

Satellites	Number of Planes	Satellites per Plane
	60	10
	75	8
	100	6
	120	5
	150	4
	200	3
	300	2
	600	1
700	1	700
	2	350
	4	175
	5	140
	7	100
	10	70
	14	50
	20	35
	25	28
	28	25
	35	20
	50	14
	70	10
	100	7
	140	5
	175	4
	350	2
	700	1
800	1	800
	2	400
	4	200
	5	160
	8	100
	10	80
	16	50
	20	40
	25	32
	32	25
	40	20
	50	16
	80	10
	100	8
	160	5

Table A.1 continued from previous page

Satellites	Number of Planes	Satellites per Plane
	200	4
	400	2
	800	1
900	1	900
	2	450
	3	300
	4	225
	5	180
	6	150
	9	100
	10	90
	12	75
	15	60
	18	50
	20	45
	25	36
	30	30
	36	25
	45	20
	50	18
	60	15
	75	12
	90	10
	100	9
	150	6
	180	5
	225	4
	300	3
	450	2
	900	1
1000	1	1000
	2	500
	4	250
	5	200
	8	125
	10	100
	20	50
	25	40
	40	25
	50	20
	100	10

Table A.1 continued from previous page

Satellites	Number of Planes	Satellites per Plane
	125	8
	200	5
	250	4
	500	2
	1000	1

A.2 Optimizer Results

A.2.1 Non Linear Optimizer 5 Satellites Combination 2 Results

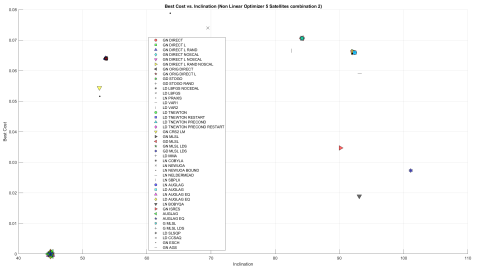

(a) Best Coverage Vs Semi Major Axis

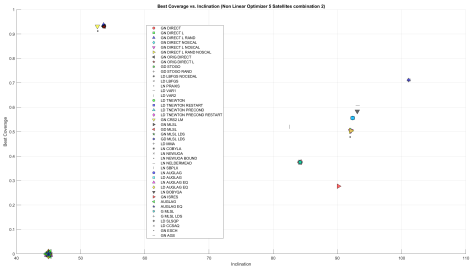

(b) Best Coverage Vs Inclination

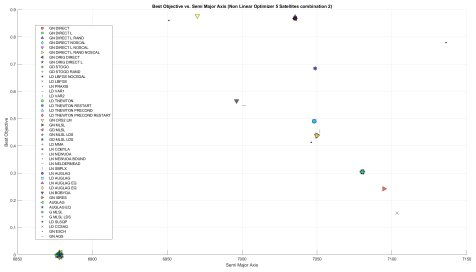

(c) Best Objective Vs Semi Major Axis

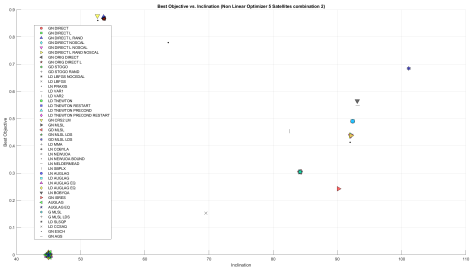

(d) Best Objective Vs Inclination

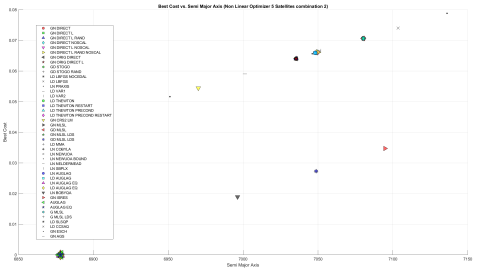

(e) Best Cost Vs Semi Major Axis

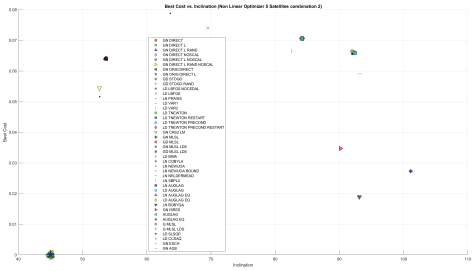

(f) Best Cost Vs Inclination

Figure A.1 Non Linear Optimizer (NLOPT) comparison 5 Satellites combination 2

The detailed table is presented in Annex Table. A.21

A.2.2 5 Satellites Combination 1

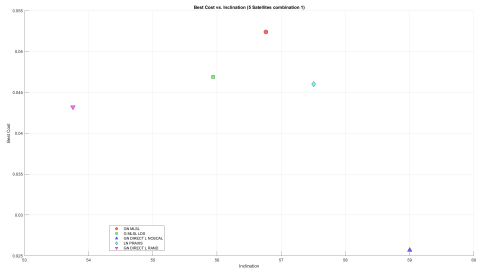

(a) Best Coverage Vs Semi Major Axis

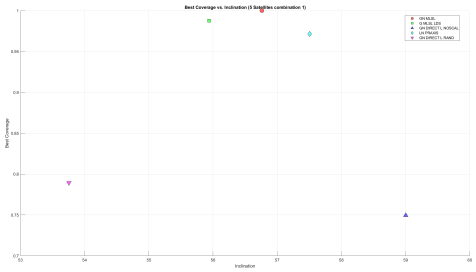

(b) Best Coverage Vs Inclination

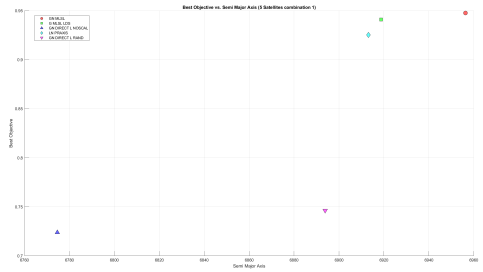

(c) Best Objective Vs Semi Major Axis

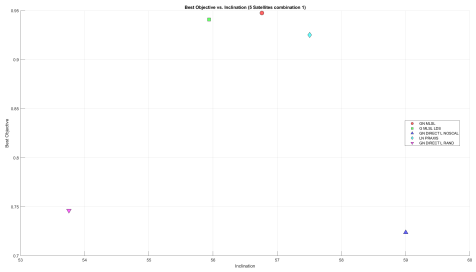

(d) Best Objective Vs Inclination

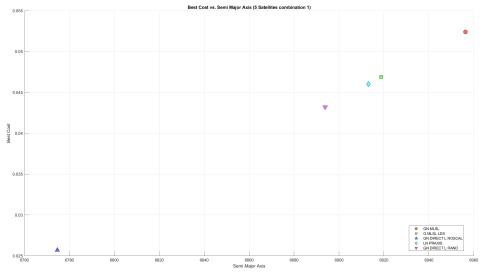

(e) Best Cost Vs Semi Major Axis

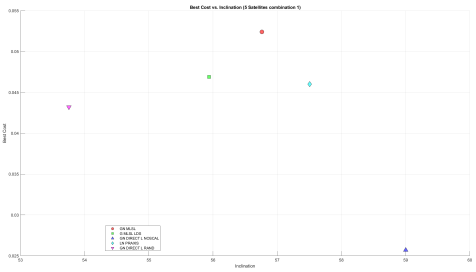

(f) Best Cost Vs Inclination

Figure A.2 5 Satellites combination 1

Table A.2 5 Satellites combination 1

Type	Name	Number of Planes	Satellites per plane	Best Coverage fraction	Best Cost	Best Objective	Best Semi Major Axis	Best Inclination
20	GN MLSL	1	5	1	0,0524	0,9476	6956,2773	56,761
39	G MLSL LDS	1	5	0,9877	0,0469	0,9409	6918,7491	55,9375
4	GN DIRECT L NOSCAL	1	5	0,7495	0,0257	0,7238	6774,6391	59,0017
12	LN PRAXIS	1	5	0,9714	0,046	0,9253	6913,132	57,5044
2	GN DIRECT L RAND	1	5	0,7894	0,0432	0,7462	6893,8272	53,755

A.2.3 5 Satellites Combination 2 Results

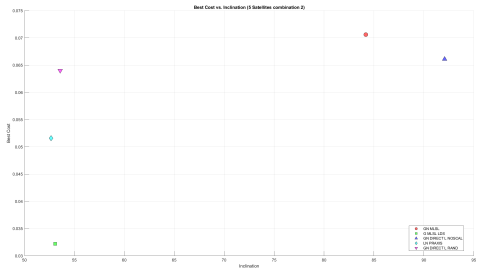

(a) Best Coverage Vs Semi Major Axis

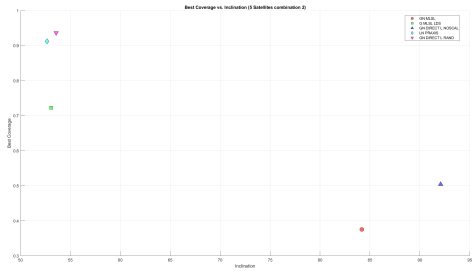

(b) Best Coverage Vs Inclination

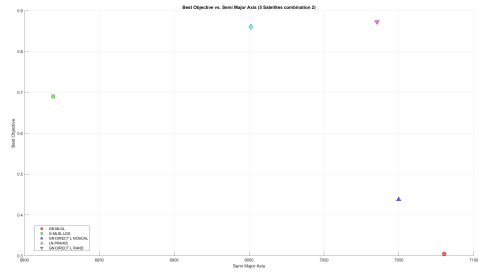

(c) Best Objective Vs Semi Major Axis

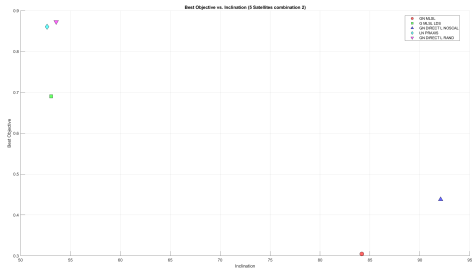

(d) Best Objective Vs Inclination

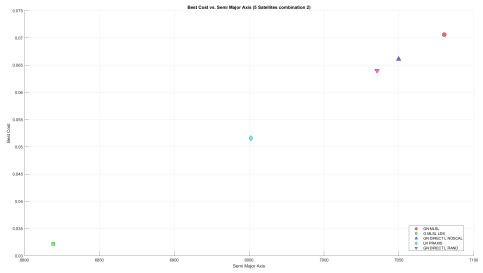

(e) Best Cost Vs Semi Major Axis

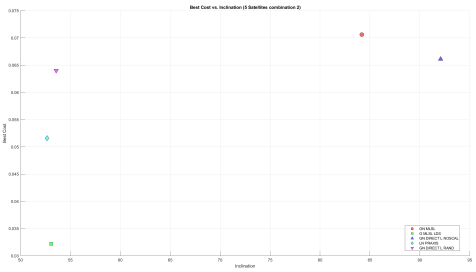

(f) Best Cost Vs Inclination

Figure A.3 5 Satellites combination 2

The Same simulation was done for 10 Satellites in all 4 combinations

Table A.3 5 Satellites combination 2

Type	Name	Number_of_Planes	Satellites_per_plane	Best_Coverage_fraction	Best_Cost	Best_Objective	Best_Semi_Major_Axis	Best_Inclination
20	GN MLSL	5	1	0,3753	0,0706	0,3046	7080,2599	84,1829
39	G MLSL LDS	5	1	0,7229	0,0322	0,6907	6819,1397	53,0664
4	GN DIRECT L NOSCAL	5	1	0,5041	0,0661	0,4379	7049,8098	92,075
12	LN PRAXIS	5	1	0,9121	0,0516	0,8604	6951,1265	52,6717
2	GN DIRECT L RAND	5	1	0,9366	0,064	0,8726	7035,3859	53,578

A.2.4 10 Satellites combination 1

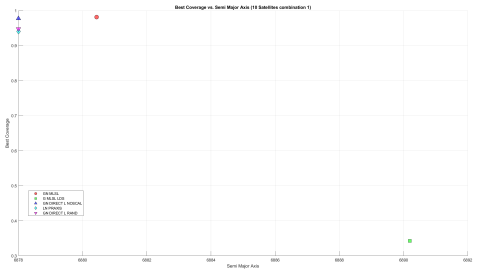

(a) Best Coverage Vs Semi Major Axis

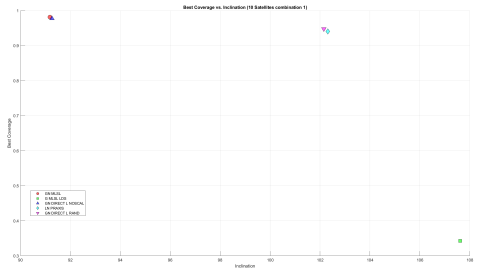

(b) Best Coverage Vs Inclination

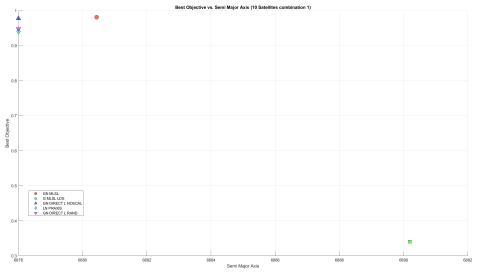

(c) Best Objective Vs Semi Major Axis

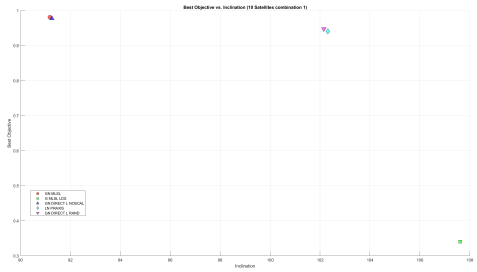

(d) Best Objective Vs Inclination

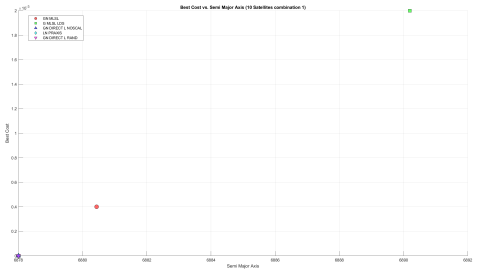

(e) Best Cost Vs Semi Major Axis

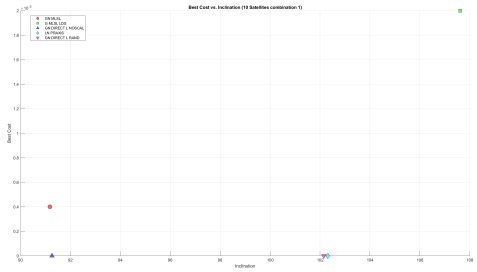

(f) Best Cost Vs Inclination

Figure A.4 10 Satellites comparison combination 1

Table A.4 10 Satellites combination 1

Type	Name	Number_of_Planes	Satellites_per_plane	Best_Coverage_fraction	Best_Cost	Best_Objective	Best_Semi_Major_Axis	Best_Inclination	Best_Inclination
20	GN MLSL	1	10	0,9816	0,0004	0,9812	6880,435	91,1795	91,1795
39	G MLSL LDS	1	10	0,3425	0,002	0,3406	6890,194	107,6172	107,6172
4	GN DIRECT L NOSCAL	1	10	0,9775	0	0,9775	6878	91,2634	91,2634
12	LN PRAXIS	1	10	0,9407	0	0,9407	6878,001	102,311	102,311
2	GN DIRECT L RAND	1	10	0,9479	0	0,9479	6878	102,152	102,152

A.2.5 10 Satellites combination 2

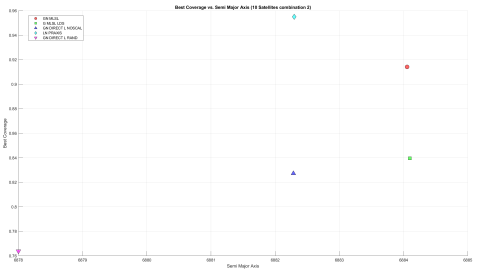

(a) Best Coverage Vs Semi Major Axis

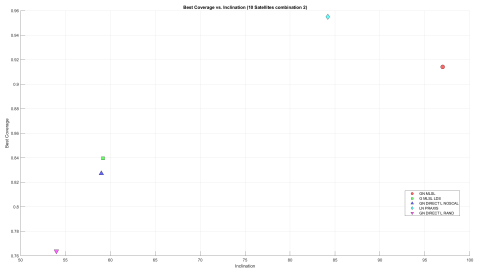

(b) Best Coverage Vs Inclination

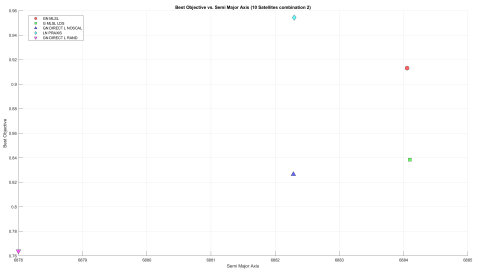

(c) Best Objective Vs Semi Major Axis

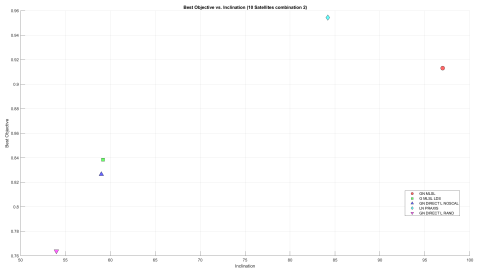

(d) Best Objective Vs Inclination

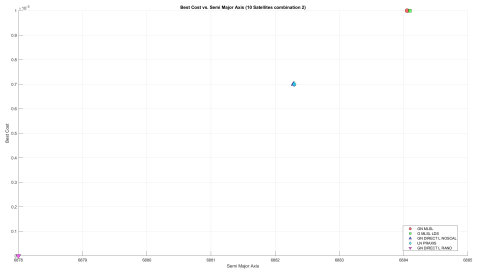

(e) Best Cost Vs Semi Major Axis

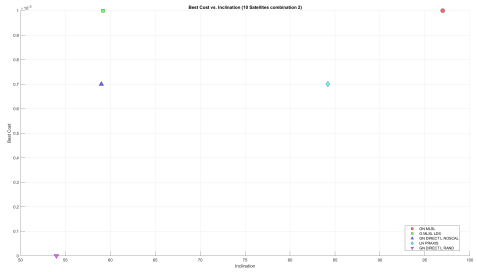

(f) Best Cost Vs Inclination

Figure A.5 10 Satellites comparison combination 2

Table A.5 10 Satellites combination 2

Type	Name	Number_of_Planes	Satellites_per_plane	Best_Coverage_fraction	Best_Cost	Best_Objective	Best_Semi_Major_Axis	Best_Inclination	Best_Inclination
20	GN MLSL	2	5	0,9141	0,001	0,9131	6884,054	96,9791	91,1795
39	G MLSL LDS	2	5	0,8395	0,001	0,8385	6884,097	59,1914	107,6172
4	GN DIRECT L NOSCAL	2	5	0,8272	0,0007	0,8265	6882,283	59	91,2634
12	LN PRAXIS	2	5	0,955	0,0007	0,9543	6882,297	84,1963	102,311
2	GN DIRECT L RAND	2	5	0,7638	0	0,7638	6878	54	102,152

A.2.6 10 Satellites combination 3

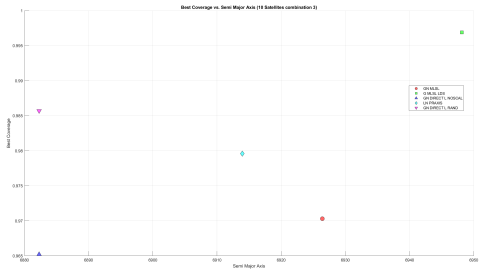

(a) Best Coverage Vs Semi Major Axis

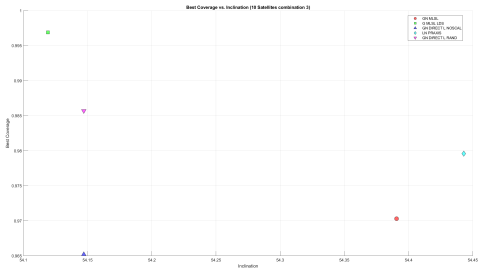

(b) Best Coverage Vs Inclination

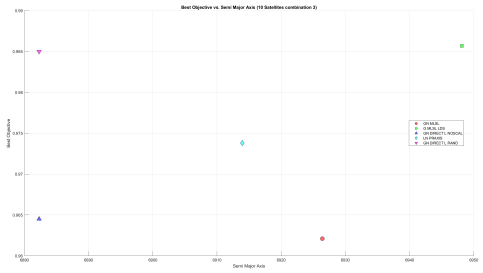

(c) Best Objective Vs Semi Major Axis

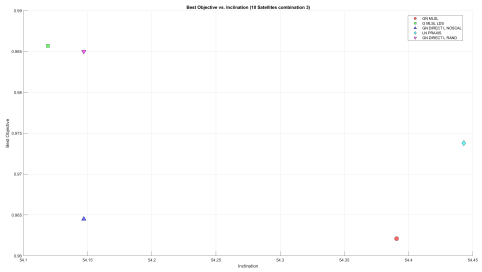

(d) Best Objective Vs Inclination

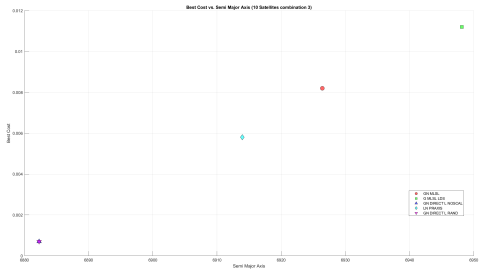

(e) Best Cost Vs Semi Major Axis

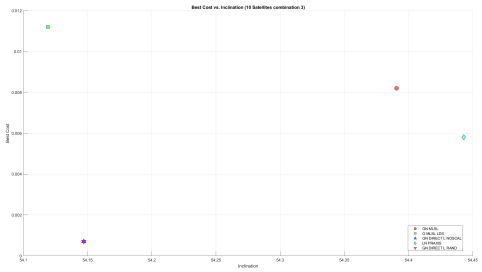

(f) Best Cost Vs Inclination

Figure A.6 10 Satellites comparison combination 3

Table A.6 10 Satellites combination 3

Type	Name	Number_of_Planes	Satellites_per_plane	Best_Coverage_fraction	Best_Cost	Best_Objective	Best_Semi_Major_Axis	Best_Inclination	Best_Inclination
20	GN MLSL	5	2	0,9703	0,0082	0,9621	6926,403	54,3906	91,1795
39	G MLSL LDS	5	2	0,9969	0,0112	0,9857	6948,122	54,1191	107,6172
4	GN DIRECT L NOSCAL	5	2	0,9652	0,0007	0,9645	6882,283	54,147	91,2634
12	LN PRAXIS	5	2	0,9796	0,0058	0,9738	6913,938	54,443	102,311
2	GN DIRECT L RAND	5	2	0,9857	0,0007	0,985	6882,283	54,147	102,152

A.2.7 10 Satellites combination 4

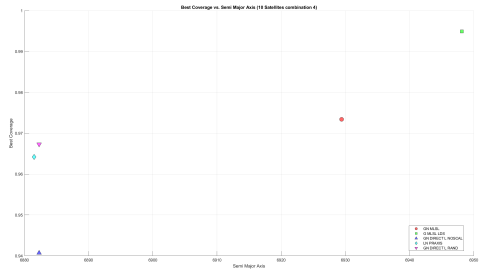

(a) Best Coverage Vs Semi Major Axis

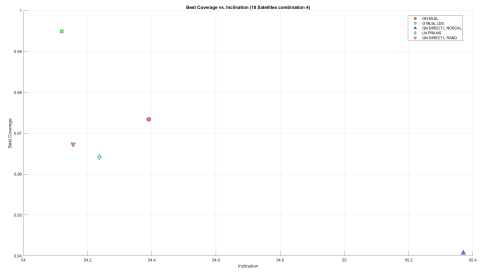

(b) Best Coverage Vs Inclination

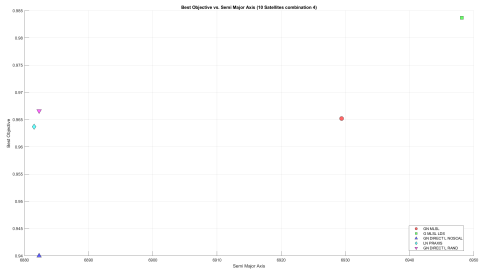

(c) Best Objective Vs Semi Major Axis

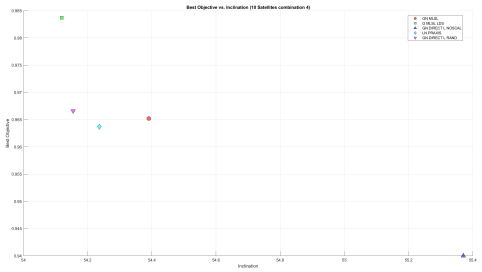

(d) Best Objective Vs Inclination

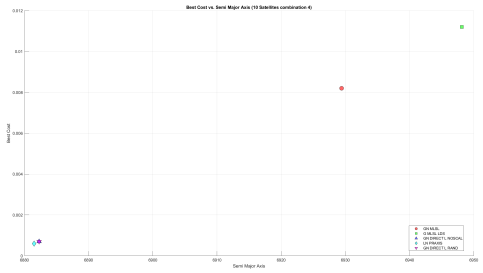

(e) Best Cost Vs Semi Major Axis

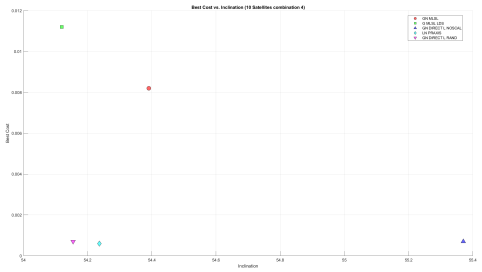

(f) Best Cost Vs Inclination

Figure A.7 10 Satellites comparison combination 4

Table A.7 10 Satellites combination 4

Type	Name	Number_of_Planes	Satellites_per_plane	Best_Coverage_fraction	Best_Cost	Best_Objective	Best_Semi_Major_Axis	Best_Inclination	Best_Inclination
20	GN MLSL	10	1	0,9734	0,0082	0,9652	6929,403	54,3906	91,1795
39	G MLSL LDS	10	1	0,9949	0,0112	0,9837	6948,122	54,1191	107,6172
4	GN DIRECT L NOSCAL	10	1	0,9407	0,0007	0,94	6882,283	55,3704	91,2634
12	LN PRAXIS	10	1	0,9642	0,0006	0,9637	6881,495	54,2367	102,311
2	GN DIRECT L RAND	10	1	0,9673	0,0007	0,9666	6882,283	54,1547	102,152

A.2.8 20 Satellites combination 1

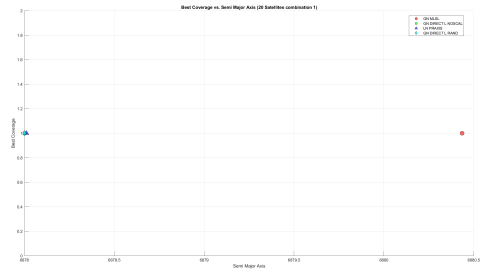

(a) Best Coverage Vs Semi Major Axis

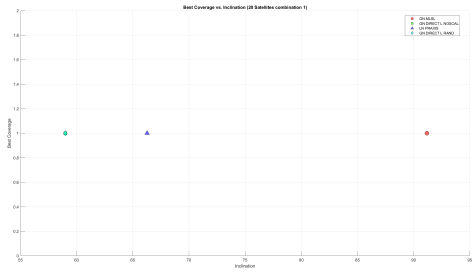

(b) Best Coverage Vs Inclination

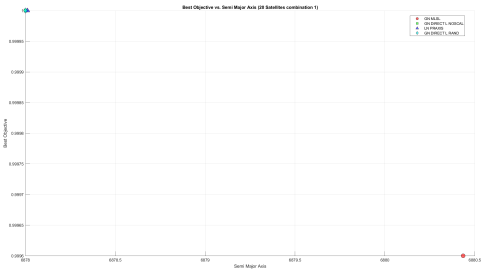

(c) Best Objective Vs Semi Major Axis

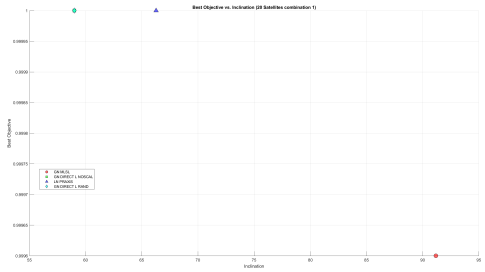

(d) Best Objective Vs Inclination

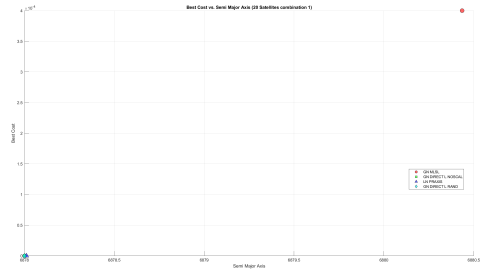

(e) Best Cost Vs Semi Major Axis

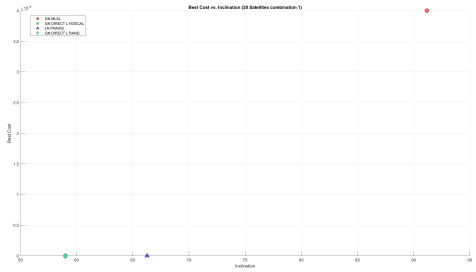

(f) Best Cost Vs Inclination

Figure A.8 20 Satellites comparison combination 1

Table A.8 20 Satellites combination 1

Type	Name	Number_of_Planes	Satellites_per_plane	Best_Coverage_fraction	Best_Cost	Best_Objective	Best_Semi_Major_Axis	Best_Inclination
20	GN MLSL	1	20	1	0,0004	0,9996	6880,435	91,1795
4	GN DIRECT L NOSCAL	1	20	1	0	1	6878	59
12	LN PRAXIS	1	20	1	0	1	6878,011	66,2733
2	GN DIRECT L RAND	1	20	1	0	1	6878	58,9999

A.2.9 20 Satellites combination 2

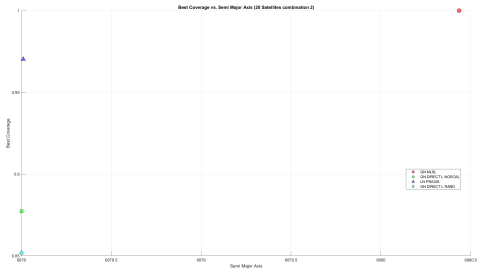

(a) Best Coverage Vs Semi Major Axis

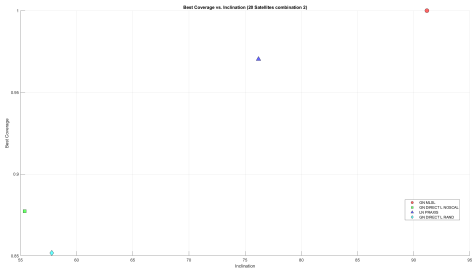

(b) Best Coverage Vs Inclination

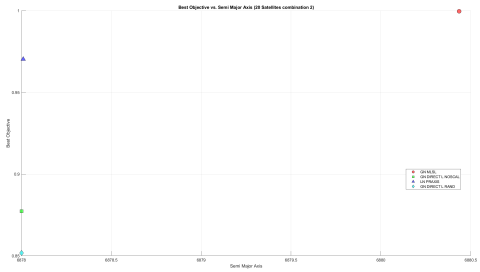

(c) Best Objective Vs Semi Major Axis

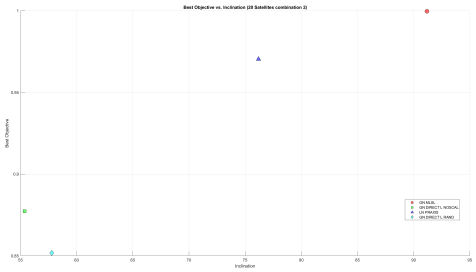

(d) Best Objective Vs Inclination

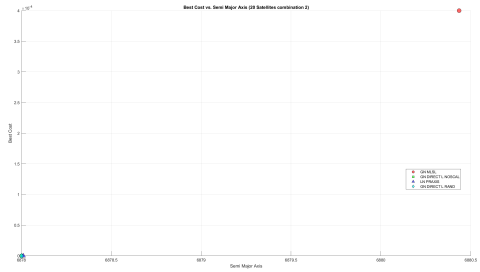

(e) Best Cost Vs Semi Major Axis

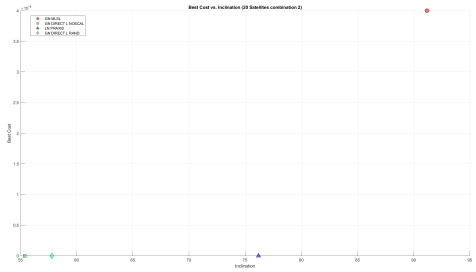

(f) Best Cost Vs Inclination

Figure A.9 20 Satellites comparison combination 2

Table A.9 20 Satellites combination 2

Type	Name	Number_of_Planes	Satellites_per_plane	Best_Coverage_fraction	Best_Cost	Best_Objective	Best_Semi_Major_Axis	Best_Inclination
20	GN MLSL	2	10	1	0,0004	0,9996	6880,435	91,1795
4	GN DIRECT L NOSCAL	2	10	0,8773	0	0,8773	6878	55,3704
12	LN PRAXIS	2	10	0,9703	0	0,9703	6878,01	76,1893
2	GN DIRECT L RAND	2	10	0,8517	0	0,8517	6878	57,7879

A.2.10 20 Satellites combination 3

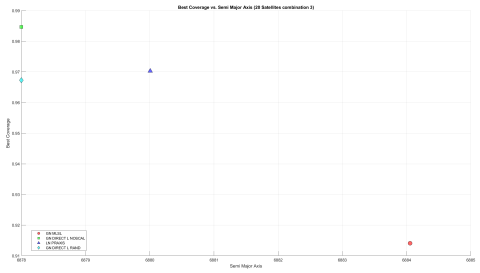

(a) Best Coverage Vs Semi Major Axis

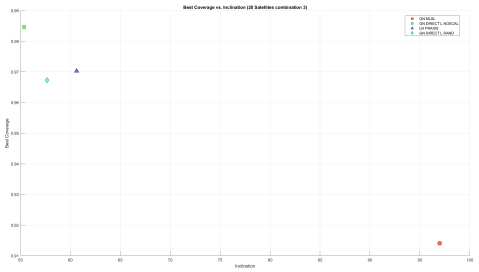

(b) Best Coverage Vs Inclination

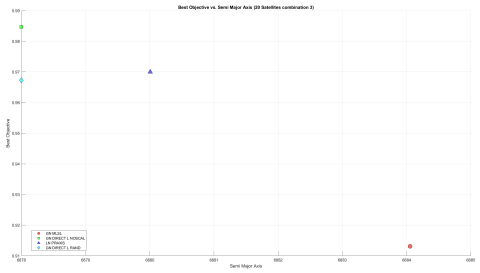

(c) Best Objective Vs Semi Major Axis

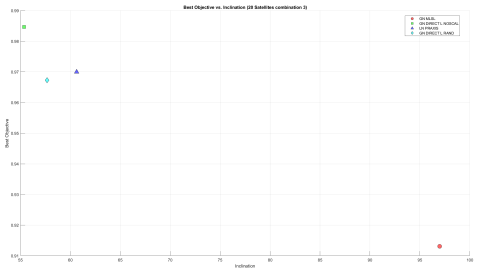

(d) Best Objective Vs Inclination

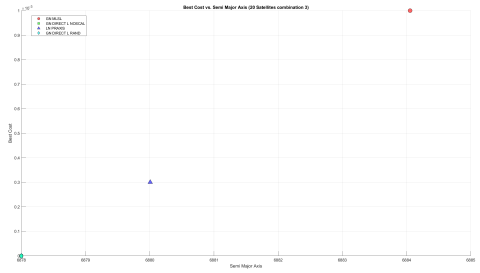

(e) Best Cost Vs Semi Major Axis

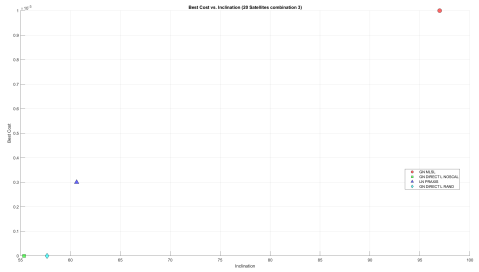

(f) Best Cost Vs Inclination

Figure A.10 20 Satellites comparison combination 3

Table A.10 20 Satellites combination 3

Type	Name	Number_of_Planes	Satellites_per_plane	Best_Coverage_fraction	Best_Cost	Best_Objective	Best_Semi_Major_Axis	Best_Inclination
20	GN MLSL	4	5	0,9141	0,001	0,9131	6884,054	96,9791
4	GN DIRECT L NOSCAL	4	5	0,9847	0	0,9847	6878	55,3704
12	LN PRAXIS	4	5	0,9703	0,0003	0,97	6880,006	60,6272
2	GN DIRECT L RAND	4	5	0,9673	0	0,9673	6878	57,6562

A.2.11 20 Satellites combination 4

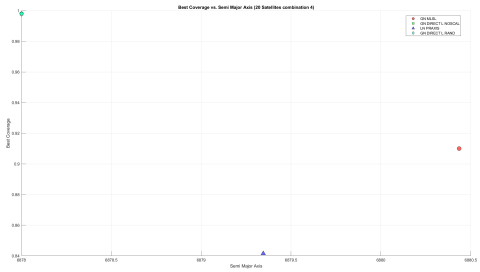

(a) Best Coverage Vs Semi Major Axis

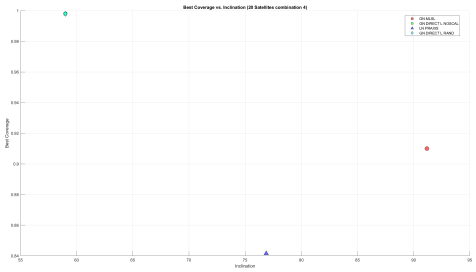

(b) Best Coverage Vs Inclination

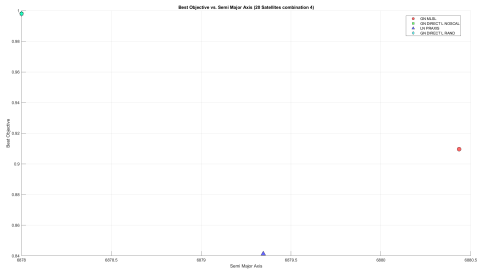

(c) Best Objective Vs Semi Major Axis

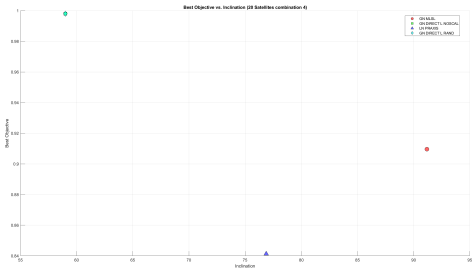

(d) Best Objective Vs Inclination

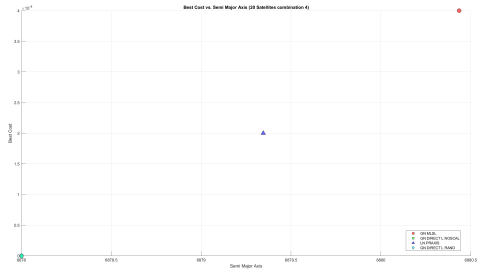

(e) Best Cost Vs Semi Major Axis

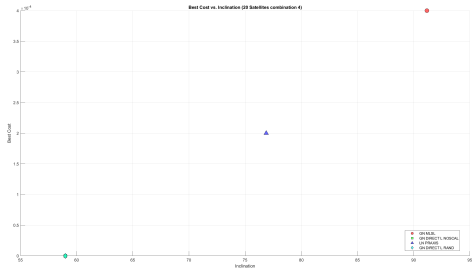

(f) Best Cost Vs Inclination

Figure A.11 20 Satellites comparison combination 4

Table A.11 20 Satellites combination 4

Type	Name	Number_of_Planes	Satellites_per_plane	Best_Coverage_fraction	Best_Cost	Best_Objective	Best_Semi_Major_Axis	Best_Inclination
20	GN MLSL	5	4	0,91	0,0004	0,9096	6880,435	91,1795
4	GN DIRECT L NOSCAL	5	4	0,998	0	0,998	6878	59
12	LN PRAXIS	5	4	0,8415	0,0002	0,8413	6879,345	76,8765
2	GN DIRECT L RAND	5	4	0,998	0	0,998	6878	58,9999

A.2.12 20 Satellites combination 5

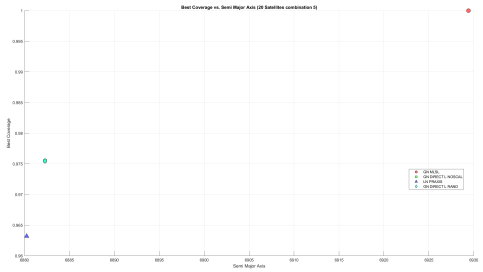

(a) Best Coverage Vs Semi Major Axis

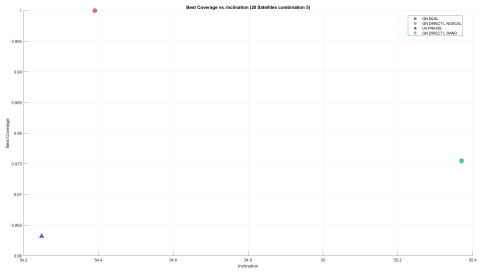

(b) Best Coverage Vs Inclination

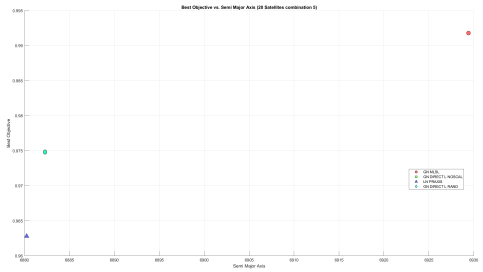

(c) Best Objective Vs Semi Major Axis

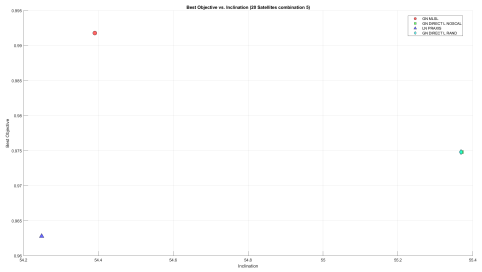

(d) Best Objective Vs Inclination

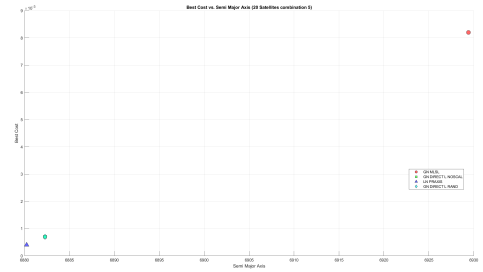

(e) Best Cost Vs Semi Major Axis

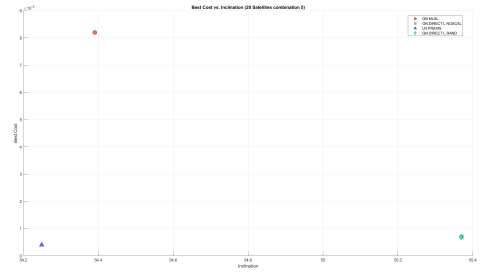

(f) Best Cost Vs Inclination

Figure A.12 20 Satellites comparison combination 5

Table A.12 20 Satellites combination 5

Type	Name	Number_of_Planes	Satellites_per_plane	Best_Coverage_fraction	Best_Cost	Best_Objective	Best_Semi_Major_Axis	Best_Inclination
20	GN MLSL	10	2	1	0,0082	0,9918	6929,403	54,3906
4	GN DIRECT L NOSCAL	10	2	0,9755	0,0007	0,9748	6882,283	55,3704
12	LN PRAXIS	10	2	0,9632	0,0004	0,9628	6880,246	54,2486
2	GN DIRECT L RAND	10	2	0,9755	0,0007	0,9748	6882,283	55,3687

A.2.13 20 Satellites combination 6

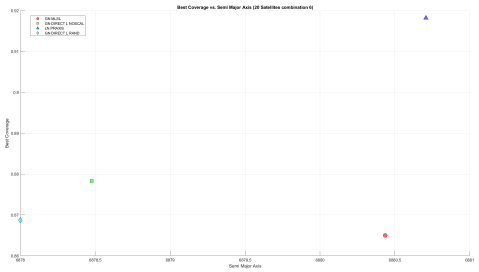

(a) Best Coverage Vs Semi Major Axis

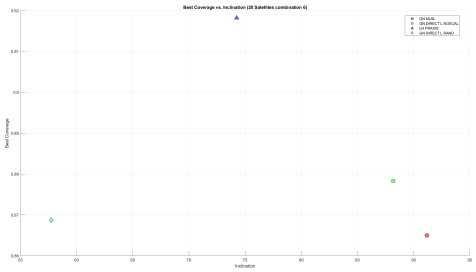

(b) Best Coverage Vs Inclination

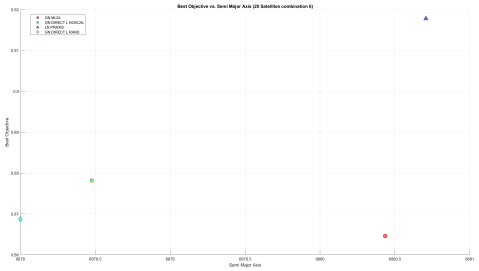

(c) Best Objective Vs Semi Major Axis

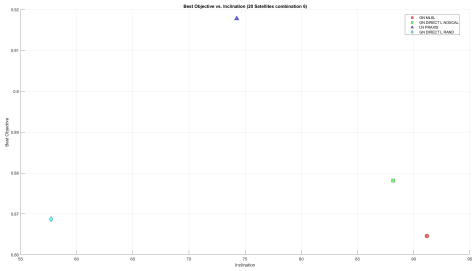

(d) Best Objective Vs Inclination

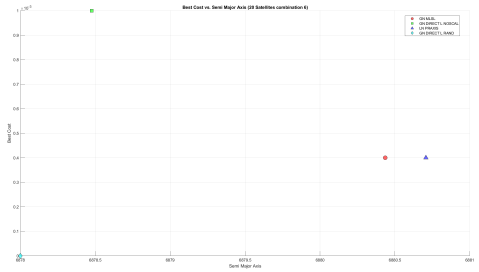

(e) Best Cost Vs Semi Major Axis

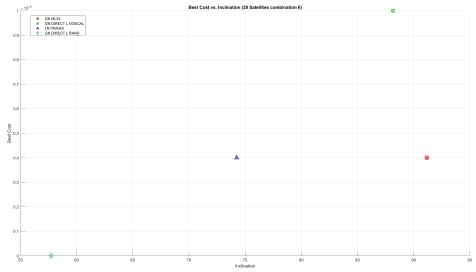

(f) Best Cost Vs Inclination

Figure A.13 20 Satellites comparison combination 6

Table A.13 20 Satellites combination 6

Type	Name	Number_of_Planes	Satellites_per_plane	Best_Coverage_fraction	Best_Cost	Best_Objective	Best_Semi_Major_Axis	Best_Inclination
20	GN MLSL	20	1	0,865	0,0004	0,8646	6880,435	91,1795
4	GN DIRECT L NOSCAL	20	1	0,8783	0,001	0,8782	6878,476	88,1715
12	LN PRAXIS	20	1	0,9182	0,0004	0,9178	6880,706	74,2486
2	GN DIRECT L RAND	20	1	0,8687	0	0,8687	6878	57,7396

A.3 Impact of Ground Stations

A.3.1 Decentralized

Table A.14 Total time taken - Decentralized

Time (min) / Satellites	One ground station	Two ground stations	Five ground stations
5	1352,6	1352,6	1334,9
10	609,95	609,95	591,05
20	90,4	39,2	39,2
30	241	241	241
40	1,25	1,25	1,25
50	44,3	40,05	40,05
100	11,65	11.65	11,65
200	1,25	1,25	1,25
300	6,1833	6,1833	6,1667
400	1,25	1,25	1,25
500	7,7	7,7	7,7
600	0,033	0,033	0,033
700	5,45	5,45	5,45
800	0,3	0,3	0,3
900	0,4833	0,4833	0,4833
1000	0,4833	0,4833	0,4833

Table A.15 Total time taken after Image capture - Decentralized

Time (min) / Satellites	One ground station	Two ground stations	Five ground stations
5	61	61	43,3
10	21,05	21,05	2,15
20	51,25	0,05	0,05
30	0,1	0,1	0,1
40	0,01667	0,01667	0,01667
50	4,3	0,05	0,05
100	0,01667	0,01667	0,01667
200	0,01667	0,01667	0,01667
300	0,033	0,033	0,01667
400	0,01667	0,01667	0,01667
500	0,01667	0,01667	0,01667
600	0,016833	0,016833	0,016833
700	0,01667	0,01667	0,01667
800	0,1667	0,1667	0,1667
900	0,01667	0,01667	0,01667
1000	0,01667	0,01667	0,01667

A.3.2 Centralized

Table A.16 Total time taken - Centralized

Time (min) / Satellites	One ground station	Two ground stations	Five ground stations
5	1352,6	1352,6	1334,9
10	611169,4	611169,4	611150
20	111,1	111,1	85,2167
30	2328,2	2303,8	2120,6
40	394,833	394,833	394,75
50	106,95	106,95	86
100	205,8	205,8	181,65
200	394,75	394,75	394,75
300	394,75	394,75	394,75
400	204,65	204,65	204,65
500	107	107	91,1667
600	204,667	204,667	204,667
700	106,95	106,95	86
800	204,667	204,667	204,667
900	204,667	107	86
1000	204,667	204,667	204,667

Table A.17 Time taken after Image captured - Centralized

Time (min) / Satellites	One ground station	Two ground stations	five ground stations
5	61	61	43,3
10	610580,5	610580,5	610561,1
20	71,95	71,95	46,083
30	2087,3	2062,83	1876,6
40	33,16	33,16	33,083
50	66,95	66,95	46
100	52,25	52,25	28,1
200	109,05	109,05	109,05
300	199	199	199
400	27	27	27
500	44	44	28,166
600	26,33	26,33	26,33
700	76,5	76,5	55
800	27	27	27
900	164,6167	66,95	45,95
1000	26,6	26,6	26,6

A.3.3 Partially Centralized

Table A.18 Total time taken - Partially Centralized

Time (min) / Satellites	One ground station	Two ground stations	Five ground stations
5	1352,6	1352,6	1334,9
10	1038,4	726,45	591,05
20	111,1	111,1	85,2
30	306,95	241	241
40	204,65	132,75	25,3667
50	106,95	106,95	86
100	11,667	12	12
200	204,633	132,7167	25,3667
300	204,633	132,7167	25,3667
400	204,65	132,75	25,3667
500	8,95	8,95	8,95
600	204,667	132,75	0,5
700	8,95	8,95	8,95
800	204,65	132,75	0,3167
900	8,95	8,95	8,95
1000	204,65	132,75	0,6

Table A.19 Time taken after Image captured - Partially Centralized

Time (min) / Satellites	One ground station	Two ground stations	five ground stations
5	61	61	43,3
10	449,5	137,55	2,15
20	71,95	71,95	46,1
30	66,05	0,1	0,1
40	203,416	131,516	24,133
50	66,95	66,95	46
100	0,033	0,033	0,033
200	203,4	131,4833	24,133
300	198,4833	126,5667	19,21667
400	203,4167	131,5167	24,133
500	1,2667	1,2667	1,2667
600	204,5	132,73	0,33
700	3,5	3,5	3,5
800	204,3667	132,4667	0,033
900	8,4833	8,4833	8,4833
1000	204,15	132,25	0,1

A.4 Non Linear Optimizer

Table A.20 Non Linear Optimizer 5 Satellites combination 1

Type	Name	Planes	Satellites	Best Coverage fraction	Best Cost	Best Objective	Best Semi Major Axis	Best Inclination
0	GN DIRECT	1	5	0,7914	0,0432	0,7482	6893,856	53,7821
1	GN DIRECT L	1	5	0,7894	0,0432	0,7462	6893,8273	53,7572
2	GN DIRECT L RAND	1	5	0,7894	0,0432	0,7462	6893,8272	53,755
3	GN DIRECT NOSCAL	1	5	0,9826	0,0062	0,9764	6916,5432	55,3704
4	GN DIRECT L NOSCAL	1	5	0,9826	0,0062	0,9764	6916,5432	55,3704
5	GN DIRECT L RAND NOSCAL	1	5	0,9826	0,0062	0,9764	6916,5432	55,3704
6	GN ORIG DIRECT	1	5	0,7986	0,0432	0,7554	6893,856	53,8418
7	GN ORIG DIRECT L	1	5	0,7975	0,0432	0,7543	6893,856	53,8363
8	GD STOGO	1	5	0	0	0	6878	45
9	GD STOGO RAND	1	5	0	0	0	6878	45
10	LD LBFGS NOCEDAL	1	5	0	0	0	6878	45
11	LD LBFGS	1	5	0	0	0	6878	45
12	LN PRAXIS	1	5	0,9714	0,046	0,9253	6913,132	57,5044
13	LD VAR1	1	5	0	0	0	6878	45
14	LD VAR2	1	5	0	0	0	6878	45
15	LD TNEWTON	1	5	0	0	0	6878	45
16	LD TNEWTON RESTART	1	5	0	0	0	6878	45
17	LD TNEWTON PRECOND	1	5	0	0	0	6878	45
18	LD TNEWTON PRECOND RESTART	1	5	0	0	0	6878	45
19	GN CRS2 LM	1	5	0,6933	0,0002	0,6931	6879,2175	53,4309
20	GN MLSL	1	5	1	0,0524	0,9476	6956,2773	56,761
21	GD MLSL	1	5	1	0,0524	0,9476	6956,2773	56,761
22	GN MLSL LDS	1	5	1	0,0524	0,9476	6956,2773	56,761
23	GD MLSL LDS	1	5	0,9877	0,0469	0,9409	6918,7491	55,9375

Table A.20 continued from previous page

Type	Name	Planes	Satellites	Best Coverage fraction	Best Cost	Best Objective	Best Semi Major Axis	Best Inclination
24	LD MMA	1	5	0,9877	0,0469	0,9409	6918,7491	55,9375
25	LN COBYLA	1	5	0	0	0	6878	45
26	LN NEWUOA	1	5	0,9509	0,0461	0,9048	6913,6658	58,3907
27	LN NEWUOA BOUND	1	5	0,9202	0,0586	0,8616	6998,8015	82,909
28	LN NELDERMEAD	1	5	0,9305	0,0586	0,8719	6998,5505	91,9989
29	LN SBPLX	1	5	0,9448	0,0551	0,8897	6974,7602	73,0402
30	LN AUGLAG	1	5	0,9172	0,0552	0,862	6975,5071	76,0405
31	LD AUGLAG	1	5	0,9172	0,0552	0,862	6975,5071	76,0405
32	LN AUGLAG EQ	1	5	0	0	0	6878	45
33	LD AUGLAG EQ	1	5	0	0	0	6878	45
34	LN BOBYQA	1	5	0,9264	0,0581	0,8683	6994,8908	93,7606
35	GN ISRES	1	5	0,8691	0,0078	0,8613	6926,9381	54,0708
36	AUGLAG	1	5	0	0	0	6878	45
37	AUGLAG EQ	1	5	0	0	0	6878	45
38	G MLSL	1	5	1	0,0524	0,9476	6956,2773	56,761
39	G MLSL LDS	1	5	0,9877	0,0469	0,9409	6918,7491	55,9375
40	LD SLSQP	1	5	0	0	0	6878	45
41	LD CCSAQ	1	5	0	0	0	6878	45
42	GN ESCH	1	5	0,9581	0,0472	0,9109	6921,1042	59,9125
43	GN AGS	1	5	0	0	0	6878	45

Table A.21 Non Linear Optimizer 5 Satellites combination 2

Type	Name	Planes	Satellites	Best Coverage fraction	Best Cost	Best Objective	Best Semi Major Axis	Best Inclination
0	GN DIRECT	5	1	0,9315	0,064	0,8675	7035,3283	53,6294
1	GN DIRECT L	5	1	0,9325	0,064	0,8685	7035,3283	53,6228
2	GN DIRECT L RAND	5	1	0,9366	0,064	0,8726	7035,3859	53,578
3	GN DIRECT NOSCAL	5	1	0,5041	0,0661	0,4379	7049,8098	92,075
4	GN DIRECT L NOSCAL	5	1	0,5041	0,0661	0,4379	7049,8098	92,075
5	GN DIRECT L RAND NOSCAL	5	1	0,5041	0,0661	0,4379	7049,8098	92,075
6	GN ORIG DIRECT	5	1	0,9315	0,064	0,8675	7035,3859	53,6377
7	GN ORIG DIRECT L	5	1	0,9305	0,064	0,8665	7035,2999	53,6451
8	GD STOGO	5	1	0	0	0	6878	45
9	GD STOGO RAND	5	1	0	0	0	6878	45
10	LD LBFGS NOCEDAL	5	1	0	0	0	6878	45
11	LD LBFGS	5	1	0	0	0	6878	45
12	LN PRAXIS	5	1	0,9121	0,0516	0,8604	6951,1265	52,6717
13	LD VAR1	5	1	0	0	0	6878	45
14	LD VAR2	5	1	0	0	0	6878	45
15	LD TNEWTON	5	1	0	0	0	6878	45
16	LD TNEWTON RESTART	5	1	0	0	0	6878	45
17	LD TNEWTON PRECOND	5	1	0	0	0	6878	45
18	LD TNEWTON PRECOND RESTART	5	1	0	0	0	6878	45
19	GN CRS2 LM	5	1	0,9315	0,0544	0,8771	6970,0854	52,6105
20	GN MLSL	5	1	0,3753	0,0706	0,3046	7080,2599	84,1829
21	GD MLSL	5	1	0,3753	0,0706	0,3046	7080,2599	84,1829
22	GN MLSL LDS	5	1	0,3753	0,0706	0,3046	7080,2599	84,1829
23	GD MLSL LDS	5	1	0,7117	0,0273	0,6843	7048,7334	101,1094
24	LD MMA	5	1	0	0	0	6878	45
25	LN COBYLA	5	1	0	0	0	6878	45

Table A.21 continued from previous page

Type	Name	Planes	Satellites	Best Coverage fraction	Best Cost	Best Objective	Best Semi Major Axis	Best Inclination
26	LN NEWUOA	5	1	0,227	0,074	0,153	7103,4247	69,5
27	LN NEWUOA BOUND	5	1	0,4785	0,0656	0,4129	7046,1101	91,9789
28	LN NELDERMEAD	5	1	0,6063	0,059	0,5473	7001,2294	93,1681
29	LN SBPLX	5	1	0,5204	0,0665	0,454	7051,9394	82,5842
30	LN AUGLAG	5	1	0,5562	0,0659	0,4903	7048,1419	92,375
31	LD AUGLAG	5	1	0,5562	0,0659	0,4903	7048,1419	92,375
32	LN AUGLAG EQ	5	1	0	0	0	6878	45
33	LD AUGLAG EQ	5	1	0	0	0	6878	45
34	LN BOBYQA	5	1	0,5838	0,0189	0,5649	6996,2757	93,0918
35	GN ISRES	5	1	0,2771	0,0347	0,2424	7094,6767	90,1582
36	AUGLAG	5	1	0	0	0	6878	45
37	AUGLAG EQ	5	1	0	0	0	6878	45
38	G MLSL	5	1	0,3753	0,0706	0,3046	7080,2599	84,1829
39	G MLSL LDS	5	1	0,7117	0,0273	0,6843	7048,7334	101,1094
40	LD SLSQP	5	1	0	0	0	6878	45
41	LD CCSAQ	5	1	0	0	0	6878	45
42	GN ESCH	5	1	0,8579	0,0788	0,779	7136,1185	63,6479
43	GN AGS	5	1	0	0	0	6878	45

A.5 Analsysis of Higher Averages: 10 Satellites

Table A.22 Analysis of Higher Averages for 10 Satellites (Note: Time is in minutes, D is Decentralized and PC is Partially Centralized)

Type	Name	Number of Planes	Satellites per plane	Best Coverage fraction	Best Cost	Best Objective	Best Semi Major Axis	Best Inclination	D	PC	D Two Ground Stations	PC Two Ground Stations	D Five Ground Stations	PC Five Ground Stations
20	GN MLSL	1	10	0,9816	0,0004	0,9812	6880,4353	91,1795	826,25	852,25	826,25	832,2	541,75	598
4	GN DIRECT L NOSCAL	1	10	0,9775	0	0,9775	6878	91,2634	825,85	851,833	825,85	832,05	541,45	597,65
20	GN MLSL	2	5	0,9141	0,001	0,9131	6884,0535	96,9791	780,95	851,85	780,95	851,85	536,55	597,65
4	GN DIRECT L NOSCAL	2	5	0,8272	0,0007	0,8265	6882,2826	59	1302,2	1330,95	1302,2	1330,95	1302,15	1312,35
20	GN MLSL	5	2	0,9703	0,0082	0,9621	6926,4026	54,3906	2768,65	2777,5	2768,65	2777,5	2753,9	2760,6
4	GN DIRECT L NOSCAL	5	2	0,9652	0,0007	0,9645	6882,2826	54,147	25989,45	26595,25	25989,45	26283,95	25989,45	26041
20	GN MLSL	10	1	0,9734	0,0082	0,9652	6929,4026	54,3906	15680,3	15695,1	15664,7	15695,1	15664,7	15675,85
4	GN DIRECT L NOSCAL	10	1	0,9407	0,0007	0,94	6882,2826	55,3704	31709,4	32277,8	31657,8	31966,9	31657,8	31724,1

A.6 Analysis of Higher Averages: 20 Satellites

Table A.23 Analysis of Higher Averages for 20 Satellites (Note: Time is in minutes, D is Decentralized and PC is Partially Centralized)

Type	Name	Number of Planes	Satellites per plane	Best Coverage fraction	Best Cost	Best Objective	Best Semi Major Axis	Best Inclination	D	PC	D Two Ground Stations	PC Two Ground Stations	D Five Ground Stations	PC Five Ground Stations
20	GN MLSL	1	20	1	0,0004	0,9996	6880,4353	91,1795	822,15	852,25	822,15	832,2	541,75	598
4	GN DIRECT L NOSCAL	1	20	1	0	1	6878	59	992,6	1037,75	715,65	728,65	487,85	499,8
20	GN MLSL	2	10	1	0,0004	0,9996	6880,4353	91,1795	826,25	852,25	826,25	832,2	541,75	598
4	GN DIRECT L NOSCAL	2	10	0,8773	0	0,8773	6878	55,3704	501,8	1038,15	501,8	726,95	482,75	483,9
20	GN MLSL	4	5	0,9141	0,001	0,9131	6884,0535	96,9791	172,1	205,8	172,1	205,8	172,1	205,8
4	GN DIRECT L NOSCAL	4	5	0,9847	0	0,9847	6878	55,3704	230,7	1038,15	229,35	229,4	229,35	229,4
20	GN MLSL	5	4	0,91	0,0004	0,9096	6880,4353	91,1795	394,8	394,8	394,8	394,8	394,75	394,8
4	GN DIRECT L NOSCAL	5	4	0,998	0	0,998	6878	59	4415,65	4462,8	4415,65	4462,8	4415,6	4438,8
20	GN MLSL	10	2	1	0,0082	0,9918	6929,4026	54,3906	2768,65	2777.5	2752,75	2777.5	2752,7	2.760.667
4	GN DIRECT L NOSCAL	10	2	0,9755	0,0007	0,9748	6882,2826	55,3704	31524,7	32277,8	31515,5	31563,3	31515,45	31522
20	GN MLSL	20	1	0,865	0,0004	0,8646	6880,4353	91,1795	374,8	394,75	323,65	394,75	323,65	394,75
4	GN DIRECT L NOSCAL	20	1	0,8783	0,001	0,8782	6878,4758	88,1715	90,4	111,1	39,2	111,1	39,2	85,2

A.7 Satellite Optimization results

Table A.24 10 Satellites Optimization

Type	Name	Number of Planes	Satellites per plane	Best Coverage fraction	Best Cost	Best Objective	Best Semi Major Axis	Best Inclination	Decentralized	Time taken after image captured	Centralized	Time taken after image captured	Decentralized Two Groundstations	Time taken after image captured	Centralized Two Groundstations	Time taken after image captured	Decentralized five Groundstations	Time taken after image captured	Centralized five Groundstations	Time taken after image captured
20	GN MLSL	1	10	0,9816	0,0004	0,9812	6880,4353	91,1795	826,25	284,55	852,25	310,55	826,25	284,55	832,2	290,5	541,75	0,05	598	56,3
39	G MLSL LDS	1	10	0,3425	0,002	0,3406	6890,1944	107,6172	2014,1	0,05	3149,95	461,45	2014,1	0,05	2983,45	294,95	2014,1	0,05	2736,1	47,6
4	GN DIRECT L NOSCAL	1	10	0,9775	0	0,9775	6878	91,2634	825,85	284,45	851,833	310,45	825,85	284,45	832,05	290,65	541,45	0,05	597,65	56,25
12	LN PRAXIS	1	10	0,9407	0	0,9407	6878,0006	102,311	708	147,85	760,15	200	708	147,85	760,15	200	560,2	0,005	596,15	36
2	GN DIRECT L RAND	1	10	0,9479	0	0,9479	6878	102,152	716,5167	156,367	760,25	200,1	716,5167	156,367	760,25	200,1	560,1667	16,833	596,15	36
20	GN MLSL	2	5	0,9141	0,001	0,9131	6884,0535	96,9791	780,95	248,4	851,85	315,35	780,95	248,4	851,85	315,35	536,55	4	597,65	61,15
39	G MLSL LDS	2	5	0,8395	0,001	0,8385	6884,0967	59,1914	27609,7	40,7	28038	469	27609,7	40,7	27728,45	159,45	27590,9	21,9	27590,95	21,95
4	GN DIRECT L NOSCAL	2	5	0,8272	0,0007	0,8265	6882,2826	59	1302,2	12,2	1330,95	40,95	1302,2	12,2	1330,95	40,95	1302,15	12,15	1312,35	22,35
12	LN PRAXIS	2	5	0,955	0,0007	0,9543	6882,297	84,1963	793,2	260,8	944,25	411,85	793,2	260,8	829,6	297,2	536,3	3,9	599,15	66,75
2	GN DIRECT L RAND	2	5	0,7638	0	0,7638	6878	54	609,95	21,05	1038,4	449,5	609,95	21,05	726,45	137,55	591,05	2,15	591,05	2,15
20	GN MLSL	5	2	0,9703	0,0082	0,9621	6926,4026	54,3906	2768,65	16	2777,5	24,85	2768,65	16	2777,5	24,85	2753,9	1,25	2760,6	7,95
39	G MLSL LDS	5	2	0,9969	0,0112	0,9857	6948,1221	54,1191	1588,95	11,9	2493,5	916,45	1588,95	11,9	1668,55	91,5	1588,95	11,9	1625,2	48,15
4	GN DIRECT L NOSCAL	5	2	0,9652	0,0007	0,9645	6882,2826	54,147	25989,45	14,3	26595,25	620,1	25989,45	14,3	26283,95	308,8	25989,45	14,3	26041	65,8
12	LN PRAXIS	5	2	0,9796	0,0058	0,9738	6913,9376	54,443	3293,55	12,45	3905,05	623,95	3293,55	12,45	3591,85	310,75	3293,55	12,45	3347,2	66,1
2	GN DIRECT L RAND	5	2	0,9857	0,0007	0,985	6882,2826	54,147	25989,45	14,3	26595,25	620,1	25989,45	14,3	26283,95	308,8	25989,45	14,3	26041	65,8
20	GN MLSL	10	1	0,9734	0,0082	0,9652	6929,4026	54,3906	15680,3	15,7	15695,1	30,5	15664,7	0,1	15695,1	30,5	15664,7	0,1	15675,85	11,26
39	G MLSL LDS	10	1	0,9949	0,0112	0,9837	6948,1221	54,1191	1629,45	52,4	2493,5	916,45	1577,1	0,05	1668,55	91,5	1577,1	0,05	1625,2	48,15
4	GN DIRECT L NOSCAL	10	1	0,9407	0,0007	0,94	6882,2826	55,3704	31709,4	51,65	32277,8	620,05	31657,8	0,1	31966,9	309,15	31657,8	0,1	31724,1	66,35
12	LN PRAXIS	10	1	0,9642	0,0006	0,9637	6881,4946	54,2367	31700,85	51,75	32269,1	620	31649,2	0,1	31957,9	308,8	31649,15	0,05	31715	65,9
2	GN DIRECT L RAND	10	1	0,9673	0,0007	0,9666	6882,2826	54,1547	26027	51,85	26595,25	620,1	25975,25	0,1	26284	308,85	25975,2	0,05	26041,05	65,9

A.8 Additional Nodes

A.8.1 Impact of Additional Central Nodes on Total Time Delay.

This analysis examines the effect of increasing the number of central nodes in the Centralized configuration. This layout is similar to the Centralized layout but includes one to ten additional central nodes, as shown in Table. A.25. All satellites can only communicate with one central node, including the additional ones, which can downlink images to the ground station. These additional nodes provide redundancy and potentially increase the robustness of the network while also helping reduce bottlenecks in the network. The total time delays are compared across configurations with one, two, and five ground stations to understand the impact of these additional central nodes.

Given that the centralized configuration demonstrated the worst performance with maximum delays, it is interesting to explore whether adding additional nodes that can downlink data will help reduce delays and improve overall performance.

Table A.25 Additional Nodes

Satellites	Nodes	Central Nodes									
5	1	const[0]									
10	1	const[0]									
20	2	const[0]	const[10]								
30	3	const[0]	const[10]	const[20]							
40	4	const[0]	const[10]	const[20]	const[30]						
50	5	const[0]	const[10]	const[20]	const[30]	const[40]					
100	10	const[0]	const[10]	const[20]	const[30]	const[40]	const[50]	const[60]	const[70]	const[80]	const[90]
200	10	const[0]	const[20]	const[40]	const[60]	const[80]	const[100]	const[120]	const[140]	const[160]	const[180]
300	10	const[0]	const[30]	const[60]	const[90]	const[120]	const[150]	const[180]	const[210]	const[240]	const[270]
400	10	const[0]	const[40]	const[80]	const[120]	const[160]	const[200]	const[240]	const[280]	const[320]	const[360]
500	10	const[0]	const[50]	const[100]	const[150]	const[200]	const[250]	const[300]	const[350]	const[400]	const[450]
600	10	const[0]	const[60]	const[120]	const[180]	const[240]	const[300]	const[360]	const[420]	const[480]	const[540]
700	10	const[0]	const[70]	const[140]	const[210]	const[280]	const[350]	const[420]	const[490]	const[560]	const[630]
800	10	const[0]	const[80]	const[160]	const[240]	const[320]	const[400]	const[480]	const[560]	const[640]	const[720]
900	10	const[0]	const[90]	const[180]	const[270]	const[360]	const[450]	const[540]	const[630]	const[720]	const[810]
1000	10	const[0]	const[100]	const[200]	const[300]	const[400]	const[500]	const[600]	const[700]	const[800]	const[900]

A.8.1.1 Total Time Taken to complete the task

One Ground Station

- General Trend: There is a slight decrease in total time compared to the centralized configuration.
- No Change: Satellite counts of 20, 400, 600, 800, and 1000 show no change.

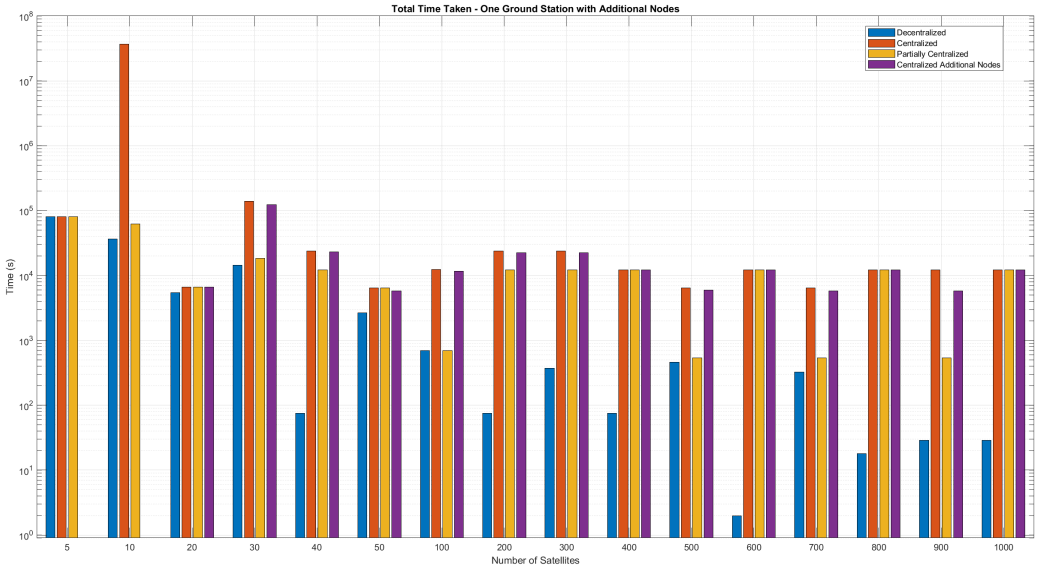

Figure A.14 Total Time Taken - One Ground Station with Additional Nodes.

Two Ground Stations

- General Trend: Slight decrease in total time for most satellite counts compared to the centralized configuration.
- No Change: Satellite counts of 20, 400, 600, 800, and 1000 remain unchanged.

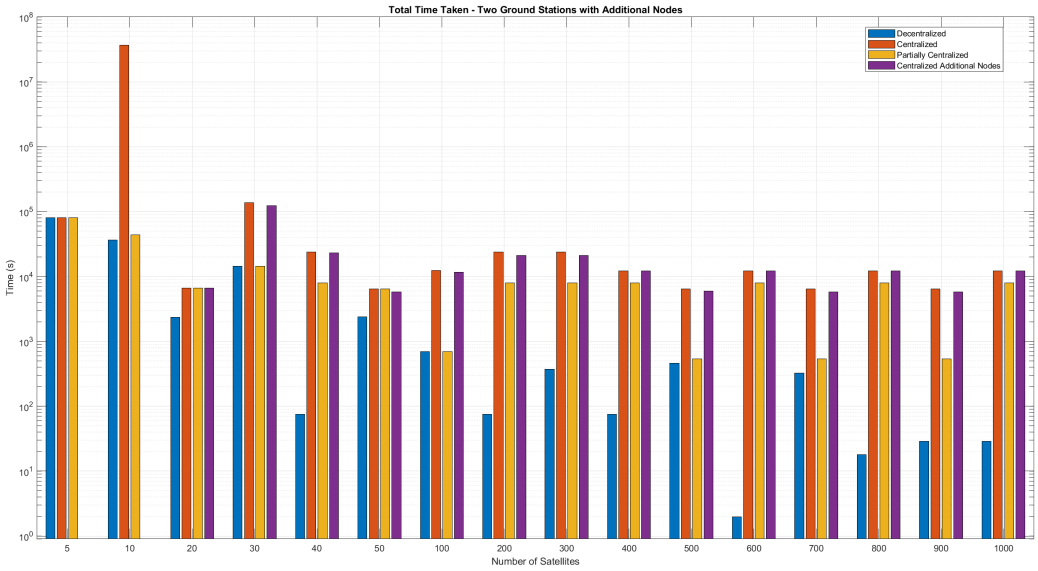

Figure A.15 Total Time Taken - Two Ground Stations with Additional Nodes.

Five Ground Stations

- General Trend: Slight changes in total time for various satellite counts.
- Slight Changes: Satellite counts of 20, 30, 50, 100, 300, 500, 700, and 900 show slight improvements.
- No Change: Satellite counts of 400, 600, 800, and 1000 remain the same, similar to the two ground station configuration.

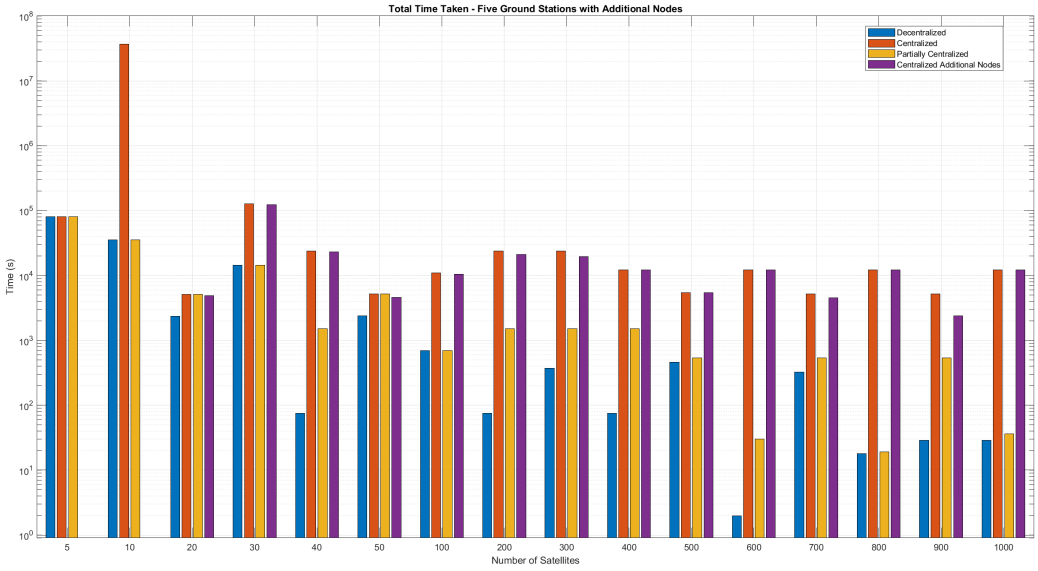

Figure A.16 Total Time Taken - Five Ground Stations with Additional Nodes.

A.8.1.2 Time taken after first Image was captured

One Ground Station

- General Trend: Minimal changes observed.
- No Change: Satellite counts of 20, 400, 600, 800, and 1000 show no change.

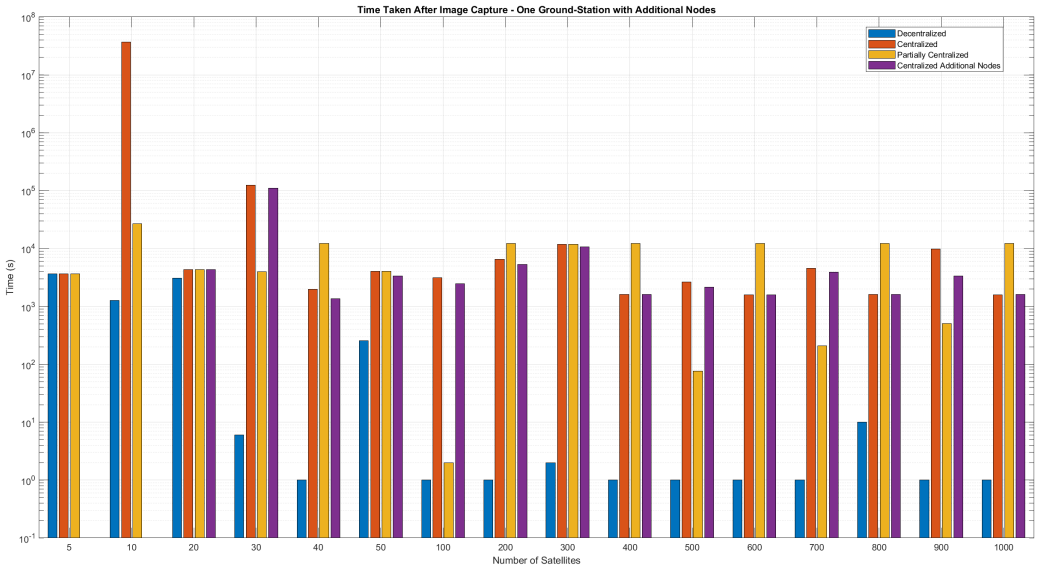

Figure A.17 Time Taken After Image Capture - One Ground-Stations with Additional Nodes

Two Ground Stations

- General Trend: Slight improvement in time for most satellite counts.
- No Change: Satellite counts of 20, 400, 600, 800, and 1000 remain unchanged.

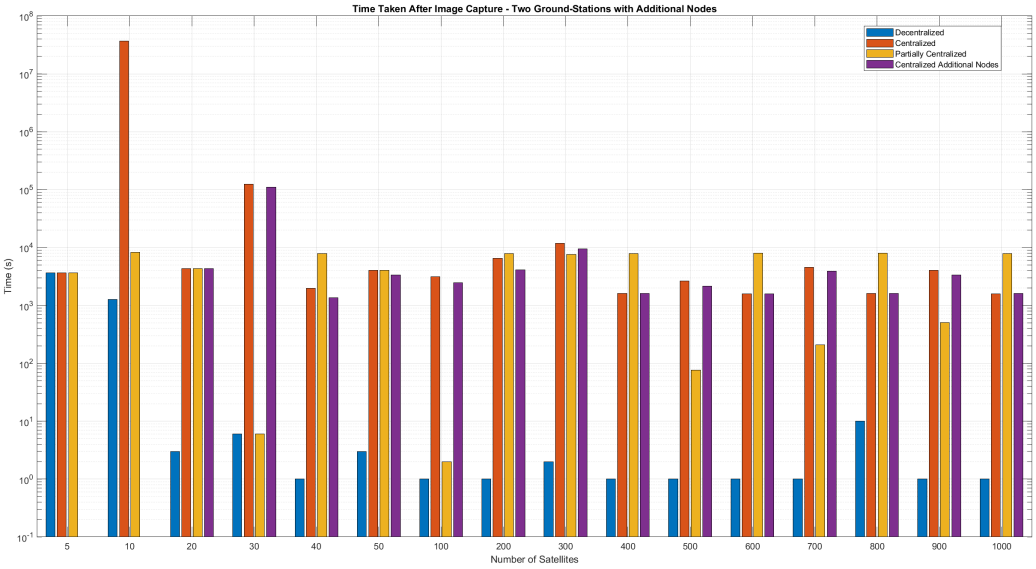

Figure A.18 Time Taken After Image Capture - Two Ground-Stations with Additional Nodes

Five Ground Stations

- General Trend: Slight improvements observed for various satellite counts.
- No Change: Satellite counts of 400, 600, 800, and 1000 show no change.

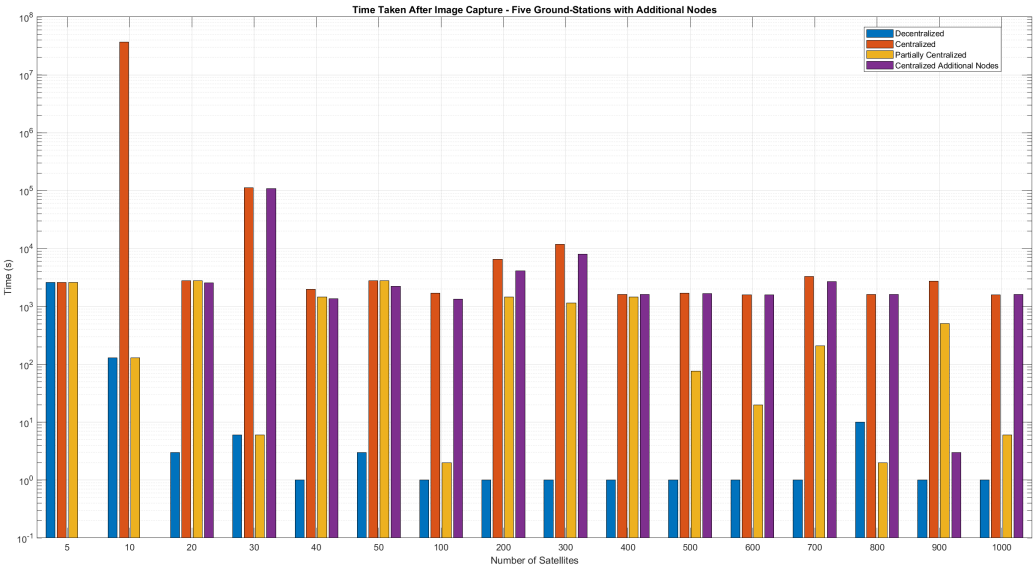

Figure A.19 Time Taken After Image Capture - Five Ground-Stations with Additional Nodes

A.9 Link Budget

The link budget analysis for the five satellites at different contact points with the ground station reveals varying performance levels across different parameters. These parameters include distance, elevation, transmitter Equivalent isotropic radiated power (EIRP), propagation losses, and received power, among others. The key indicators for assessing link performance are the Carrier-to-Noise density ratio (C/No), Carrier-to-Noise ratio (C/N), and link margin.

A.9.0.1 Contact at Start

As shown in Fig.3.15a,at the beginning of the contact, the received isotropic power for L1 is -156.46 dBW, resulting in a C/No of 95.14 dB-Hz, a C/N of 1.71 dB, and a margin of 16.15 dB. These values indicate that L1 has a viable communication link at the start. However, L2 shows significantly lower received power levels (-188.05 dBW), with a negative C/N value (-37.87 dB). While the link can be established, L2 may require robust error correction techniques and adaptive coding to maintain data integrity. L3 shows a received isotropic power of -187.46 dBW, a C/No of 64.14 dB-Hz, and a margin of 10.17 dB it should still perform better due to higher margin.

Table A.26 Link Budget 5 Satellites Contact Start

Tag	Name	L1	L2	L3
N1	Distance (km)	1.3180e+04	1.3101e+04	1.5768e+04
N2	Elevation (deg)	-12.6338	-12.9094	-36.2193
N3	Tx EIRP (dBW)	32	-0.2000	1.8000
N4	Polarization loss (dB)	3.0103	3.0103	3.0103
N5	FSPL (dB)	182.4505	181.8372	183.2519
N6	Rain attenuation (dB)	-	-	-
N7	Total atmospheric losses (dB)	-	-	-
N8	Total propagation losses (dB)	182.4505	181.8372	183.2519
N9	Received isotropic power (dBW)	-156.4608	-188.0475	-187.4622
N10	C/No (dB-Hz)	95.1384	55.5516	64.1370
N11	C/N (dB)	1.7142	-37.8726	-29.2872
N12	Received Eb/No (dB)	28.1487	4.5825	13.1679
N13	Margin (dB)	16.1487	1.5825	10.1679

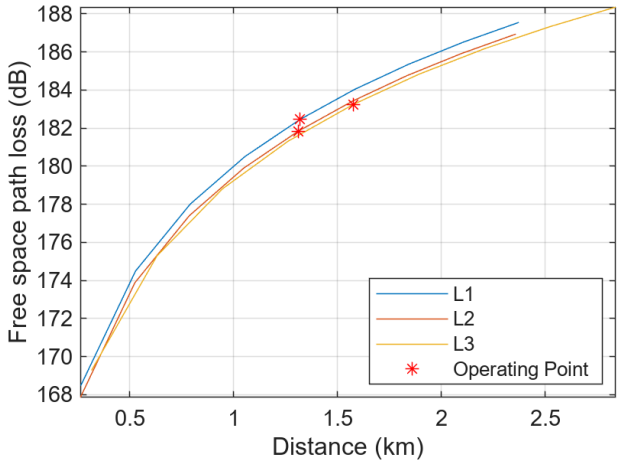

(a) Free Space Path Loss (dB)

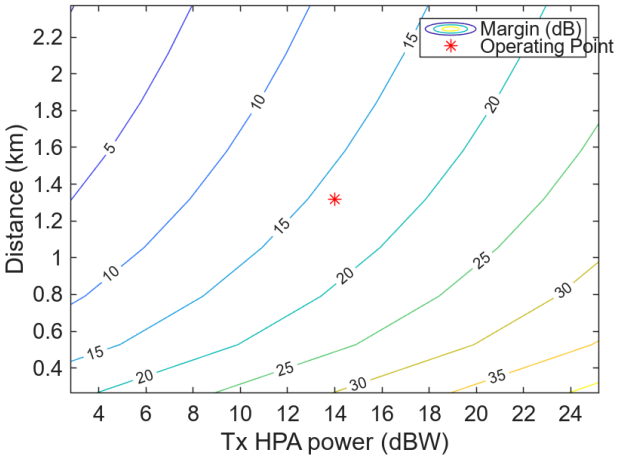

(b) Margin L1 (dB)

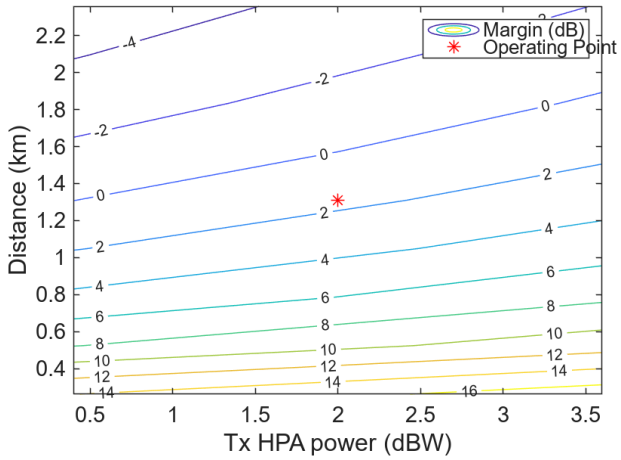

(c) Margin L2 (dB)

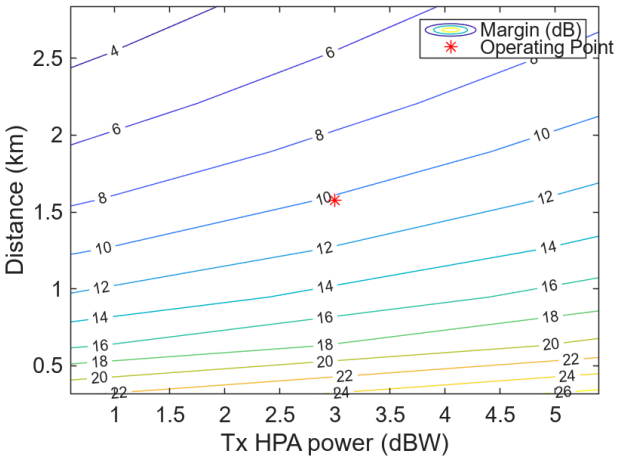

(d) Margin L3 (dB)

Figure A.20 5 Satellites Link Budget Analysis

A.9.0.2 Contact at Ground Station Zenith

As shown in Fig.3.15b, as the satellites progress to the ground station zenith position, the received power improves slightly for L1 and L2. L1 shows a received power of -155.99 dBW, a C/No of 95.60 dB-Hz, a C/N of 2.18 dB, and a margin of 16.61 dB, maintaining a reliable link. L2's performance also improves with a C/No of 56.37 dB-Hz and a slightly negative C/N of -37.05 dB. With advanced modulation schemes and error correction, L2 can achieve reliable communication. L3 exhibits a received isotropic power of -187.49 dBW, a C/No of 64.11 dB-Hz, and a margin of 10.14 dB.

Table A.27 Link Budget 5 Satellites Contact at Ground Station Zenith

Tag	Name	L1	L2	L3
N1	Distance (km)	1.0714e+04	1.0477e+04	1.5815e+04
N2	Elevation (deg)	9.3263	10.5735	-36.3846
N3	Tx EIRP (dBW)	32	-0.2000	1.8000
N4	Polarization loss (dB)	3.0103	3.0103	3.0103
N5	FSPL (dB)	180.6509	179.8963	183.2776
N6	Rain attenuation (dB)	0.0262	0.0192	-
N7	Total atmospheric losses (dB)	1.3347	1.1211	-
N8	Total propagation losses (dB)	181.9856	181.0174	183.2776
N9	Received isotropic power (dBW)	-155.9959	-187.2277	-187.4879
N10	C/No (dB-Hz)	95.6033	56.3715	64.1113
N11	C/N (dB)	2.1791	-37.0528	-29.3130
N12	Received Eb/No (dB)	28.6136	5.4024	13.1422
N13	Margin (dB)	16.6136	2.4024	10.1422

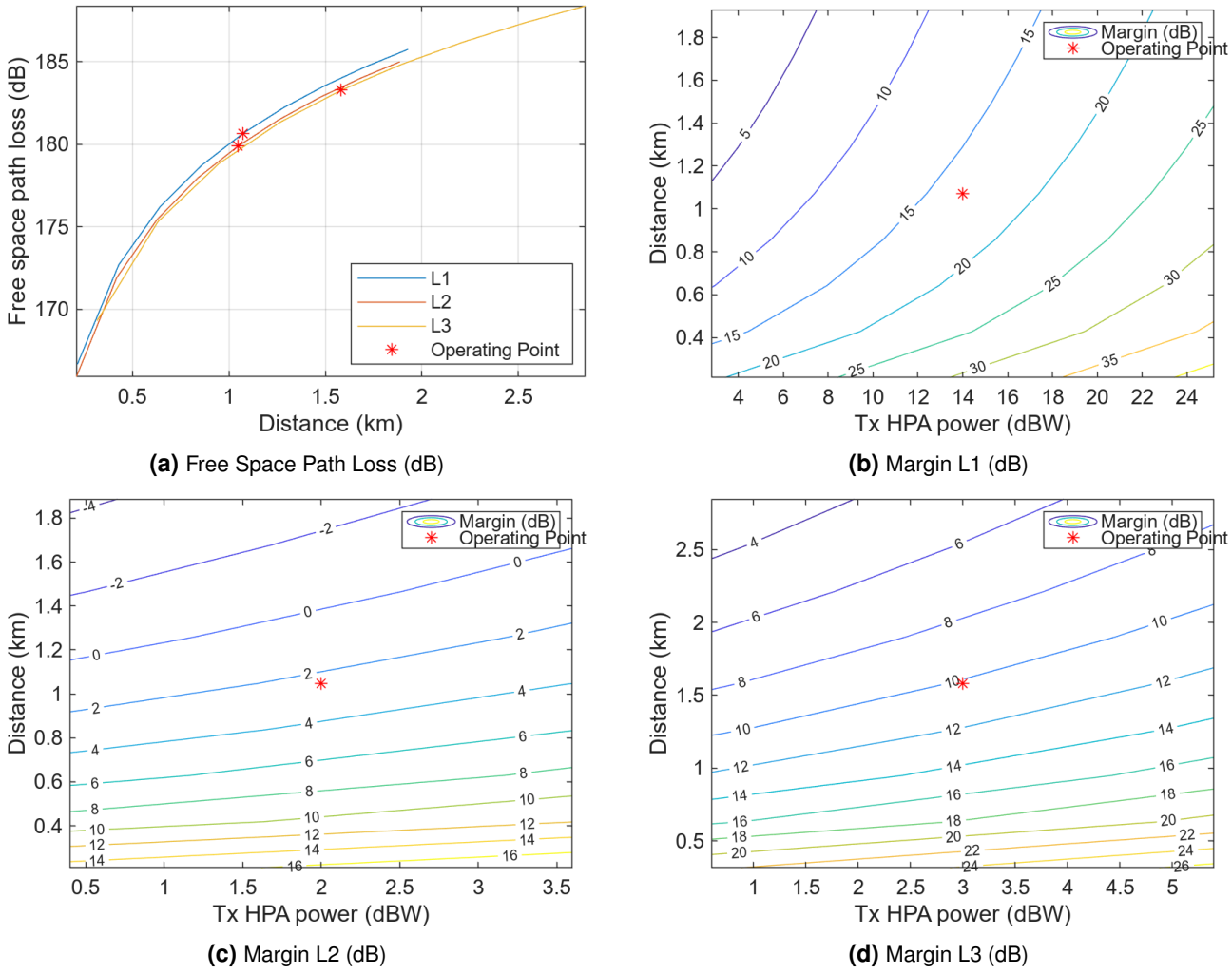

(a) Free Space Path Loss (dB)

(b) Margin L1 (dB)

(c) Margin L2 (dB)

(d) Margin L3 (dB)

Figure A.21 5 Satellites Link Budget Analysis

A.9.0.3 Contact at End

As shown in Fig.3.15c, by the end of the contact, the performance parameters further improve. L1 shows a significant enhancement with a received power of -153.29 dBW, a C/No of 98.31 dB-Hz, a C/N of 4.89 dB, and a margin of 19.32 dB. This indicates a robust and reliable link. L2, although still facing challenges, shows better margins (4.79 dB) and slightly improved C/No values. However L2 can be improved. L3 demonstrates a received isotropic power of -183.31 dBW, a C/No of 68.29 dB-Hz, and a margin of 14.32 dB, indicating that the link is strong despite FSPL losses.

Table A.28 Link Budget 5 Satellites Contact End

Tag	Name	L1	L2	L3
N1	Distance (km)	8.8026e+03	8.7157e+03	9.7784e+03
N2	Elevation (deg)	31.9790	31.6481	-21.5061
N3	Tx EIRP (dBW)	32	-0.2000	1.8000
N4	Polarization loss (dB)	3.0103	3.0103	3.0103
N5	FSPL (dB)	178.9442	178.2974	179.1016
N6	Rain attenuation (dB)	0.0046	0.0038	-
N7	Total atmospheric losses (dB)	0.3340	0.3304	-
N8	Total propagation losses (dB)	179.2782	178.6279	179.1016
N9	Received isotropic power (dBW)	-153.2885	-184.8382	-183.3119
N10	C/No (dB-Hz)	98.3107	58.7610	68.2873
N11	C/N (dB)	4.8864	-34.6632	-25.1370
N12	Received Eb/No (dB)	31.3210	7.7919	17.3182
N13	Margin (dB)	19.3210	4.7919	14.3182

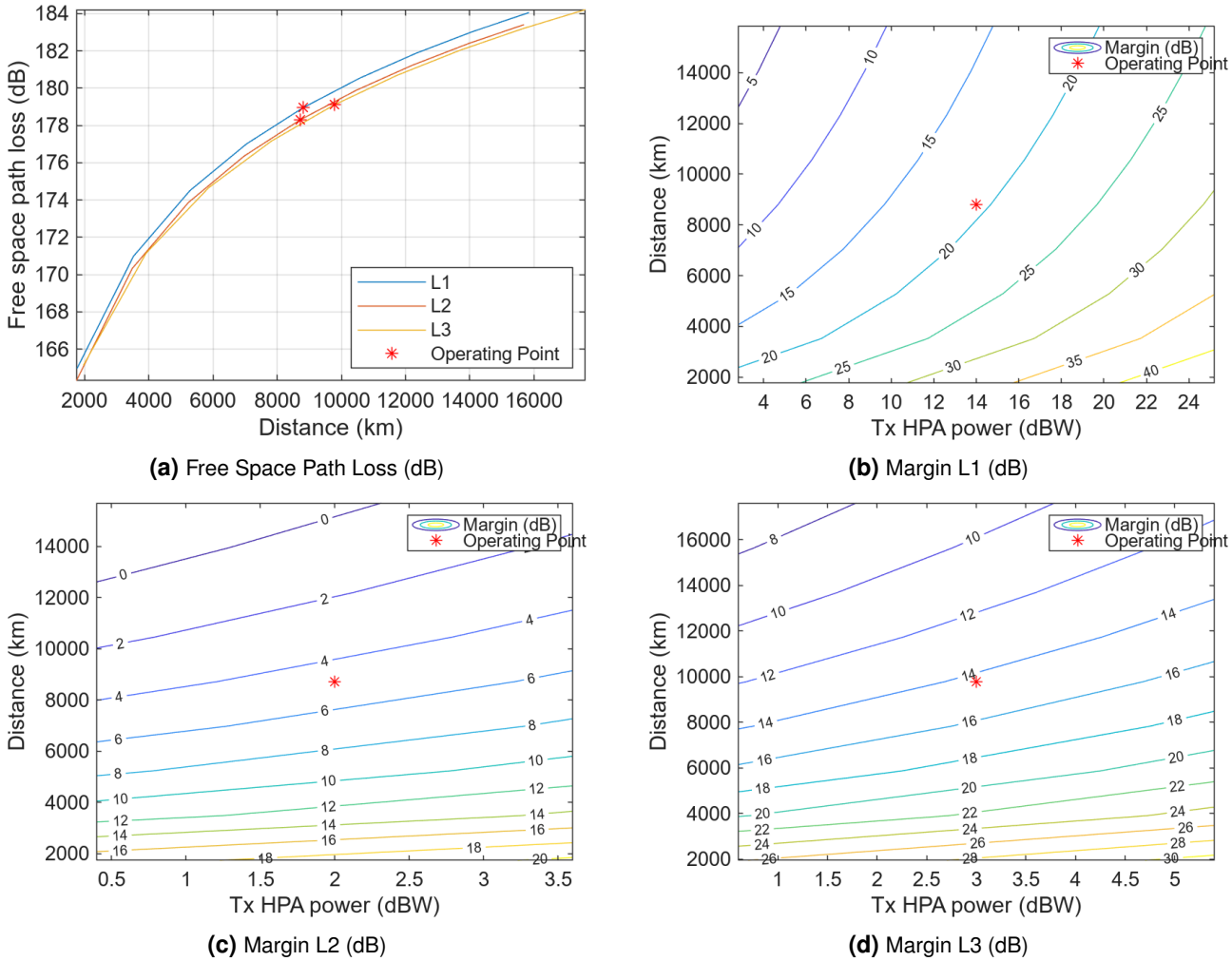

(a) Free Space Path Loss (dB)

(b) Margin L1 (dB)

(c) Margin L2 (dB)

(d) Margin L3 (dB)

Figure A.22 5 Satellites Link Budget Analysis

Bibliography

[1] P H Krisko. The predicted growth of the low-earth orbit space debris environment — an assessment of future risk for spacecraft. *Proceedings of the Institution of Mechanical Engineers, Part G: Journal of Aerospace Engineering*, 221(6):975–985, Jun 2007.

[2] 10 years of planned satellites - spacecast 28, url=https://www.youtube.com/watch?v=8sYtPe9ycWQt=0s, journal=YouTube, publisher= Ansys Government Intiatives (AGI), year=2019, month=Dec.

[3] Marco Schmidt. *Ground Station Networks for Efficient Operation of Distributed Small Satellite Systems*. doctoralthesis, Universität Würzburg, 2011.

[4] Alessandro Golkar Vincenzo Messina. Initial formulation of a time varying dynamic graph decentralized optimization framework for scaled satellite network infrastructure operations. In *IAC 2023 Congress Proceedings, 74th International Astronautical Congress*, Oct 2023.

[5] Gene M. Belanger, Slava Ananyev, Jason L. Speyer, David F. Chichka, and J. Russell Carpenter. Decentralized control of satellite clusters under limited communication. *Journal of Guidance, Control, and Dynamics*, 29(1):134–145, 2006.

[6] Juan A. Fraire and Elías L. Gasparini. Centralized and decentralized routing solutions for present and future space information networks. *IEEE Network*, 35(4):110–117, 2021.

[7] Ramón María García Alarcia Jaspar Sindermann Alessandro Golkar Simone Scrocciolani, Vincenzo Messina. Advancing satellite network performance: Distributed simulation for earth observation satellite federations. *IEEE Access*, 12:45616–45630, Mar 2024.

[8] Fabricio S Prol, R Morales Ferre, Zainab Saleem, Petri Välisuo, Christina Pinell, Elena Simona Lohan, Mahmoud Elsanhoury, Mohammed Elmusrati, Saiful Islam, Kaan Çelikbilek, et al. Position, navigation, and timing (pnt) through low earth orbit (leo) satellites: A survey on current status, challenges, and opportunities. *IEEE Access*, 10:83971–84002, 2022.

[9] Chris Daehnick, Isabelle Klinghoffer, Ben Maritz, and Bill Wiseman. Large leo satellite constellations: Will it be different this time. *McKinsey & Company*, 4, 2020.

[10] Oltjon Kodheli, Eva Lagunas, Nicola Maturo, Shree Krishna Sharma, Bhavani Shankar, Jesus Fabian Mendoza Montoya, Juan Carlos Merlano Duncan, Danilo Spano, Symeon Chatzinotas, Steven Kisseleff, et al. Satellite communications in the new space era: A survey and future challenges. *IEEE Communications Surveys & Tutorials*, 23(1):70–109, 2020.

[11] John G Walker. Satellite constellations. *Journal of the British Interplanetary Society*, 37:559, 1984.

[12] S. Huang, C. Colombo, and F. Bernelli-Zazzera. Multi-criteria design of continuous global coverage walker and street-of-coverage constellations through property assessment. *Acta Astronautica*, 188:151–170, 2021.

[13] Yupeng Gong, Anshou Li, and Xuan Peng. Geometrical design method of walker constellation in non-terrestrial network. *Acta Astronautica*, 219:618–626, 2024.

[14] Der-Ming Ma, Zuu-Chang Hong, Tzung-Hang Lee, and Bo-Jyun Chang. Design of a micro-satellite constellation for communication. *Acta Astronautica*, 82(1):54–59, 2013.

[15] Bassel Al Homssi, Akram Al-Hourani, Ke Wang, Phillip Conder, Sithamparanathan Kandeepan, Jinho Choi, Ben Allen, and Ben Moores. Next generation mega satellite networks for access equality: Opportunities, challenges, and performance. *IEEE Communications Magazine*, 60(4):18–24, 2022.

[16] Leonardo Pedroso and Pedro Batista. Distributed decentralized ekf for very large-scale networks with application to satellite mega-constellations navigation. *Control Engineering Practice*, 135:105509, 2023.

[17] Xiaogang Wang, Wutao Qin, Yuliang Bai, and Naigang Cui. A novel decentralized relative navigation algorithm for spacecraft formation flying. *Aerospace Science and Technology*, 48:28–36, 2016.

[18] Quan Chen, Giovanni Giambene, Lei Yang, Chengguang Fan, and Xiaoqian Chen. Analysis of inter-satellite link paths for leo mega-constellation networks. *IEEE Transactions on Vehicular Technology*, 70(3):2743–2755, 2021.

[19] Juan A Fraire and Elias L Gasparini. Centralized and decentralized routing solutions for present and future space information networks. *IEEE Network*, 35(4):110–117, 2021.

[20] Gene M Belanger, Slava Ananyev, Jason L Speyer, David F Chichka, and J Russell Carpenter. Decentralized control of satellite clusters under limited communication. *Journal of guidance, control, and dynamics*, 29(1):134–145, 2006.

[21] J Russell Carpenter. Decentralized control of satellite formations. *International Journal of Robust and Nonlinear Control: IFAC-Affiliated Journal*, 12(2-3):141–161, 2002.

[22] ai solutions. Brouwer lyddane j2.

[23] ai solutions. Keplerian elements.

[24] Cavu Aerospace SatCatalog. Camera s.ldu.345.

[25] Endurosat s band transceiver, Apr 2023.

[26] Sample coverage time optimization, url = https://ai-solutions.com/_help_files/optimization_smp.htm#achr_coveragetimeopt, note = Accessed: 2023-11-15.

[27] Powered by mapbox, url = https://geojson.io/#map=8.06/-17.22/123.638, journal=geojson.io, author=mapbox note = accessed: 2023-11-20 .

[28] Bushfire, url = https://www.ga.gov.au/education/natural-hazards/bushfire#:~:text=in%20terms%20of%20the%20total,of%20western%20australia%20and%20queensland., journal = geoscience australia, publisher = commonwealth of australia, author = geoscience australia, year = 2023, month = sep .

[29] Ground stations, url = https://www.dlr.de/en/eoc/about-us/german-remote-sensing-data-center/national-ground-segment/ground-stations, journal = deutsches zentrum für luft- und raumfahrt.

[30] L- / s- / x-band receiving station, url = https://www.dlr.de/en/research-and-transfer/research-infrastructure/l-s-x-band-receiving-station, journal =dlr.

[31] Sansa space operations - hbk-5, url = https://www.sansa.org.za/wp-content/uploads/2018/08/a5-antennae-factsheets-out.pdf, journal=sansa space operations - hbk-5, author=sansa.

[32] Indian dsn.

[33] Kourou station, url = https://www.esa.int/enabling_support/operations/esa_ground_stations/kourou_station, journal=esa, author=esa.

[34] 2025-2110 mhz band allocations.

[35] James Richard Wertz, Wiley J Larson, Douglas Kirkpatrick, and Donna Klungle. *Space mission analysis and design*, volume 8. Springer, 1999.

[36] Shkelzen Cakaj, Bexhet Kamo, Vladi Kolici, and Olimpjon Shurdi. The range and horizon plane simulation for ground stations of low earth orbiting (leo) satellites. *IJCNS*, 4:585–589, 01 2011.

[37] Steven G. Johnson. The NLopt nonlinear-optimization package. https://github.com/stevengj/nlopt, 2007.

[38] A. H. G. Rinnooy Kan and G. T. Timmer. Stochastic global optimization methods part II: Multi level methods. *Mathematical Programming*, 39:57–78, 1987.

[39] J. M. Gablonsky and C. T. Kelley. A locally-biased form of the DIRECT algorithm. *Journal of Global Optimization*, 21:27–37, 2001.

[40] D. R. Jones, C. D. Perttunen, and B. E. Stuckman. Lipschitzian optimization without the Lipschitz constant. *Journal of Optimization Theory and Applications*, 79:157–181, 1993.

[41] Optimization engines, url= https://ai-solutions.com/_help_files/optimization_engines.htm, journal=optimization engines, author=ai solutions.